THE STUDY OF THE EFFECTS OF SOME KENYAN SOILS ON THE CORROSION OF THE UNDERGROUND PIPES

BY

SIMON P.K. KARUU

A Thesis submitted in fulfilment for the Degree of Doctor of Philosophy in the University of Nairobi.

OCTOBER 1989

Dedicated to my wife GLADYS and CHILDREN.

This thesis is my original work and has not been presented for a degree in any other University.

SIMON P.K. KARUU

This thesis has been submitted for examination with our approval as University Supervisors.

PROF. A.H.S. EL-BUSAIDY
CHEMISTRY DEPARTMENT
UNIVERSITY OF NAIROBI

DR. N. DESAI
CHEMISTRY DEPARTMENT
UNIVERSITY OF NAIROBI

TABLE OF CONTENTS

CHAPTER 3

ANALYTICAL TECHNIQUES

CHAPTER 4

EXPERIMENTAL

ACKNOWLEDGEMENT

I wish to express my sincere gratitude to Professor A.H.S. El-Busaidy, my supervisor, for all the valuable guidance and support, he has accorded me during this research project. I wish to thank him for his concern particularly in providing ideas, enthusiasm and thought-provoking discussions together with his tireless efforts to obtain research funds, that have made the present work possible.

I am deeply indebted to the Norwegian Agency for International Development (NORAD) for providing the funds to enable me to carry out this work. I am grateful to the British Council for granting me a scholarship to do part of my project at the University of Manchester Institute of Science and Technology (U.M.I.S.T.), Britain.

My personal thanks go to Dr. Cottis, my supervisor at U.M.I.S.T., for his instructions on the polarization techniques and use of various instruments during my stay in U.M.I.S.T.

Special thanks are due to my colleagues at U.M.I.S.T. for their valuable advice and discussions on the project. I am particularly indebted to Mr. David Mackomic of Manchester Polytechnic who introduced me into the computer classes. These computer lectures helped me in the understanding, operating and following computer data analysis which was applied in my project.

My thanks are also due to my wife, Gladys and children for their patience during my absence from home. I wish also to extend my sincere thanks to members of my family and

friends for the support they afforded me throughout.

Last but not least, I wish to extend my thanks to Mrs. Mary Kihara who typed the thesis with extra attention and wishful thinking.

EXPLANATORY NOTES:

NHE	-	Normal Hydrogen Electrode
SCE	-	Saturated Calomel Electrode
C_L	-	Clay type of soil
S_L	-	Silt type of soil
SC_L	-	Sandy clay type of soil
Y_1, Y_2, Y_3	-	Codes for pipes with smallest wall thickness
B_1, B_2, B_3	-	Codes for pipes with the higher wall thickness
R_1, R_2, R_3	-	Codes for pipes with the highest wall thickness
R_p	-	Polarization resistance
η	-	Overpotential
I_L	-	Limiting current density
β_a, β_c	-	Anodic and cathodic Tafel slopes respectively

ABSTRACT

Corrosion of metallic structures buried in the soil, or in contact with soils, has been a serious engineering and economic problem in most parts of the world. A research programme was conducted to investigate the corrosive properties of the soils in which underground pipes were laid. Domestic water-supply pipes were laid both in the field and in the laboratory.

Soil samples were collected from various sites in Nairobi City. The soils were placed half-way in plastic containers measuring 153mm x 245mm x 225mm. Three preweighed metal pipes, cut to size of 153mm long, were laid horizontally in each of the containers. Soil was added to cover the pipes and an air-tight lid was used to cover each container.

The pipes were unearthed at intervals of four months, cleaned and examined for the extent and type of corrosion that had taken place. After drying, each pipe was weighed and the mass lost during burial calculated.

After one year of laboratory experiment six soil samples were selected according to their respective corrosivity. Metal pipes, cut to lengths of one meter were buried half a meter deep in selected sites in the field and unearthed three times at intervals of six months. The pipes were cleaned and assessed for the extent and nature of corrosion that had taken place. The observed nature of corrosion was compared with that observed for the laboratory-buried pipes. The difference in

mass in the laboratory-buried pipes gave an indication of the extent of corrosion that had taken place.

The soil samples were analysed in the laboratory for both chemical and physical properties. These included soil-moisture content, pH, acidity and alkalinity, Redox potential, electrical conductivity, sulphate and chloride ions concentrations, presence of trace metals and the mechanical analysis. The observed corrosion was correlated with the properties analysed and the corrosive nature of each soil determined.

The rate of corrosion was also electrochemically determined as corrosion current. This was conducted by various methods that included Tafel extrapolation, polarization resistance determination, electrical impedance determination and electrochemical noise analysis.

The corrosion rate has been found to be high in moist soils rather than dry or water-saturated. The same observation was made when the chloride and sulphate ions concentrations were low rather than high. Soils with low electrical resistivity showed high corrosion rate, as was also observed for those with high acidity and low pH.

The laboratory-buried pipes showed a decrease in mass which ranged between 0.06% and 3.26% in one year of investigation. The observed loss in mass decreased with time of burial due to formation of corrosion products on the surface of the corroding pipe. However the field-buried pipes showed progressively increasing deterioration with time. This was mainly due to washing away of the corrosion products from the surface of the pipe, by rain.

Electrochemical methods were used for quick determination of corrosion currents which varied slightly with the technique used. The Tafel Extrapolation technique showed corrosion currents ranging between 6.0 and 17.0 ± 0.5μA while the Polarization Resistance technique showed corrosion currents ranging between 7.0 and 29.0 ± 0.5μA. The values for electrical impedance analysis showed just about the same values as those obtained for Polarization Resistance technique, and the electrochemical noise determination. This showed that each of the last three techniques was good enough for fast determination of corrosion rate.

The electrochemical determination of corrosion rate for both aerated and deaerated soil-water extracts showed a high corrosion current for aerated electrolyte. This indicated that oxygen was an important parameter in the corrosion process.

Observation of the unearthed pipe specimens showed that highest corrosion was on the upper part of the specimen. This is due to mixed anodic and cathodic areas close to one another forming microscopic corrosion cells.

The physical and chemical properties listed above were all found to be important parameters on the corrosion of buried underground pipes.

CHAPTER 1

INTRODUCTION

Corrosion is the destructive attack of a metal by chemical or electrochemical reaction with its environments. Deterioration by physical causes is described as erosion, galling or wear but not corrosion. However, in some cases, chemical attack accompanies physical deteriorations as described by terms such as corrosion-erosion, corrosive wear, or fretting corrosion.

Rusting, as used in this investigation, generally applies to corrosion of iron or iron-based alloys with formation of corrosion products consisting largely of ferrous and ferric oxides. Non-ferrous metals corrode but do not rust.

The importance of corrosion studies is threefold. The first area of significance is the economic factor including the objective of reducing material losses resulting from corrosion of pipelines, tanks, metal components of machines, ships, bridges, marine structures and so on.

The second area of importance is the improved safety of operating equipment which, through corrosion, may fail with catastrophic consequences. Examples of these include pressure vessels, boilers, metallic containers for corrosive materials, turbine blades and rotors, bridges, aeroplane components and automotive steering mechanisms.

The third importance of corrosion studies is conservation of materials,primarily those of metal resources.

Conservation of human effort entering the design and rebuilding the corroded metal pipes, equipment or structures adds to the economic importance of corrosion studies [Romanoff, 1957].

The economic factor is the prime motive for much of the current investigation in underground pipeline corrosion. Losses sustained by industry, by municipalities and by military, amount to many billions of dollars [Uhlig, H. and R. Revie, 1985]. Economic losses are either direct or indirect.

The direct economic losses are those losses that are encountered by replacing corroded structures and machinery and their components. These include condenser tubes, mufflers, pipelines and metal roofing together with the necessary labour. Other examples are, the repainting of the structures where prevention of rusting is the prime objective and the capital costs plus the upkeep of the cathodically protected pipes.

Indirect losses are more difficult to assess. However, a brief survey of typical losses of this kind compels the conclusion that they add several billions of dollars to the direct losses outlined above. Examples of these indirect losses include: shutdown; loss of production; loss of efficiency; contamination of the products; and overdesign.

Obviously, indirect losses are a substantial part of the economic tax imposed by corrosion, although it is difficult to arrive at a reasonable estimate of the total losses from this source.

The corrosion of metallic structures buried in the soil or in contact with soils has long been a serious engineering and economic problem. In 1957, corrosion affected about one million miles of gas, water, and oil pipelines, half a million of railroad tracks and quarter of a million of buried communications, signal and power cable systems in the U.S.A. [Romanoff, 1957]. The annual loss to the American pipeline industry alone, from actual destruction by corrosion and the cost of preventing corrosion was estimated to be in the order of 600 million dollars. Because the corrosion rates are often unknown, engineers often overdesign underground structures by specifying extra thickness of metal required to ensure adequate life and strength. This leads to needless consumption of appreciable tonnage of critical metals.

In Kenya, there is the famous Kenya Pipeline running from the Port of Mombasa to Nairobi. This pipeline carries the petroleum products between the two Kenyan towns. There are plans to extend the pipeline to other large towns of the country to ease the transportation of the petroleum products.

All towns in Kenya have piped water systems that supplies both the industry, and the commercial and residential premises with water. Plans are under way to make sure that every Kenyan citizen has clean piped water by the year 2000 A.D.

90% of the water pipes used in the country are made of iron alloys and are buried underground. They are therefore prone to corrode due to aggressive properties of soils in which they are buried. The corrosion of pipes has both direct and indirect economic factors, as mentioned above.

Corrosion and bursting of a water pipe would lead to replacement of the pipe, loss of water, and inconvenience the water consumers, and employment of labour required for the respective repairs and maintenance. If the consumer was an industry, the processes requiring water would be closed down, the products are delayed or wasted, time is lost and the employees are paid for work not done.

On the other hand the corrosion and bursting of the petroleum pipeline would lead to catastrophic effects. These include explosions and possibly loss of life, waste of product, including contamination and lack of services to the intended customers. These effects are in addition to the cost of replacing the pipe and the shutdown of all the pipeline processes. The environment would also be highly polluted.

The corrosivity of a soil towards buried metals depends on both the physical and chemical compositions of the soil. It was therefore found necessary to study the nature of the soil, chemical and physical properties that would lead to corrosion of metal pipes buried underground.

The investigation started by collecting soil samples at twenty six sites within the city of Nairobi. These samples were analysed in the laboratory for physical and chemical compositions as well as mechanical analysis from which texture of each of the soils was determined. The following factors were thoroughly tested and determined: (1) soil moisture content, (2) redox potential, (3) electrical conductivity/resistivity, (4) pH, (5) acidity/alkalinity, (6) metal ions which included Cu, Zn, Mn, Mg and Fe, (7) concentrations of sulphate and chloride ions.

The analyses were conducted using field-condition soil, soil-water slurry and soil-water extracts (see chapter 4). Each of the soils under investigation was mechanically tested for texture determination.

After the soils were analysed for the above properties, their corrosive effects due to these properties were studied. This was done by burying some pipes in the field and others in plastic containers in the laboratory.

Preweighed metal pipes with a $\frac{1}{2}$" diameter, cut to lengths of six inches were buried in plastic containers in the laboratory. The pipes were unearthed three times at intervals of four months. The pipes were thoroughly cleaned with hot water to remove the soil stuck on the pipes. This was followed by a thorough cleaning using a mixture of hot water, hydrochloric acid and stannous chloride to remove the corrosion stains from the surface of the pipes. The pipes were then degreased using acetone, dried and weighed. The difference in mass before burial and after unearthing was recorded (Appendix 1). The highest mass loss indicated the highest corrosion undergone by the pipe. This in turn indicated the most corrosive soil to the pipes.

After the above experiment was done, six sites were selected for field testing. Metal pipes, with the same diameter as above, but one meter long were buried in respective sites in the field. Three pipes were buried in each site and these pipes were unearthed at intervals of six months. The unearthed pipes were cleaned as above, degreased with acetone and left overnight to dry.

Both the field- and laboratory-buried pipes were visually examined for the type and extent of corrosion that had taken place during the period of burial. The type of corrosion was similar for both the laboratory and field pipes. However, the field pipes were more corroded because of the washing away of the corrosion products by rain. The pitting corrosion was also more pronounced in the field pipes than the laboratory pipes. The freshly cut ends of the pipes showed more corrosion than the other parts of the pipes.

After establishing that the field and laboratory pipes suffered similar types of corrosion, it was found necessary to study the rate of corrosivity of the soils. This was done by using two polarization techniques, namely: Tafel extrapolation technique and linear or polarisation resistance technique (Section 5.9.2).

The rate of corrosion was determined by:

(1) direct extrapolation of anodic and cathodic Tafel slopes. The point of intersection of the two lines was noted and extrapolated to the current axis from which corrosion current was determined. Extrapolation of this point to the potential axis indicated the respective corrosion potential. The method for accurate determination of the corrosion potential of the working electrode is discussed in Section 4.12.1.

(2) the values of applied current and the overvoltage were used to calculate the corrosion current by using the Butler-Volmer Equation (Section 2.5.2.2).

(3) the anodic and cathodic Tafel slopes obtained in (1)

above were used to calculate the corrosion current by the Stern-Geary Equation (Section 5.9.2).

In this investigation, it was found necessary to study the effect of oxygen absorbed in the soil-water extracts. This was achieved by deaerating the soil-water extracts by bubbling oxygen-free nitrogen gas through the solution for one hour. Polarization measurements, carried out above, were repeated for the deaerated soil-water extracts and the results are presented in figures 1-24 (last pages of thesis).

From these experiments it was found that the corrosivity of the soil towards buried pipe, depended very much on the soil texture. The soils with large grains and hence large pores, such as sands and gravels, have low water-retention capacity. They were found to contain low amounts of soluble salts (chlorides and sulphates) and were generally found to have low corrosive capacity.

The soils with small grain sizes such as silt and clay were found to have high water retention capacity, high acidity, and high concentrations of soluble sulphates and chlorides. They were found to be more corrosive than the soils with large grains.

The visual examination of the unearthed pipes showed that those pipes buried in large-grain soils showed uniform type of corrosion. Those unearthed from small-grain soils showed highly localised corrosion. The mass losses recorded for pipes unearthed from clay soils were generally higher than those recorded for sandy soils.

It was generally found that the corrosion of underground pipeline increased with time. That is the longer the pipe was in service, the greater was the deterioration. However this depends on the composition of the soils because different components have different corrosivities towards buried pipes. The climatic conditions also have effect on the corrosivity of the underground pipes. Too much rainfall would lead to washing away of the corrosion products accelerating the rate of corrosion of the pipe. Dry weather conditions lead to very little corrosion and hence the pipe would have a longer service life.

Polarization measurements showed that there was a direct relationship between the observed mass losses and the corrosion currents measured (sec. 4.12). This method can therefore be used to determine the corrosion rate of systems whose loss of mass is not easy to determine. These systems include underground pipelines, ship hauls, aeroplane or bridge components, only to name a few.

The deaeration experiment showed that corrosion current was generally lower for deaerated soil-water extracts samples. This indicates that soil samples with high moisture contents and no oxygen would corrode metals only very slowly as compared to the high corrosion in aerated soils rich in soil moisture. In the presence of oxygen the main cathodic reaction, during the ferrous metal corrosion, is the oxidation of oxygen leading to the formation of ferrous or ferric oxide on the surface of the metal. In the absence of oxygen then other cathodic reactions would take place.

In this investigation, most of the soils were found to be acidic. Therefore, in absence of oxygen, the hydrogen evolution would be the effective cathodic reaction. On the other hand, in presence of sulphate-reducing bacteria, the cathodic reaction would be the sulphide-reduction reaction (Section 5.9.3).

It has been established that the major cause of corrosion of water pipelines laid underground in Nairobi is low pH and the high concentrations of chlorides in the soils. The low electrical resistivity is due to the presence of soluble salts, among which are sulphates and chlorides in addition to the presence of various metal ions in the soils. However, the electrical resistivity is not so much a threat to the underground pipes as are the acidity and the high chloride concentration.

It is therefore concluded that soils which are low in acidity, low metal ion concentrations, and low concentrations of both chloride and sulphate should be used for backfilling the trenches after laying the pipes. The soil should be free from pieces of paper, wood, tins or stones. The soils should have high drainage and high pH values.

The life of underground pipeline could further be increased by coating it. The coating could be either metallic, such as galvanised iron, or non-metallic such as bitumen. Both should be capable of increasing the life of the pipeline and are recommended for future investigation.

The investigation should be extended to other towns and rural areas of Kenya. The investigations should be recommended as part of District Focus for Development of rural parts of Kenya,

in readiness for the supply of the clean piped water by the year 2000 A.D.

CHAPTER 2

THEORETICAL ASPECTS OF CORROSION

2.1 CHARACTERISTICS OF SOILS

2.1.1 Definition

In general, the word soil is applied to the first few feet of finely divided modified rock material covering the level and moderately inclined portion of the earth. Crushed rock and unmodified rock on mountain tops are not soils and earth removed from its original position is not soil if it has lost its structure.

Vegetation and climate are two active factors of soil development that change the parent material from an inert mass to a body that has morphology. Drainage, aeration, the quantity of water that percolates through the soil, the rate of natural erosion, sun and wind, affect the effects of climate and vegetation to varying degrees.

2.1.2 Classification

The classification of soils according to their characteristics is based on their physical and chemical properties. Soils may be divided into two broad classes: (a) Pedacols - soils in which lime accumulates in the subsoil. (b) Pedafers - soils in which lime does not accumulate in the subsoil [Romanoff 1957].

2.1.3 Chemical properties

Quite a large number of chemical elements exist in the soils, but most of them are combined to complex soluble compounds

which exert little direct chemical influence on corrosion. These inert compounds of soils are chiefly combinations of oxygen with silicon, aluminium and iron. Iron in various degrees of oxidation is responsible for the colour of many soils, and this colour is an indicator of the degree of aeration of the soil. In well-aerated soils, the iron compounds are oxidized to the ferric state. These soils are generally indicated by their brown, red or yellow colours. In poorly-aerated soils the soils are predominantly grey in colour indicating reduced forms of iron. Accumulation of organic matter in humid areas favour the formation of darker-coloured soils.

Chemical analyses of soils for corrosion studies are limited to the determinations of the constituents that are soluble in water under standardized conditions. The soils are usually analysed for sodium, calcium, magnesium and other substances such as carbonates, bicarbonates, chlorides, nitrates and sulphates. The nature and amount of soluble salts together with moisture content of the soil, largely determine the ability of the soil to conduct an electric current [Byers, 1938; Piper 1947 and Gerhood, H. 1979].

The development of acidity in soils is a result of the natural process of weathering under humid conditions. In regions of moderate rainfall, soluble salts do not accumulate except where soil waters seep to lower levels and collect in depressions. In regions of high rainfall, not only are soluble salts removed from the soils but the absorbed bases normally present in the colloidal materials of the soil are partially removed, and this results in increased acidity. The depths to which this leaching of bases

occurs varies with rainfall, drainage, type of vegetation and the nature of the material present.

The degree or intensity of acidity or alkalinity of a soil is expressed as a pH. The terms used for soil reaction are defined by Romanoff (1957) and are presented in the following table:

Term	pH
Extremely acid	Below 4.5
Very strongly acid	4.5 - 5.0
Strongly acid	5.1 - 5.5
Medium acid	5.6-6.0
Slightly acid	6.1-6.5
Neutral	6.6-7.3
Mildly alkaline	7.4-7.8
Moderately alkaline	7.9-8.4
Strongly alkaline	8.5-9.0
Very strongly alkaline	9.1 and higher

Table 2.1: pH descriptions for soil analysis.

2.1.4 Physical properties

The physical properties of soils that are of importance in corrosion are those that determine the permeability of the soil to oxygen or air and to water. The particle size distribution of the soil is an important factor with respect to both aeration and moisture content. In soils of coarse texture, such as sands and gravels, where there is free circulation of air, corrosion

approaches the atmospheric type. Soils that are free of clay and silt have low plasticity, low water-content and are not much affected by changes in moisture content.

Clay and silt soils are characterised by fine texture, high water-holding capacity and by poor aeration and poor drainage. The clay particles are highly plastic and become sticky and impervious when saturated with water. Such soils shrink and crack when dry and swell on wetting. Soils containing silt have some plasticity and expand and contract considerably on wetting and drying but to a much less degree than clay.

Diffusion of gases into the soils is enhanced by a number of climatic factors. Temperature changes from day to night conditions cause expansion and contraction of the soil surface pores. Variations in barometric pressure affect diffusion of gases. Biological activity within the soil tends to decrease the oxygen content and replace it with gases from metabolic activity such as carbon dioxide. Factors which tend to increase microbial respiration such as the addition of large amounts of readily decomposed organic matters or factors which decrease diffusion rates (e.g. water saturation), will lead to development of anaerobic conditions within the soil.

2.2 MECHANISM OF UNDERGROUND CORROSION

2.2.1 Electrochemical mechanism

Iron and many other metals used in the underground constructions become coated with a thin film of an oxide immediately upon being exposed to air. Such a film on iron may

be merely of molecular thickness but furnishes some degree of protection against further oxidation or corrosion. At higher temperatures, oxygen diffuses into the metal increasing the film thickness. If this film flakes off it exposes fresh metal surface for the continuation of the reaction.

Most of the corrosion of iron and other metals in the underground surface at normal or moderate temperatures is the result of an electrochemical reaction. In this type of reaction the overall chemical reaction of the electrolyte with the metal is divided into two largely independent processes.

(i) Anodic process

This process involves the transfer of metal into solution as hydrated ions with an equivalent number of electrons left in the metal. i.e.

$$M_{(s)} \xrightarrow{xH_2O} M^{n+}_{(aq)} \cdot xH_2O_{(l)} + ne^-_{(aq)}$$

(ii) Cathodic process

This process involves assimilation of the excess electrons in the metal by depolarizers (atoms, molecules or ions in the solution that can be reduced at the cathode). The examples of cathodic reactions taking place in underground corrosion are given by the following equations:-

(a) In acidic soils:

$$O_{2\,(dissolved)} + 4H^+_{(aq)} + 4e^- \longrightarrow 2H_2O_{(l)}$$

(b) Neutral or alkaline soils:

$$O_{2\,(dissolved)} + 2H_2O_{(l)} + 4e^- \longrightarrow 4OH^-_{(aq)}$$

The spatial separation of the anodic and the cathodic reactions is energywise more advantageous in as much as the reactions can proceed with greater ease. For this reason, electrochemical corrosion is characterised by the localization of the anodic and cathodic processes in different regions. This results in some areas of the pipe corroding while other adjacent areas show no deterioration at all.

In the electrochemical theory, corrosion occurs through the loss of electrons at the anodic areas and freeing of the metal ions which detach from the metal base. However, correlation of this theory with the actual corrosion of metals underground is complicated because of the many factors that singly or in combination affect the course of the electrochemical reaction. These factors (Section 2.3) determine both the rate and extent at which corrosion occurs and also the type of corrosion taking place. The major types are uniformly distributed type and these are considered relatively less aggressive, and the localised type such as the pitting type of corrosion. The latter type of corrosion is much more dangerous because a few small perforations can greatly reduce the efficiency of a pipeline even though there is only a very small or negligible loss in weight of the pipe as a whole.

2.2.2 Kinetics and thermodynamics of the corrosion process

Thermodynamics provides a means of predicting the equilibrium state of a system of specified components, but provides no information on the detailed course of the reaction nor that of the rate at which the system proceeds to equilibrium. By use of

suitable catalysts the reaction can be made to proceed by a different mechanism and different rates. The final position of the equilibrium which can be predicted by the thermodynamics remains unchanged.

Kinetic factors that control the rate of processes frequently outweigh thermodynamic tendency of the metal to corrode so that the final position of equilibrium i.e. complete conversion to corrosion products is attained only slowly or not at all. Although the formation of oxide film or films of other corrosion products are of vital importance in controlling the rate of a corrosion reaction in aqueous solution, it must be emphasized that in certain circumstances the activation energy of the process or the rate of diffusion of species to and from the metal surface may be more significant than the film formation.

The magnitude of the free energy change, ΔG, of a specific corrosion reaction provides a measure of the spontaneity of the reaction and of the extent to which it will proceed before equilibrium is attained. If $\Delta G \ll 0$ (negative) the tendency of the metal to react with species in solution will be high but whether or not the reaction proceeds to any extent will depend on the kinetic factors. If $\Delta G = 0$ the system is at equilibrium and there will be no net direction of the reaction. If $\Delta G \gg 0$ (positive) the metal is stable and no further consideration need be given to kinetics.

The applications of thermodynamics to the corrosion phenomena have been generalized by means of potential-pH plots

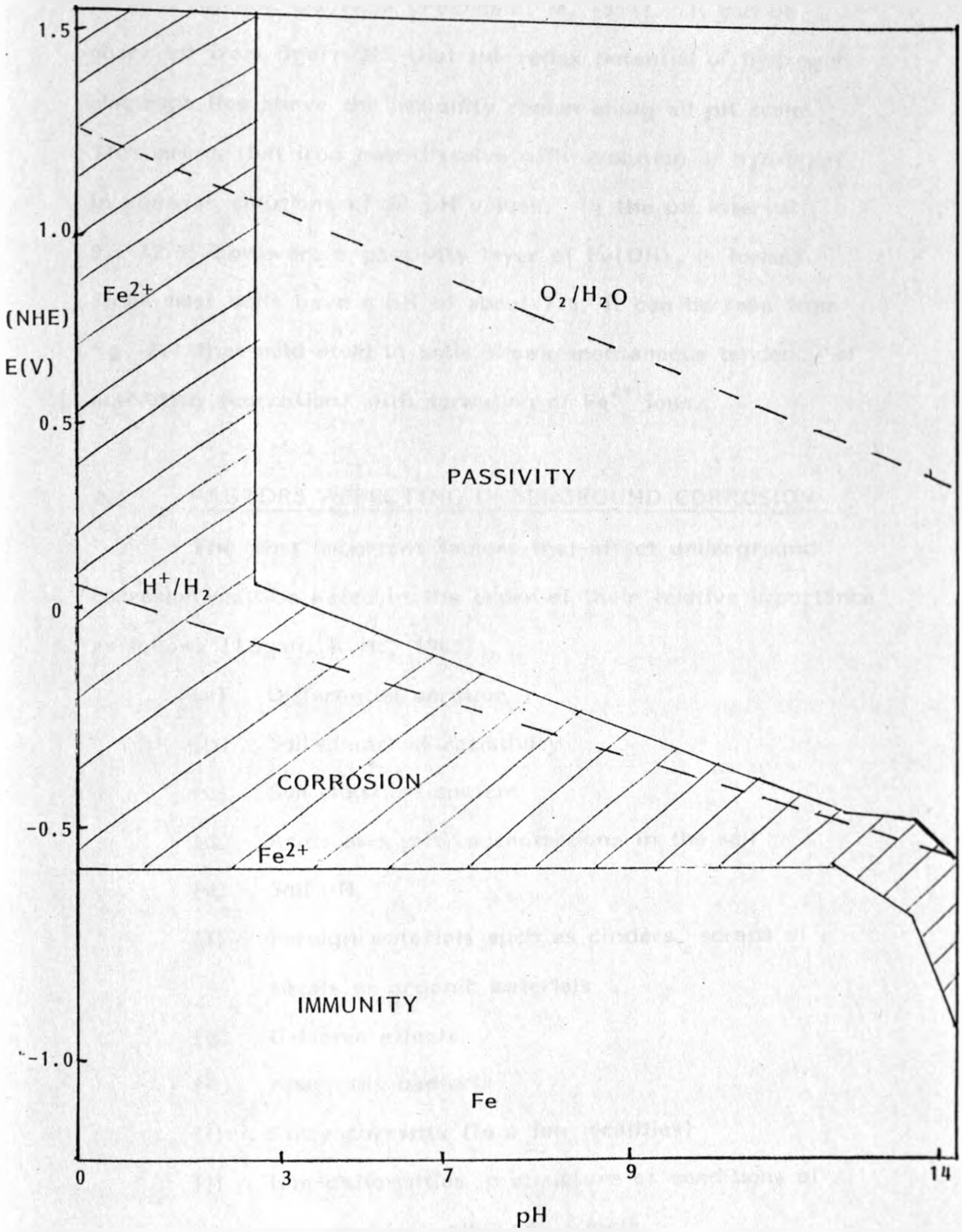

Fig. 2.1: Potential-pH diagram for iron [Pourbaix, M., 1954].

in the Pourbaix diagrams [Pourbaix, M. 1954]. It can be observed from figure 2.1 that the redox potential of hydrogen electrode lies above the immunity region along all pH scale. This means that iron may dissolve with evolution of hydrogen in aqueous solutions of all pH values. In the pH interval 9.5-12.5, however, a passivity layer of $Fe(OH)_2$ is formed. Since most soils have a pH of about 7.5, it can be seen from fig. 2.1 that mild steel in soils shows spontaneous tendency of activation (corrosion) with formation of Fe^{2+} ions.

2.3 FACTORS AFFECTING UNDERGROUND CORROSION

The most important factors that affect underground corrosion may be listed in the order of their relative importance as follows [Logan, K.H., 1945]:

(a) Differential aeration

(b) Soil electrical resistivity

(c) Soil moisture content

(d) Acids and salt concentrations in the soil

(e) Soil pH

(f) Foreign materials such as cinders, scraps of metals or organic materials

(g) Galvanic effects

(h) Anaerobic bacteria

(i) Stray currents (in a few localities)

(j) Non-uniformities in structure or conditions of the metal eg. mill scale effects.

The major factors in soil corrosion are discussed in more details. In this discussion, it is relatively difficult to avoid some repetition because the same phenomenon or factor may be operative in more than one grouping and besides, various factors are frequently interrelated [Romanoff, 1957].

2.3.1 Differential aeration

Evans, in his Differential Aeration Principle [Evans, 1961] stated that any geometrical factor that results in higher concentration of oxygen at one part of the metal and a lower concentration (or zero concentration) at another will result in the former becoming the cathode and the latter the anode of the corrosion cell resulting in a localized attack. Pourbaix has however shown by means of Potential-current diagrams that the Differential Aeration Principle is applicable only at certain pH values [Pourbaix, 1954].

In the soil, oxygen either from the atmospheric sources or from oxidising salts or compounds, stimulates corrosion by combining with metal ions to form oxides, hydroxides, or salts of the metal. The aeration characteristics of a soil are dependent primarily upon the physical characteristics such as particle size, particle size distribution and apparent specific gravity, all of which are related to size and continuity of the pore space. Local differences in the packing of the soil and in its moisture content may develop oxygen concentration cells where the area with the least oxygen is anodic in which corrosion may occur (figs. 2.2 and 2.3).

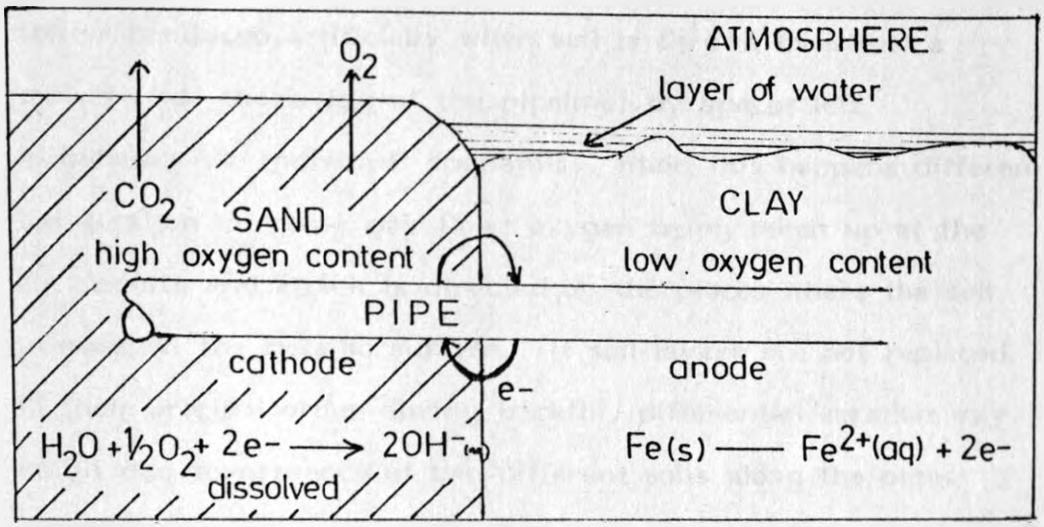

Fig 2.2 Differential Aeration Corrosion in the soil

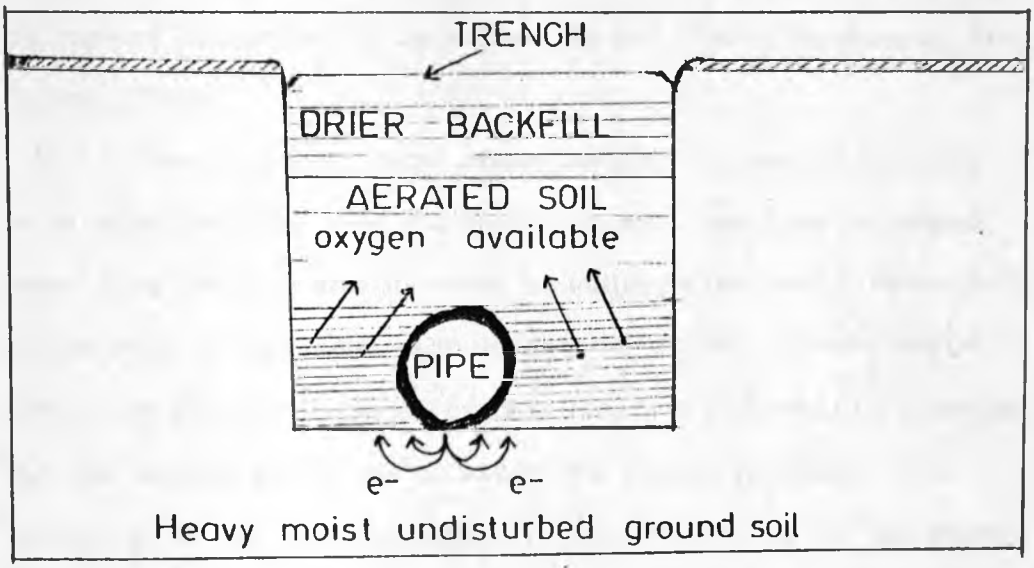

Fig 2.3 Corrosion caused by differential aeration

Soils of intermediate character may produce corrosion which is localised and accordingly intense, if air pockets are present. These are present either as a natural feature of the soil or produced artificially when soil is thrown back into a trench after the laying of the pipeline, by spaces left in-between the individual spadefuls. When this happens differential aeration currents may flow; oxygen being taken up at the air pockets and attack is directed on the places where the soil presses on the metallic surface. If soil layers are not replaced in their original order during backfill, differential aeration may result due to presence of two different soils along the pipe. Occasionally serious corrosion has been reported because of stones, sticks and other foreign material that come into contact with the pipe when the trench is backfilled [Evans, 1963; Bondurant, 1971; Gupta, 1978].

The phenomena that affect aeration characteristics also have other effects. For example most soils decrease in volume when they are dry and increase in volume when wet. Particularly in the case of clay soils high in organic matter, the shrinkage in volume on drying produces cracks that provide effective channels for the oxygen of the air to reach the buried pipeline. The shrinking of the soil also tends to pull the coating off the coated pipe, whereas the coating may be deformed in compression when the soil expands [Scott, 1929]. Logan was unable to observe that swelling of the soil forced the coating of rag-felt-reinforced asphalt on pipe into cracks [Logan, 1945].

Since oxygen reduction is the principal cathodic reaction, aeration has a pronounced effect on underground corrosion. For most materials, the rate is under cathodic control and is a direct function of the degree of aeration. Tomashov has described soil as a stationary electrolyte where oxygen diffusion is the rate determining step or parameter [Tomashov, 1966]. The mechanism of diffusion of oxygen into the soil is shown in figure 2.4 and consists of three zones.

Zone A: Gaseous convection of oxygen in pores of soil occurs here.

Zone B: Gaseous diffusion in pores of the soil occurs here.

Zone C: Diffusion of oxygen in a continuous liquid film (or corrosion products) takes place here.

Any of these transport mechanisms may be the limiting factor for corrosion in the soil.

Differential aeration cells due to stones, lumps of soil crevices formed by shielding jackets or other conditions which cause unequal oxygen distribution are readily established in the soil. The static nature of the electrolyte as well as small concentrations of ions such as chloride and hydrogen which break down the passive film, enhance differential aeration effects. This effect was clearly reported by Pearlstein and Teitell for aluminium exposed at a tropical rain forest for one year [Pearlstein and Teitell, 1974]. The weight loss for the aluminium in the soil where differential aeration occurred was higher than

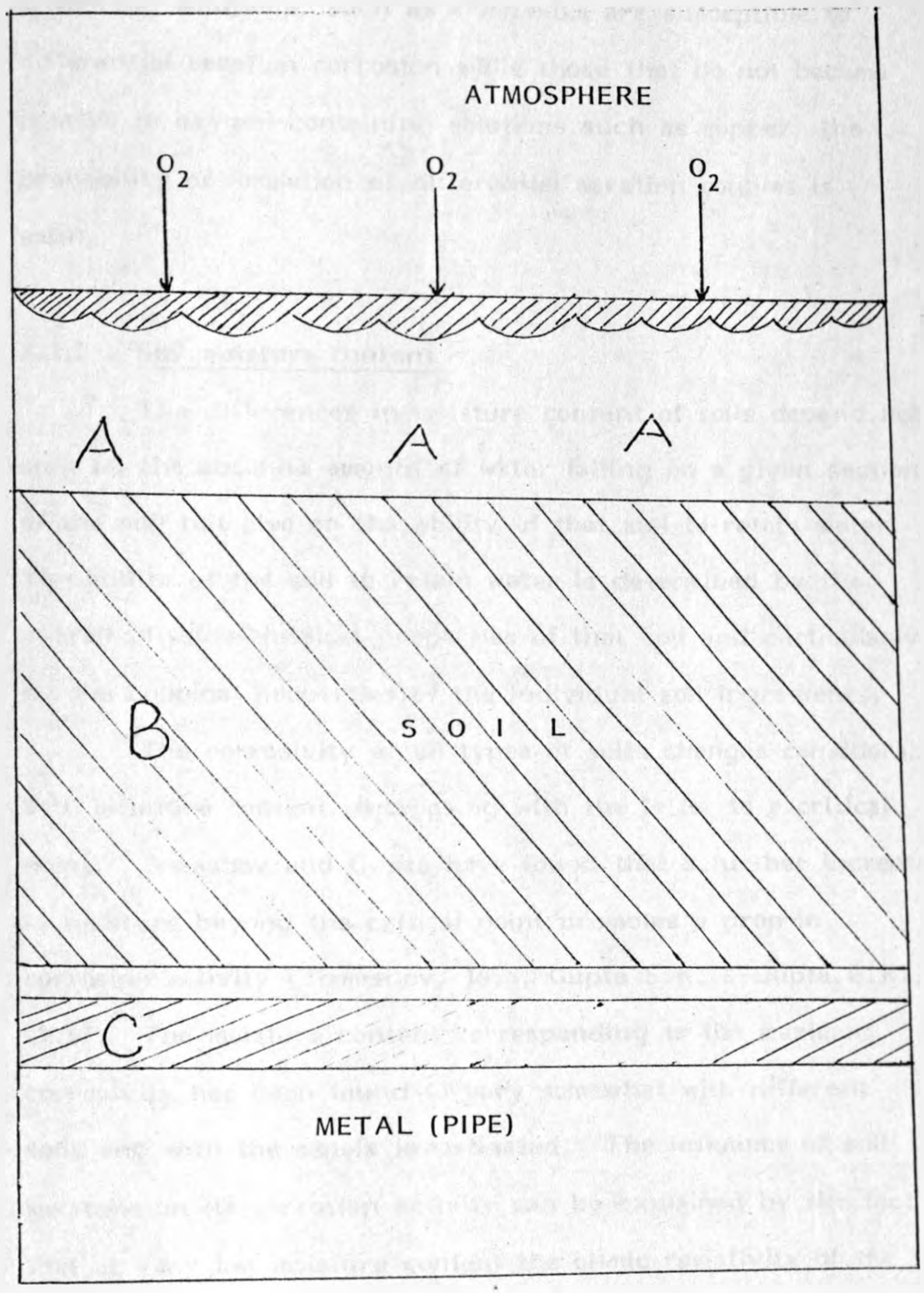

Fig. 2.4 Mechanism of oxygen transport in the soil towards the corroding metal surface (schematic).

the weight loss in the atmosphere where oxygen was readily available. Metals which are readily passive in oxygen-containing solutions, such as aluminium are susceptible to differential aeration corrosion while those that do not become passive in oxygen-containing solutions such as copper, the probability of formation of differential aeration couples is small.

2.3.2 Soil moisture content

The differences in moisture content of soils depend not only on the absolute amount of water falling on a given section of the soil but also on the ability of that soil to retain water. The ability of the soil to retain water is determined by the overall physico-chemical properties of that soil and particularly by the colloidal properties of the individual soil ingredients.

The corrosivity of all types of soils changes considerably with moisture content, increasing with the latter to a critical point. Tomashov and Gupta have found that a further increase in moisture beyond the critical point promotes a drop in corrosion activity [Tomashov, 1966; Gupta S.K. & Gupta, B.K., 1979]. The moisture content corresponding to the maximum corrosivity has been found to vary somewhat with different soils and with the metals investigated. The influence of soil moisture on its corrosion activity can be explained by the fact that at very low moisture content the ohmic resistivity of the soil is high and the anodic and cathodic processes are retarded.

At extremely high moisture content the oxygen supply needed for the cathodic depolarization is reduced resulting in decreased corrosion activity. Markovic claims that the rate of attack of unprotected iron is influenced greatly by the water content of the soil and increases from negligible value in perfectly dry soils to a maximum at a point where the soil is saturated with water [Markovic, T. 1956]. Beyond this point a sudden fall occurs to a low rate of attack when free water becomes present. Gupta et al investigating the relationship between soil resistivity, moisture content and corrosivity, have found that corrosivity of soils increases with decrease in the soil electrical resistivity up to a point when the minimum value is reached [Gupta B. and Gupta S., 1978]. At this point there is a sudden increase, followed by a decrease in the corrosivity without corresponding changes in resistivity values (Fig. 2.5). The relationship between resistivity and water content of the soil is shown in figure 2.6. The point of minimum resistivity comes much before saturation of soils with water is observed.

According to Schaschl and Marsh, the cathodic activity of oxygen is most vigorous when a soil contains 50-95% of water needed for saturation [Schaschl and Marsh, 1963].

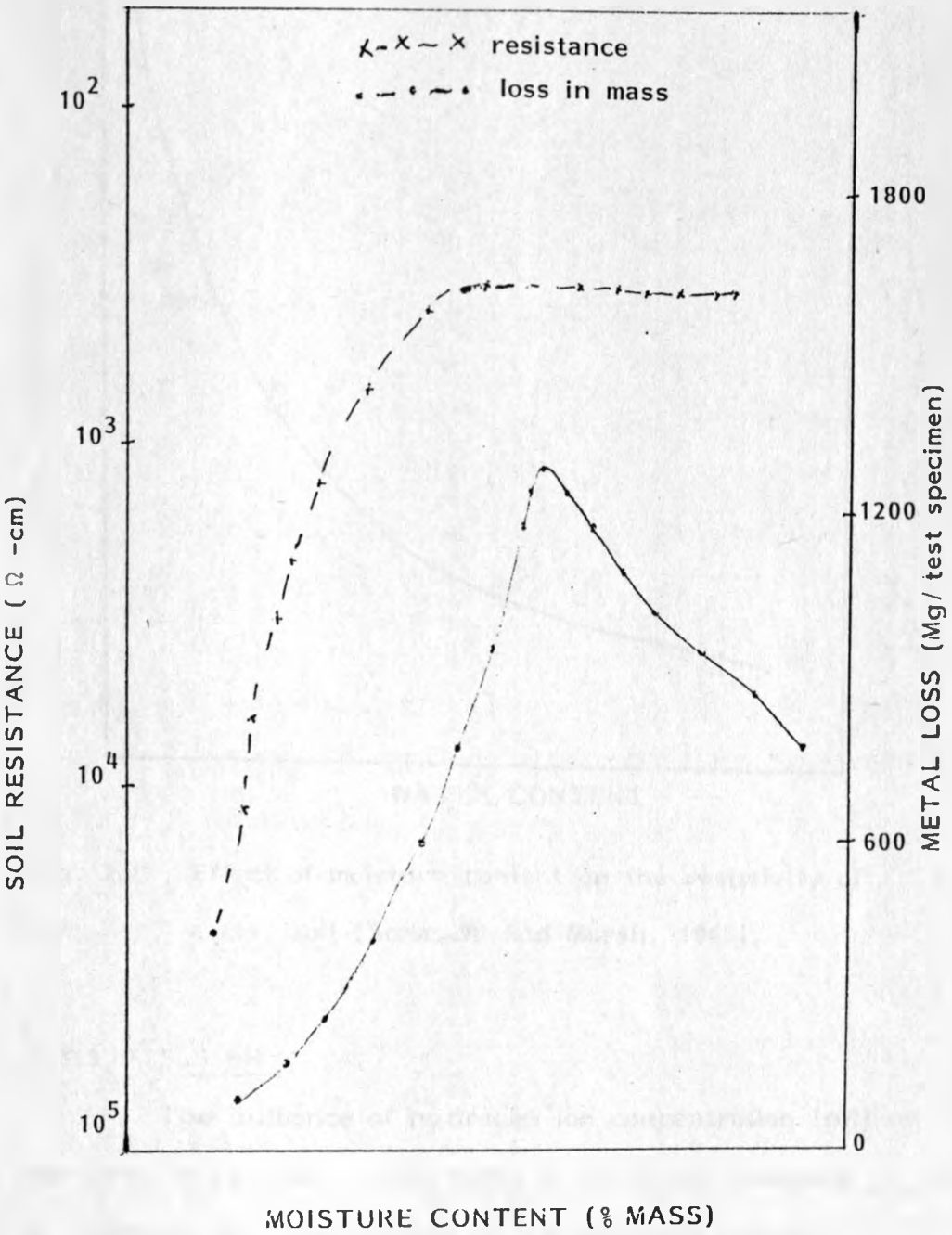

Fig. 2.5 Relationship between soil corrosivity and soil resistance at different moisture contents [Gupta and Gupta,. 1979].

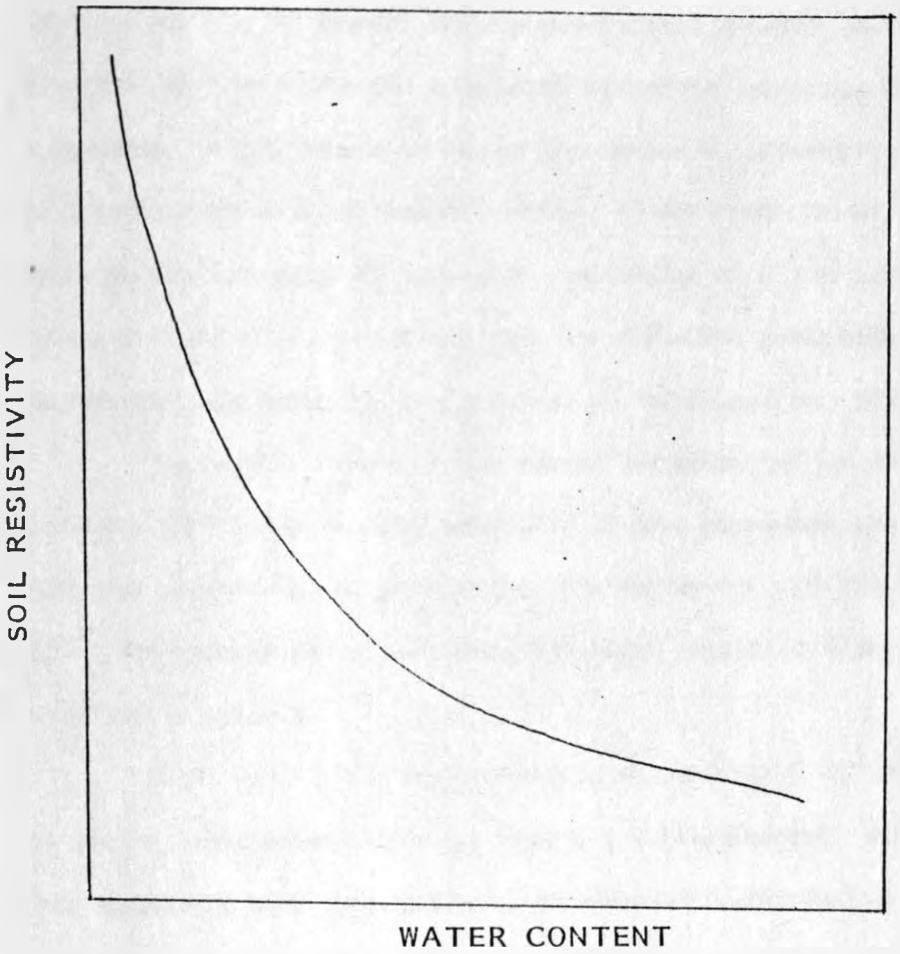

Fig. 2.6 Effect of moisture content on the resistivity of a clay soil [Schaschl and Marsh, 1963].

2.3.3 Soil pH

The influence of hydrogen ion concentration (pH) on corrosion is two fold. First there is the direct influence of hydrogen ion concentration on the electrode process. The potential of hydrogen and oxygen electrodes changes by 0.059V for every unit change in pH. Since a decrease in pH

(increasing the hydrogen ion concentration) results in the potential of the hydrogen electrode becoming more positive, a decrease in pH would enhance the cathodic processes of hydrogen and oxygen depolarization. This leads to an increase in the rate of corrosion, particularly if the corrosion process is chiefly controlled, not by diffusion processes on to the cathode but, by the process of hydrogen ion discharge.

Secondly, there is the direct influence of pH which consists of change in the solubility of the corrosion products and the possibility of protective film formation with change in pH. This depends on whether the metal oxides are soluble in acids or alkalis.

The role of pH in underground corrosion for copper is shown diagrammatically in figure 2.7 [Bondurant, 1971]. For most alloys the corrosion increases with decreasing pH of the soil. In strongly acid soils (pH<4.5), corrosion rates for some of the more resistant materials such as copper are significantly higher [Gerhoold and Cann, 1976]. Except for amphoteric metals like aluminium which are subject to higher corrosion rates in alkaline soils (fig. 2.7), most alkaline soils are less corrosive.

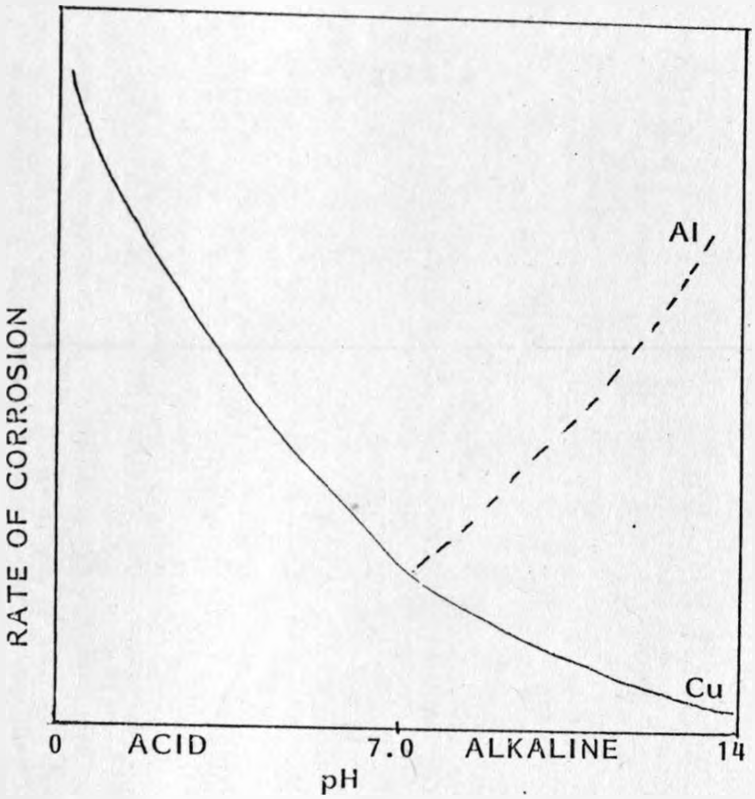

Fig. 2.7 Relationship between pH and soil corrosivity [Bondurant, 1971].

In aerated water of pH values between 4-10, the corrosion rates of iron and steel depend on the amount of dissolved oxygen in the water. Also whatever the initial pH of the solution in this range, the surface of the iron is always covered with $Fe(OH)_2$ and free hydroxyl ions which can give a cathode a pH of about 9.5. When the pH is between 4-6 iron dissolves with hydrogen gas evolution. At a further increase in pH between 10-12.6 a lowering of the corrosion rate for iron is observed, due primarily to a decrease in the solubility of the corrosion products in alkali (hydrate formation). An increase in pH above 13 however again causes an increase in corrosion rate due to the solubility of corrosion

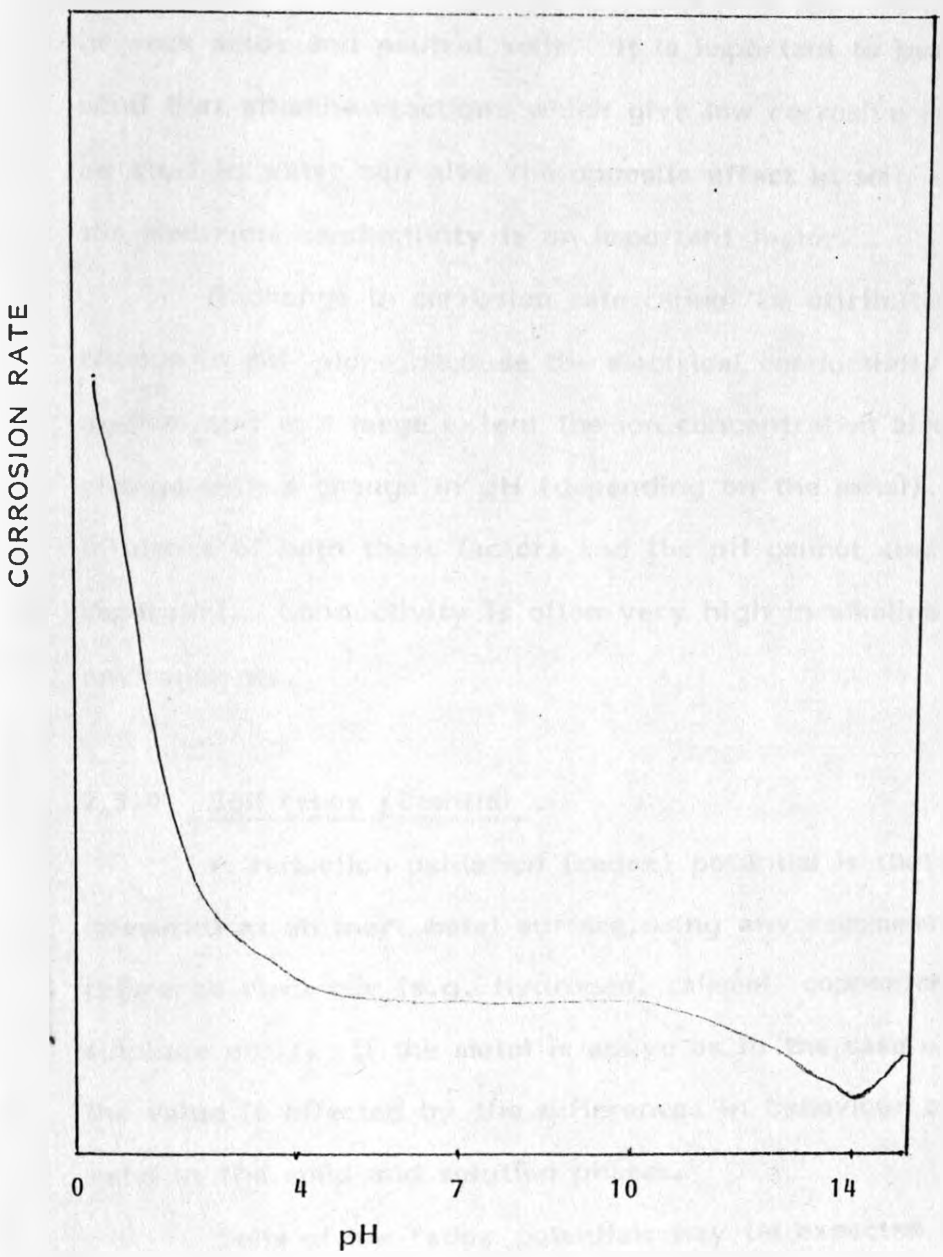

Fig. 2.8 Corrosion rate of steel in water at various pH values [Pourbaix Atlas, 1954].

products in the concentrated alkali (Fig. 2.8) [Pourbaix Atlas, 1954].

The pH value in the soil is not so serious a factor for iron and steel as it is for copper and zinc. However, steel corrodes more rapidly in acid soils (pH 3.5-4.5) than in weak acids and neutral soils. It is important to bear in mind that alkaline reactions which give low corrosive rates on steel in water can give the opposite effect in soil, where the electrical conductivity is an important factor.

A change in corrosion rate cannot be attributed to change in pH alone, because the electrical conductivity of the medium, and to a large extent the ion concentration also usually change with a change in pH (depending on the metal). The influence of both these factors and the pH cannot always be separated. Conductivity is often very high in alkaline environments.

2.3.4 Soil redox potential

A reduction-oxidation (redox) potential is that potential measured at an inert metal surface, using any recommended reference electrode (e.g. hydrogen, calomel, copper/copper sulphate etc.). If the metal is active as in the case of iron, the value is affected by the differences in behaviour of the metal in the solid and solution phases.

Soils of low redox potentials may be expected to provide a suitable environment for the proliferation of sulphate

reducing bacteria (SRB) and hence support microbiological corrosion or to provide a localized anodic zone for corrosion due to differential aeration. It should be noted that pH of the soil influences the redox potentials.

To establish the feasibility of the use of the redox potential as an index of corrosivity of a soil, Starkey and Wight measured the redox potentials in many soils along pipeline distribution systems [Starkey and Wight, 1945]. The results so obtained were correlated with severity of corrosion on the pipes and the resulting corrosion criteria derived (Table 2.1).

Redox potentials (NHE)	Corrosivity (description)
Below 100mV	Severe corrosion
100mV-200mV	Moderate corrosion
200mV-400mV	Slight corrosion
Above 400mV	Non corrosive

Table 2.1 Relationship between corrosivity and Redox potentials. Potentials corrected to pH = 7.0 [Starkey and Wight, 1945].

2.3.5 Galvanic effects of soils due to dissimilarity of soils and surface conditions and other factors

A galvanic cell results when similar metal electrodes are placed in dissimilar electrolytes. When the two electrodes are connected by a wire, an electric current will flow just as in the case with dissimilar metals. This type of galvanic cell may occur when a pipeline passes through different soils, and may result in what is called long-line currents being formed between parts of the pipe that are anodic and cathodic sites. The lower the resistance of the soils the higher the rate of corrosion. Other factors like variations in pH, salt content, and differential aeration can contribute to this galvanic cell formation (Fig. 2.9).

Dissimilarity of pipe surface conditions can also cause corrosion of pipe (Fig. 2.10). Bright pipe metal such as scratches caused by pipe wrenches and shallow threads adjacent to coupling or fitting are anodic to the pipe surface. These cells can be very active due to the unfavourable ratio of anodic to cathodic areas.

Galvanic cells may also result from repairing already corroded pipes. The newly repaired section of the pipe becomes anodic region whereas the old section becomes cathodic. Corrosion hence begins and the pipe is pitted once again (Fig. 2.11).

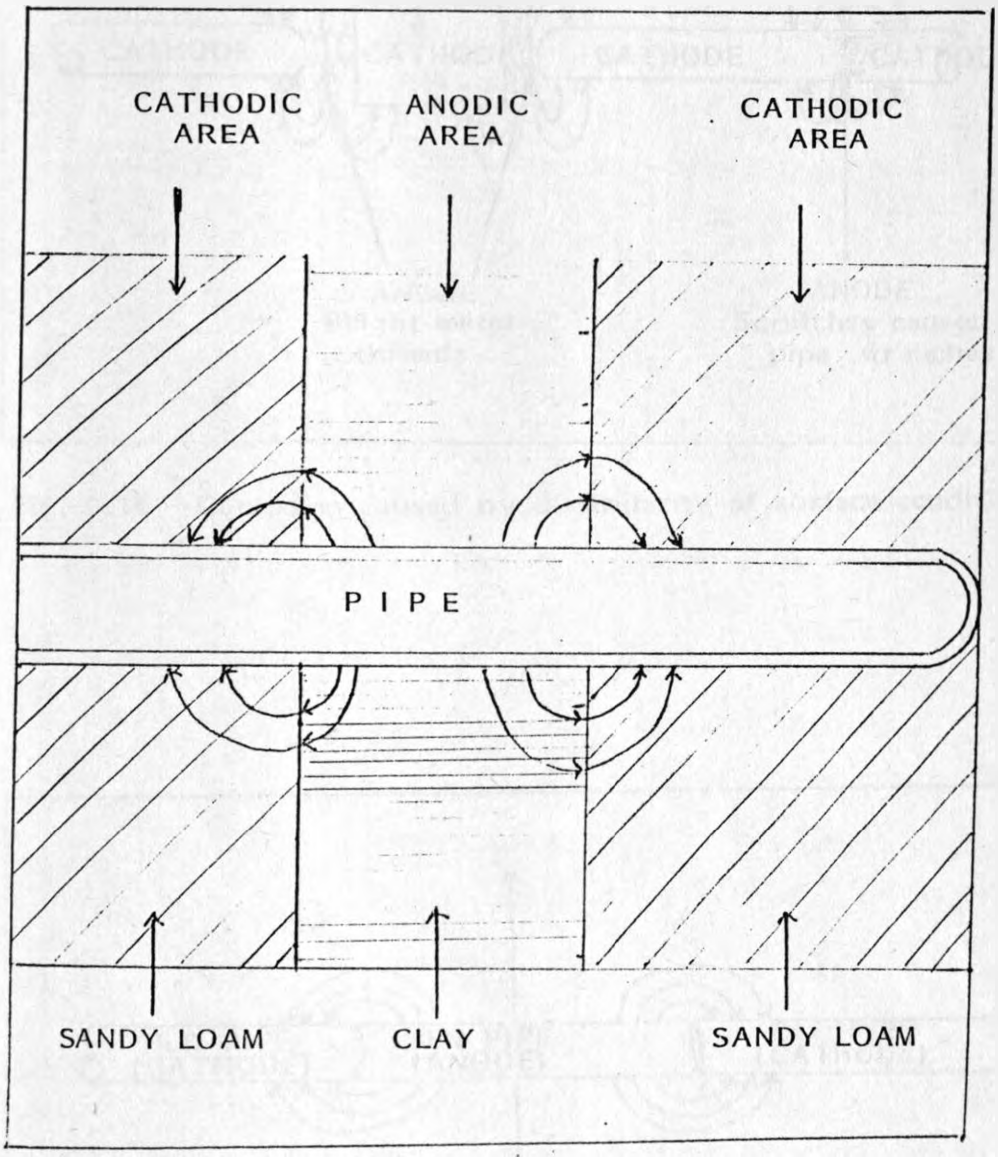

Fig. 2.9 Corrosion caused by dissimilar soils.

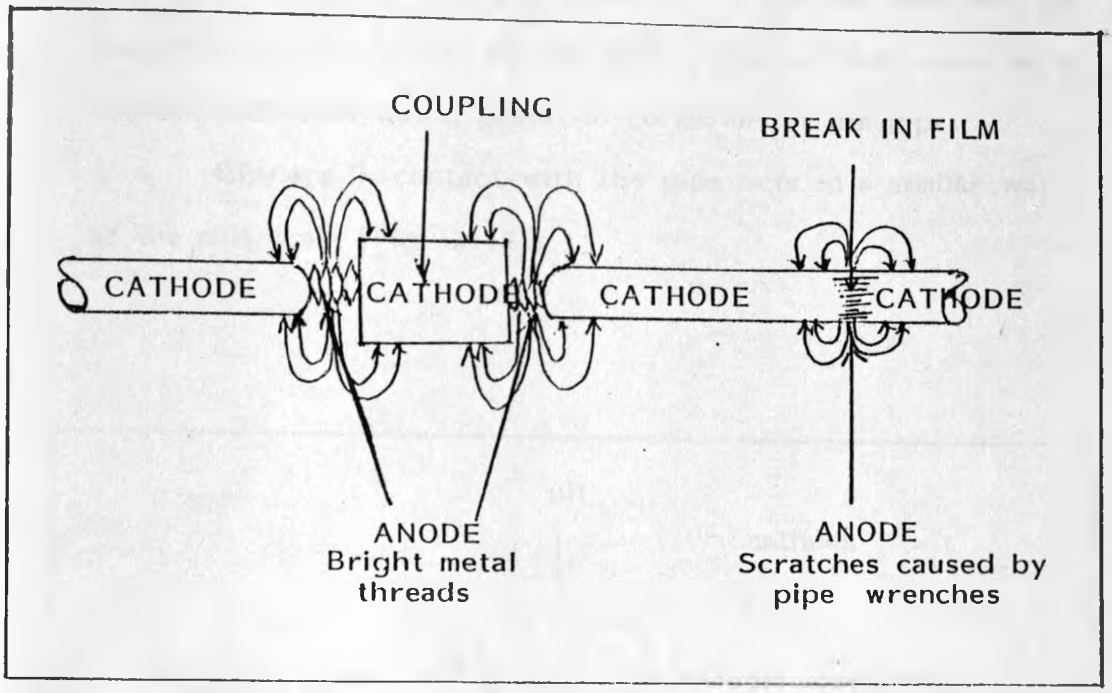

Fig. 2.10 Corrosion caused by dissimilarity of surface conditions.

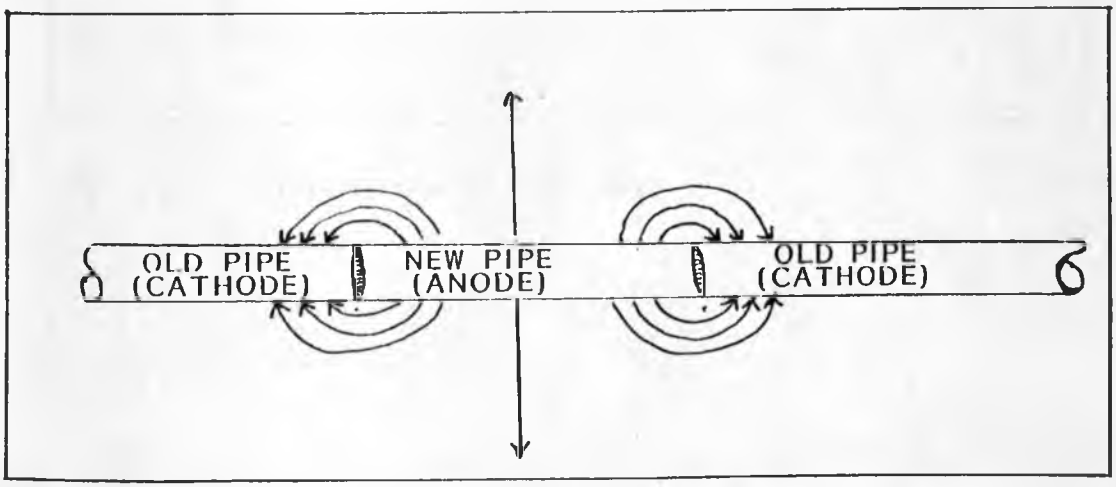

Fig. 2.11 Galvanic cell, dissimilar metals, new and old pipe.

There can also be pitting due to mill scale (Fig. 2.12). During the pipe manufacture, particles of the mill scale may be embedded on the surface of the pipe. The mill scale acts as a cathodic site that would result in corrosion of the pipe.

Cinders in contact with the pipe acts in a similar way as the mill scale (Fig. 2.13).

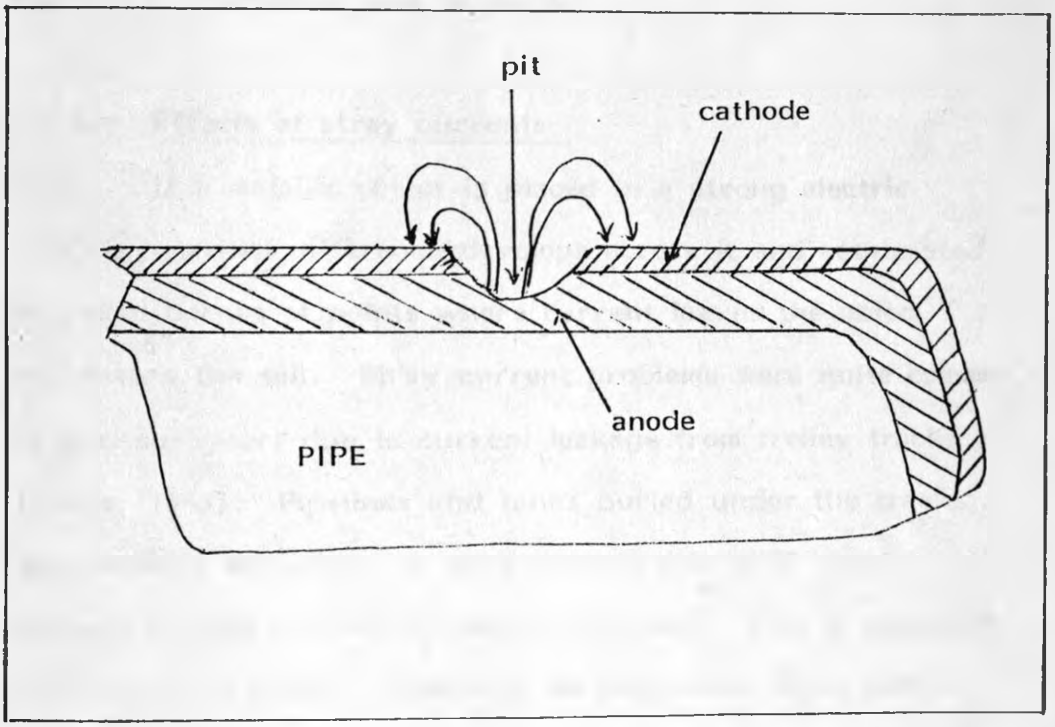

Fig. 2.12 Pitting due to mill scale.

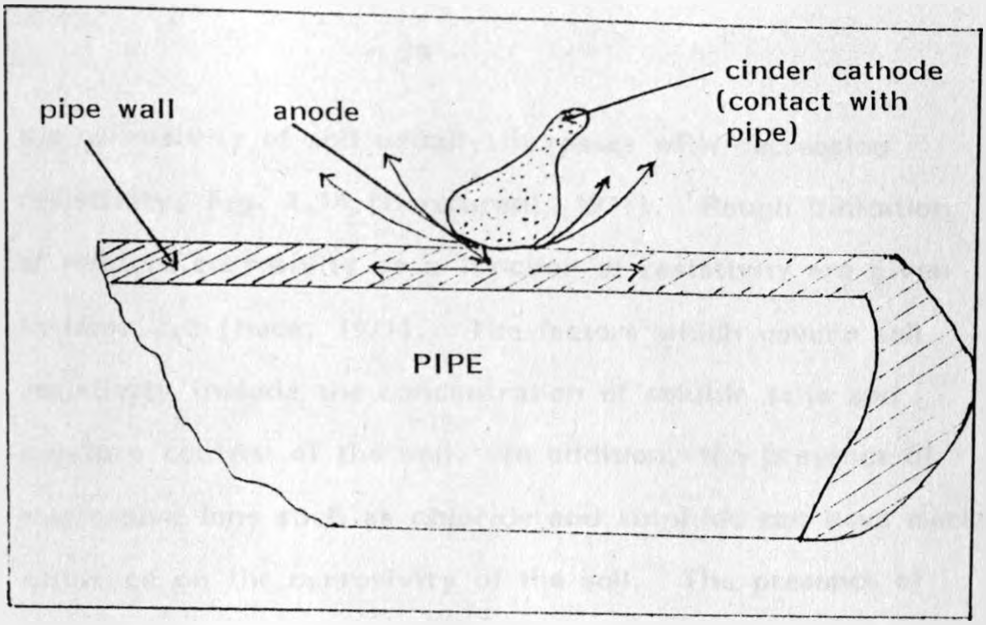

Fig. 2.13 Corrosion due to cinders.

2.3.6 Effects of stray currents

If a metallic object is placed in a strong electric field, a potential difference develops across it and accelerated corrosion occurs at points where current leaves the object and enters the soil. Stray current problems were quite common in previous years due to current leakage from trolley tracks [Evans, 1963]. Pipelines and tanks buried under the tracks were rapidly corroded. A more common source of stray current is from cathodic protection systems. This is especially pronounced in densely populated oil production fields and within industrial complexes containing numerous buried pipelines.

2.3.7 Soil electrical resistivity

Soil electrical resistivity is used as an indication of soil corrosivity. Although other factors must be considered

the corrosivity of soil usually increases with decreasing resistivity, Fig. 2.14 [Bondurant, 1971]. Rough indication of relative corrosivity as a function of resistivity are given in table 2.2 [Nace, 1971]. The factors which govern soil resistivity include the concentration of soluble salts and moisture content of the soil. In addition, the presence of aggressive ions such as chloride and sulphide can have marked influence on the corrosivity of the soil. The presence of chloride can result in localized corrosion of materials with passive films while the presence of sulphide can result in altered corrosion rate due to change in electrode process.

The latest work reported on this subject is that conducted by G.H. Booth et al at the National Physical Laboratory who sought to establish criteria for soil aggressiveness towards buried metals among them, iron [Booth,G.H., Cooper, Wakerley, 1967). The soil properties they examined for this purpose are electrical resistivity, redox potentials, water content and soluble iron contents, pH and activity of the bacteria. From their studies of 87 sites in both England and Wales, they concluded that reliable estimates of aggressiveness of soils towards buried ferrous metals can be made from measurements of its resistivity and redox potentials. Marginal cases can be solved by knowledge of water content.

Gupta et al found that soil corrosivity increases with decrease in the electrical resistivity value upto a point when minimum resistivity is reached [Gupta S. and Gupta B., 1978]. At this point there is a sudden increase followed by

a decrease in the corrosivity without corresponding values of resistivity (Fig. 2.5).

Resistivity Ω -cm	Corrosivity (description)
Below 500	Very corrosive
500 - 1000	Corrosive
1000- 2000	Moderately corrosive
2000-10,000	Mildly corrosive
Above 10,000	Progressively less corrosive

Table 2.2 Rough indication of soil corrosivity versus resistivity [Nace, 1971].

2.3.8 Salt concentrations in the soil

A change in the concentration of a soluble salt in the soil can influence the rate of corrosion. The effect of an increase in the concentration of oxidising salts is analogous to the effect of an increasing amount of oxidising inhibitor and leads (with absence of active ions) to an almost cessation of corrosion by changing to a passive state. However, this comes about if oxidising salts (such as dichromates) act principally as passivators. If however, the oxidising agent (salt) acts primarily as a cathodic depolarizer (eg persulphate), then an increase in its concentration will increase the rate of corrosion.

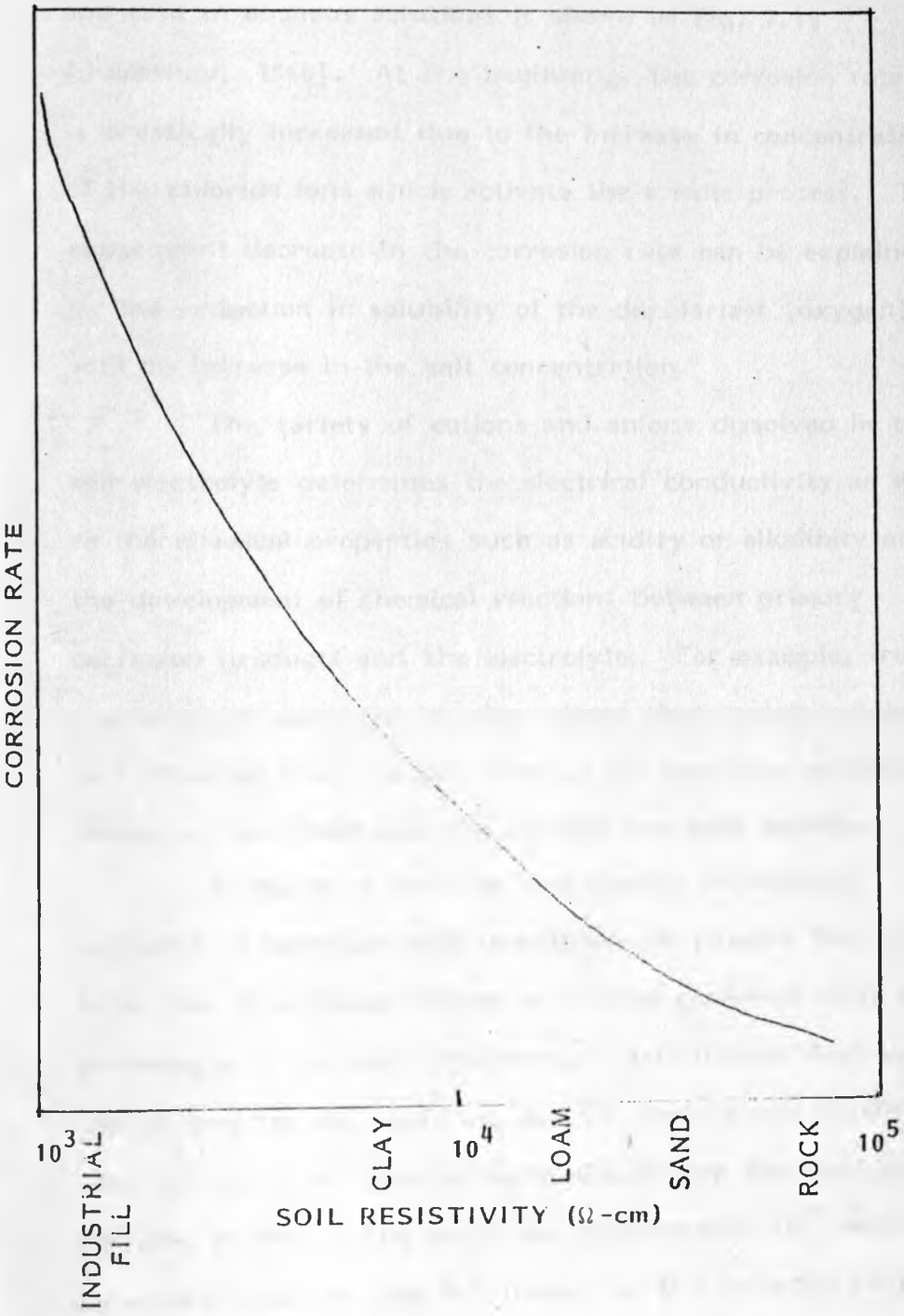

Fig. 2.14 Relationship between soil resistivity and soil corrosivity, [Bondurant, 1971].

The dependence of the rate of corrosion of iron or steel on the concentration of such salts as NaCl, KCl and LiCl in aqueous solutions is shown in Fig. 2.15 [Tomashov, 1966]. At the beginning, the corrosion rate is drastically increased due to the increase in concentration of the chloride ions which activate the anodic process. The subsequent decrease in the corrosion rate can be explained by the reduction in solubility of the depolarizer (oxygen) with an increase in the salt concentration.

The variety of cations and anions dissolved in the soil electrolyte determines the electrical conductivity as well as the chemical properties such as acidity or alkalinity and the development of chemical reactions between primary corrosion products and the electrolyte. For example, iron and steel are corroded by electrolytes that contain sulphates and chlorides from the soil because the corrosion products formed at the anode and the cathode are both soluble.

Presence of chloride ions results in localised corrosion of materials with destruction of passive films, while that of sulphide results in altered corrosion rates due to changes in electrode processes. The chloride destroys the passive film by replacing the OH^- ions of the $Fe(OH)_2$ film, by virtue of chloride being specifically adsorbed on the iron surface. The sulphides combine with Fe^{2+} ions in deaerated soils to form FeS instead of the expected $Fe(OH)_2$ film. This happens only in presence of sulphur-reducing bacteria.

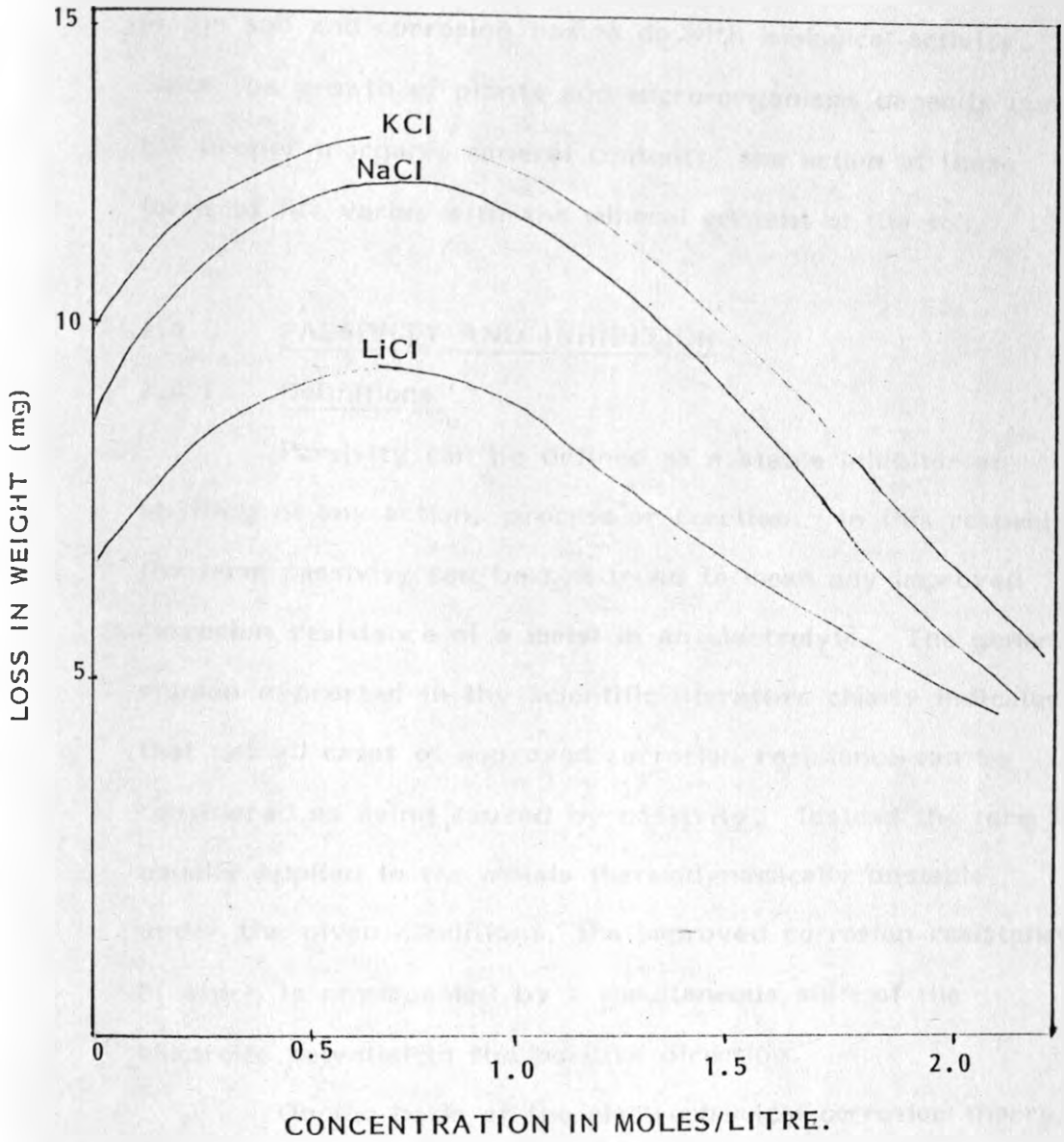

Fig. 2.15 Effect of concentration of KCl, NaCl and LiCl on the corrosion of low-carbon cold-rolled steel at 35°C [Tomashov, 1966].

Another important relationship between the salts in the soil and corrosion has to do with biological activity. Since the growth of plants and micro-organisms depends upon the proper inorganic mineral contents, the action of these forms of life varies with the mineral content of the soil.

2.4 PASSIVITY AND INHIBITION

2.4.1 Definitions

Passivity can be defined as a stable inhibitor or strifling of any action, process or reaction. In this respect the term passivity can be construed to mean any improved corrosion resistance of a metal in an electrolyte. The general opinion expressed in the scientific literature clearly indicates that not all cases of improved corrosion resistance can be considered as being caused by passivity. Instead the term is usually applied to the metals thermodynamically unstable under the given conditions, the improved corrosion resistance of which is accompanied by a simultaneous shift of the electrode potential in the positive direction.

On the basis of the electrochemical corrosion theory, Tomashov gives a rational definition of the phenomenon of passivity of metals as follows;"Passivity is a state of high corrosion resistance of metals or alloys (under conditions when their reactions are thermodynamically possible) caused by inhibition of anodic process; that is a passive state is a state of corrosion resistance caused by an increased anodic control" [Tomashov, 1966].

2.4.2 Mechanism of passivity

Many theories have been put forward to explain the mechanism of passivation, but the most fundamental and generally accepted theories are those explaining the passive state on the basis of a film or adsorption mechanism accounting for inihibition of anodic dissolution [Bockris and Reddy, 1970; Tomashov and Chernova, 1967].

The film theory of passivation explains the passive state as the appearance of a very thin, often visible protective film of products formed by the reaction of the metal with the environment. Very often this film represents some form of metallic oxide.

Another quite different view regards the essential cause of passivation as arising from the formation of a monolayer of adsorbed oxygen or oxygen which is "in" and not "on" the metal surface. In some versions of this view, the sudden fall of current characteristics of passivation is supposed to occur as a result of the presence on the surface of a much less than a monolayer of O^{2-}, OH^{-} or other anions.

The reasons of such small amounts of material being absorbed on an electrode causing such dramatic happenings are rationalised in various ways. For example, the absorbed ion may block a kink site in the dissolving metal and this may lower free energy of the initial state of the atom in its dissolution reaction. It then no longer dissolves with the former rate because dissolution has been dropped by several orders of magnitude.

2.5 POLARIZATION

2.5.1 Polarization and overpotentials

The difference between the potentials of an electrode with and without impressed current or $E_j - E_o$ (taken in this order) is called electrochemical polarization. Polarization is a measure of irreversibility and its magnitude varies with current density, temperature and the materials taking part in the reaction.

There is however a lot of dispute in the use of the term polarization. Bockris considered this as fustysism and feels that the term overpotential or overvoltage should be used [Bockris, 1970]. Wranglen defines overpotential as polarization of a definite electrode reaction such as hydrogen evolution [Wranglen, 1972]. Paul Ruetschi gives a clear distinction between overpotential and polarization. He defines overpotential as the potential between the potential at a certain rate of current density level and potential at reversible conditions for a single electrode reaction; while polarization is the difference between potential at a certain current density and the open circuit potential (E_2=0) for instance a corroding surface where one has more than one electrode reaction going on [Ruetschi, 1972].

When the practical objective is to convert chemical energy to electrical energy or vice versa, it is important to minimize polarization. In electrochemical corrosion a high degree of polarization is desirable since it slows down the rate of attack. Many corrosion control measures are aimed at

increasing the polarization of galvanic couples. The overpotential required to reduce hydrogen ion or water hydrogen gas, a process which in absence of overpotential would take place at zero volt, is of special importance. E_{NHE} overpotential can be of real advantage in some circumstances. Cations of metals such as sodium and potassium can be reduced to free metals at a mercury cathode even though their standard potentials are more negative than NHE, because the high overvoltage of H_2 on mercury prevents its liberation. At a platinum cathode, sodium and potassium cannot be reduced from aqueous solution because the potential cannot exceed that required for hydrogen liberation.

2.5.2 Types of overpotentials

Electrochemical overpotential is substantially of three different kinds:-

(a) Concentration overpotential, η_C

(b) Activation overpotential, η_A

(c) Resistance overpotential, η_R

2.5.2.1 Concentration overpotentials

Concentration overvoltage arises when concentration of positive ions in the immediate vicinity of the cathode decreases due to the deposition. It is caused by a deviation of the concentration on the electrode surface from that of the bulk of the solution. For instance, in copper refining, copper is deposited on the cathode resulting in a lower ion

concentration at the cathode than in the bulk of the solution. At the anode, copper is dissolved, resulting in a higher concentration there than in the bulk.

Without electrolysis, we have for both electrodes, $E_o = E^o + \frac{0.059}{2} \log C_o$. Where C_o = concentration in the bulk. Under electrolysis, we have for each electrode

$E_j = E^o + \frac{0.059}{2} \log C_e$, observing $C_e < C_o$ at the cathode and $C_e > C_o$ at the anode. Hence the concentration overvoltage η_c is given as

$E_j - E_o = \eta_c = \frac{0.059}{2} \log \frac{C_e}{C_o}$, which expression is negative for the cathode and positive for the anode.

The limiting current connected with concentration overvoltage is an important quantity. This is the highest current density possible for a given electrode reaction, eg. metal deposition, due to the limitation imposed by the diffusion velocity of the reacting particles. Anodic limiting current density is often an introductory step in anodic passivation. Anodic polishing is also carried out under conditions giving anodic limiting current density.

For a cathodic process the concentration overpotential is given by

$\eta_c = \frac{0.059}{2} \log \frac{C_e}{C_o} = \frac{0.059}{2} \log \left(1 - \frac{I}{I_L}\right)$ [Wranglen, 1972].

If the limiting current density I_L, for the cathode reaction is known, this equation shows how concentration overvoltage varies with the applied current.

The concentration overvoltage decreases slowly with a rise in temperature due to an increase in diffusion velocity. The concentration overvoltage is reduced by stirring, since the diffusion layer δ then becomes thinner and limiting current density I_L is increased. I_L is inversely proportional to the thickness of the diffusion boundary layer (electrode film inside which the concentration deviates from the bulk concentration).

2.5.2.2 Activation overvoltage

Whereas metal ions are transferred in a metal/ion electrode, a redox electrode involves the transfer of electrons. The hindrance of charge transfer reaction causes the formation of charge transfer overvoltage or activation overpotential. Activation overvoltage is thus caused by a slow step in the electrode process requiring an activation energy for overcoming the reaction hindrance. This activation overvoltage gives the relation between current flow and the voltage drop just across the distance between the Helmholtz plane and electrode surface, that is the so called inner electrochemical double layer.

At the redox electrode, electrons are simultaneously accepted and donated by the metal at the same surface (Fig. 2.16). The lengths of the arrows represent a measure of the magnitude of the charge crossing the phase boundary in either direction per unit area and unit time. Hence the lengths of the arrows are measures of the densities of the two currents flowing in opposite directions; that is anodic partial

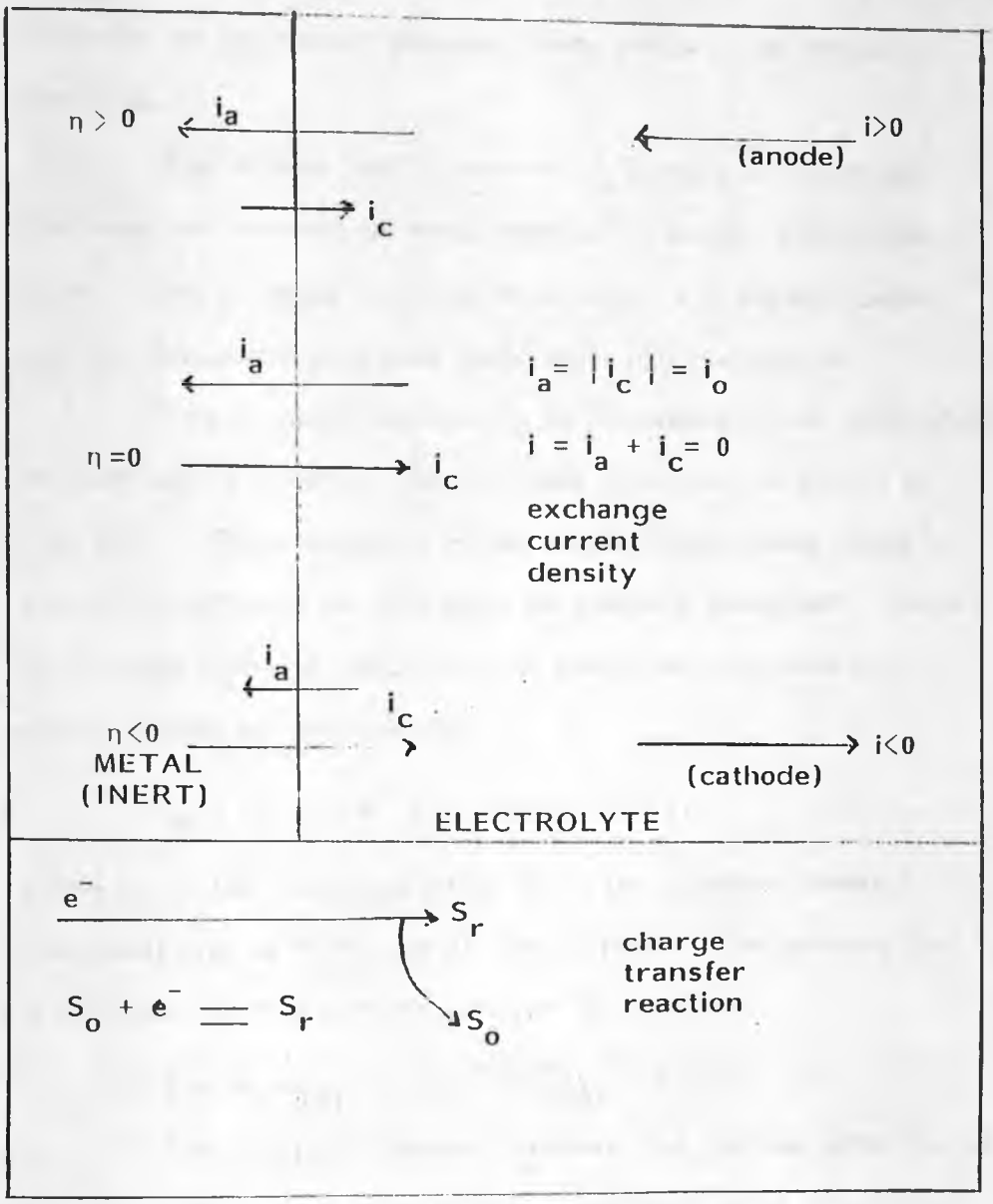

Fig. 2.16 The transfer of charge at a redox electrode.

current i_a and the cathodic partial current i_c. The charge transfer reaction taking place on a redox electrode is shown as reduced species s_r being converted into the oxidised species s_o, by donation of an electron to the inert metal electrode. This process is exemplified by the reaction $Fe^{2+}_{(aq)} \longrightarrow Fe^{3+}_{(aq)} + e^-$ (anodic direction). In the cathodic direction an equivalent process takes place in the opposite direction.

The anodic partial current i_a occurs at metal/ion electrode by transfer of metal ions M^{n+} across the double layer. This process involves rupture of the metallic bond and the formation of a new bond with the electrolyte.

The cathodic current i_c is produced by an equivalent process taking place in the opposite direction as shown in Fig. 2.17. The boundary of the metal which takes place in the electrolyte can be solvation or complex formation. Thus, the charge transfer reaction at a metal/ion electrode is characterised by the reaction

$$s_m + s_r \longrightarrow s_o \text{ [Vetter, 1967].}$$

where s_m = the adsorbed atom, s_r = the complex-forming compound and s_o = the metal-ion complex. The process is exemplified by the reaction of iron in the soil

$$Fe.xH_2O_{(s)} \longrightarrow Fe^{n+}_{(aq)} + xH_2O + ne^-$$

The relation between current and applied potential of the electrode in a charge-transfer reactions is of significant importance. It is applicable in the polarization techniques of determining the rate of corrosion of a metallic specimen.

Starting from the important Butler-Volmer equation, it can be shown that a relationship exists between current and the applied potential.

$$i = i_o \left[\exp\left(\frac{\alpha F}{RT}\eta_A\right) - \exp\left(-\frac{(1-\alpha)F}{RT}\eta_A\right)\right] \qquad (1)$$

The validity of this relationship is based on the assumption that concentrations of both the reduced and oxidized species are independent of the current density and the potential and consequently only pure charge-transfer overvoltage is involved.

For higher cathodic or anodic charge-transfer overvoltage $|\eta_A| \gg \frac{RT}{F}$, the first or second term of the Butler-Volmer equation becomes negligible depending on the sign of the current so that the following expressions are obtained for anodic and cathodic current densities:-

$$i = i_o \exp\left(\frac{\alpha F}{RT}\eta_A\right) \qquad (2)$$

for small potentials i.e. $\eta_A \ll \frac{RT}{F}$

Since $e^{x}_{x \longrightarrow o} = 1 + x$ and $e^{-x}_{x \longrightarrow o} = 1 - x$.

Hence the Butler-Volmer equation (1) becomes

$$i = i_o\left[1 + \frac{\alpha F}{RT}\eta_A - \left(1 - \frac{(1-\alpha)F}{RT}\eta_A\right)\right], \text{ as } \eta \longrightarrow o$$

$$i = i_o \frac{F}{RT}\eta_A \qquad (3)$$

From equation (3) we have

$$\eta_A / i = \frac{RT}{i_o F} = R_p \qquad (4)$$

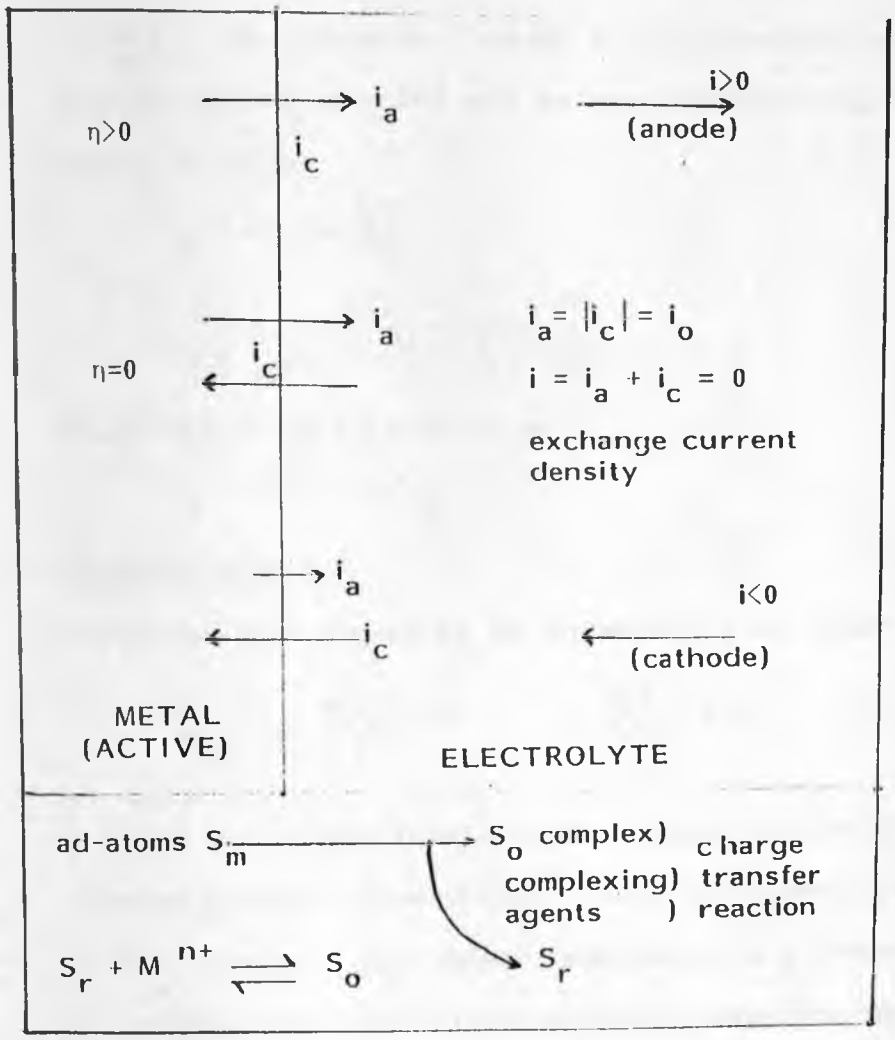

Fig. 2.17 Transfer of charge at a metal/ion electrode.

Where R_p = interfacial resistance or polarization resistance. Therefore, for very small overpotentials, there exists a linear relationship between the current density and the applied potential.

However, if the overpotentials are large, i.e. $\eta >> \frac{RT}{F}$, the relationship ceases to exist between the current and the applied potential and we have the following cases:-

Anodic direction:

$$i_a = i_o \exp \frac{\alpha F}{RT} \eta_a \qquad (5)$$

$$\eta_a = \frac{-RT \ell\eta\ i_o}{\alpha F} + \frac{RT}{\alpha F} \ell\eta\, i_a \qquad (6)$$

Equation (6) can be written as

$$\eta_a = a + b \log i_a \qquad (7)$$

Cathodic direction:

Using similar argument as for equation (5) we obtain

$$\eta_c = \frac{RT\ \ell\eta_c i_o}{(1-\alpha)\ F} - \frac{RT.\ell\eta_c i_c}{(1-\alpha)F} \qquad (8)$$

Thus at high overvoltages, a linear relationship exists between activation overvoltage η_A and the logarithm of current density. This linear relationship is a criterion for the existence of charge transfer overvoltages provided the value of charge transfer coefficient, α is taken into consideration. By extending the Tafel line to the equilibrium potential $\eta = o$, one obtains the exchange current density i_o (Fig. 2.18).

The activation overvoltage is strongly dependent on the composition of the solution, particularly its content of ions and inhibitors. It is however independent of stirring of the

solution but decreases rapidly with rising temperature, since the exchange current density i_o, increases strongly with temperature.

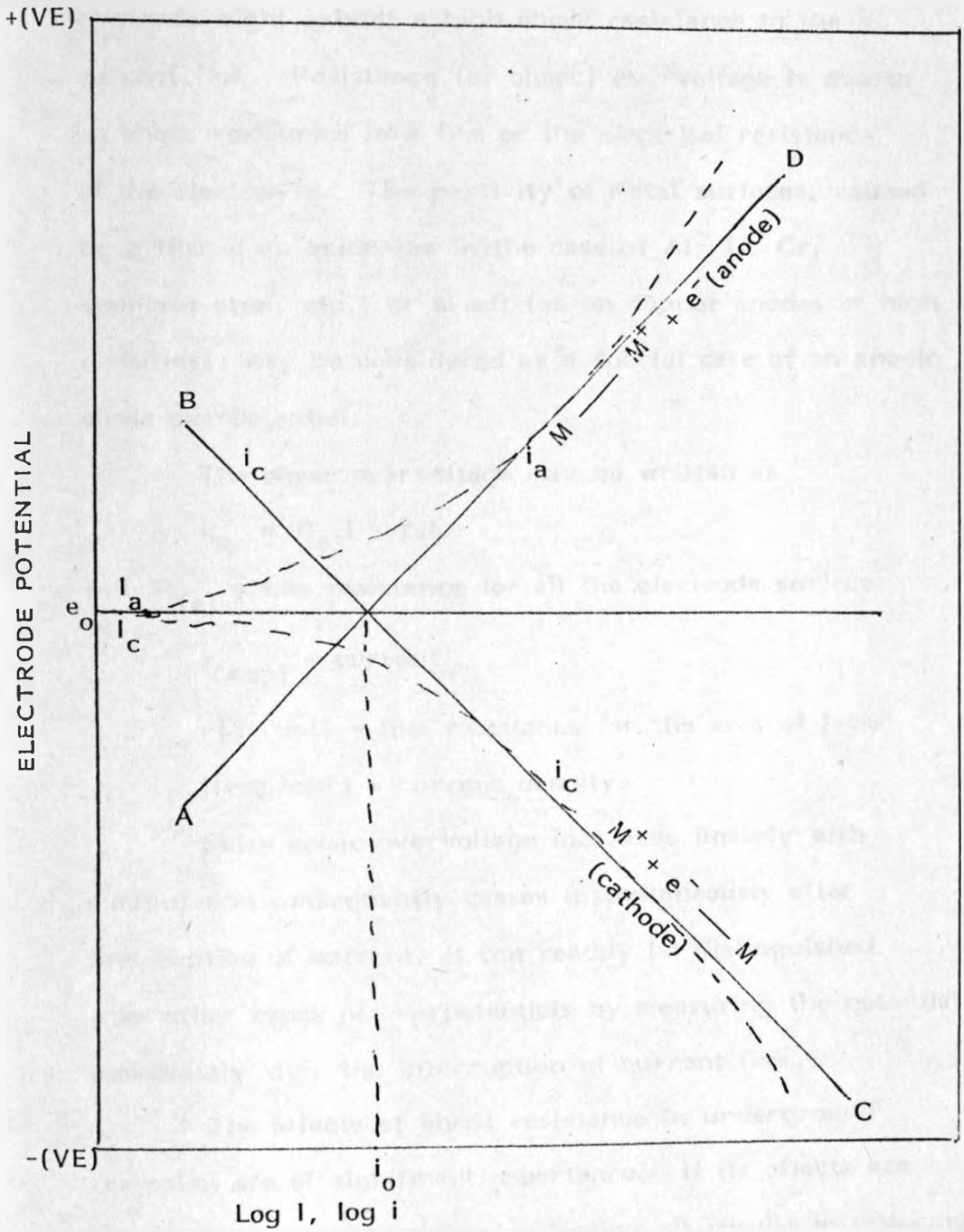

Fig. 2.18 Polarisation conditions at a non-corroding electrode.

2.5.2.3 Resistance overpotential

Most electrochemical interfaces are covered with thin oxide layers and films of relatively high resistance. Also the layer of solution in the immediate vicinity of the electrode might exhibit a high ohmic resistance to the current flow. Resistance (or ohmic) overvoltage is due to an ohmic resistance in a film or the electrical resistance of the electrolyte. The passivity of metal surfaces, caused by a film of an oxide (as in the case of Al, Ti, Cr, stainless steel, etc.) or a salt (as on copper anodes at high densities), may be considered as a special case of an anodic ohmic overpotential.

The ohmic overvoltage may be written as

$$\eta_R = R_e . I = r . i$$

with $R_{(e)}$ = film resistance for all the electrode surface

$I_{(amp)}$ = current

$r(\Omega\ cm^2)$ = film resistance for the area of 1 cm^2

$i(amp/cm^2)$ = current density.

Since ohmic overvoltage increases linearly with current and consequently ceases instantaneously after interruption of current, it can readily be distinguished from other types of overpotentials by measuring the potential immediately after the interruption of current flow.

The effects of ohmic resistance in underground corrosion are of significant importance. If its effects are not eliminated during corrosion testing, it results in reducing the corrosion current as shown in Fig. 2.19.

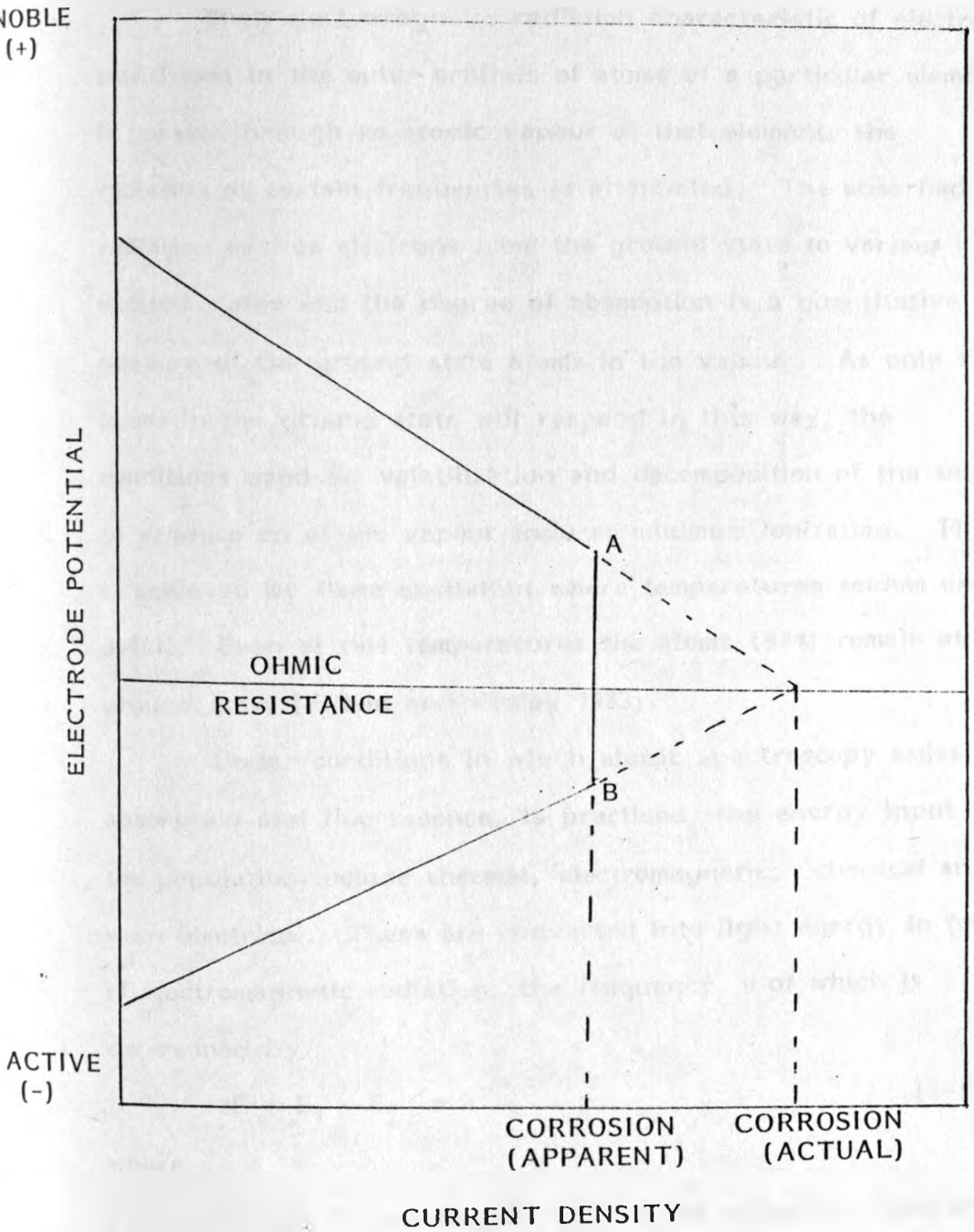

Fig. 2.19 Effect of ohmic resistance on cathodic and anodic polarization.

CHAPTER 3

ANALYTICAL TECHNIQUES

3.1 ATOMIC ABSORPTION SPECTROMETRY

3.1.1 Introduction

When electromagnetic radiation characteristic of electronic transitions in the outer orbitals of atoms of a particular element is passed through an atomic vapour of that element, the radiation at certain frequencies is attenuated. The absorbed radiation excites electrons from the ground state to various excited states and the degree of absorption is a quantitative measure of the ground state atoms in the vapour. As only the atoms in the ground state will respond in this way, the conditions used for volatilization and decomposition of the sample to produce an atomic vapour induces minimum ionization. This is achieved by flame excitation where temperatures seldom exceed 3000K. Even at this temperatures the atoms (90%) remain at the ground state [Fifield and Kealey 1983].

Under conditions in which atomic spectroscopy emission, absorption and fluorescence, is practiced, the energy input into the population include thermal, electromagnetic, chemical and even electrical. These are converted into light energy in form of electromagnetic radiation, the frequency ν of which is determined by

$$\Delta E = E_1 - E_2 = h\nu , \qquad (3\text{-}1)$$

where

E_1 and E_2 are the energies in the initial and final states respectively and h is the Planck's constant.

The absorption spectra of most elements when produced in the laboratory conditions are extremely simple. There is little possibility of coincidence of the lines and therefore very few examples of spectral interferences [Boiteux, H., 1965].

The wavelength of a resonance line is inversely proportional to its energy i.e. $\Delta E = \frac{hc}{\lambda} = h\nu$ (3-2)

The absolute amount of energy absorbed is directly dependent on the frequency and under experimental conditions one measures only the proportion of the incident energy which is absorbed.

3.1.2 Absorption and characteristic radiation

The extent to which radiation of a particular frequency is absorbed by an atomic vapour is related to the length of the path traversed and the concentration of absorbing atoms in the vapour. For a collimated monochromatic beam of radiation of incident intensity I_o passing through an atomic vapour of thickness l, the intensity of the transmitted radiation, I_ν is expressed as

$$I_\nu = I_o e^{-K_\nu l} \qquad (3-3)$$

where ν is the radiation frequency and k_ν is the corresponding absorption coefficient. The value of k_ν is determined by the concentration of atoms which can absorb at frequency ν and is given by the expression

$$\int k_\nu d_\nu = \frac{\pi e^2}{mc} N_\nu f \qquad (3-4)$$

where c is the velocity of light in m/s,

m and e represent the mass and charge of the electron, N_ν is the number of atoms per cm^3 capable of absorbing radiation of frequency ν, and f is the number of electrons per atom capable of being excited by the incident radiation. Hence, for transitions from the ground state, the integrated absorption is proportional to N_ν, which approximates to the concentration of the element in the sample [Price W.J., 1979].

3.1.3 Instrumentation

Fig. 3.1 represents a schematic diagram for a single beam atomic absorption spectrometer.

To avoid interference from emission by excited atoms in the flame and from random background emission by the flame, the output of the flame is modulated usually at 50 Hz and the detection system tuned to the same frequency.

3.1.3.1 Hollow cathode lamps

A hollow cathode lamp consists of a sealed glass envelope with a quartz end-window, containing a hollowed-out cylindrical cathode of some 2mm internal diameter, together with a tungsten wire.

The cathode is fabricated from the element to be determined. By reducing the pressure inside the envelope to about 1.3k Nm^{-2} and passing a current of 5-500 mA at an applied potential of about 300V, a low pressure discharge

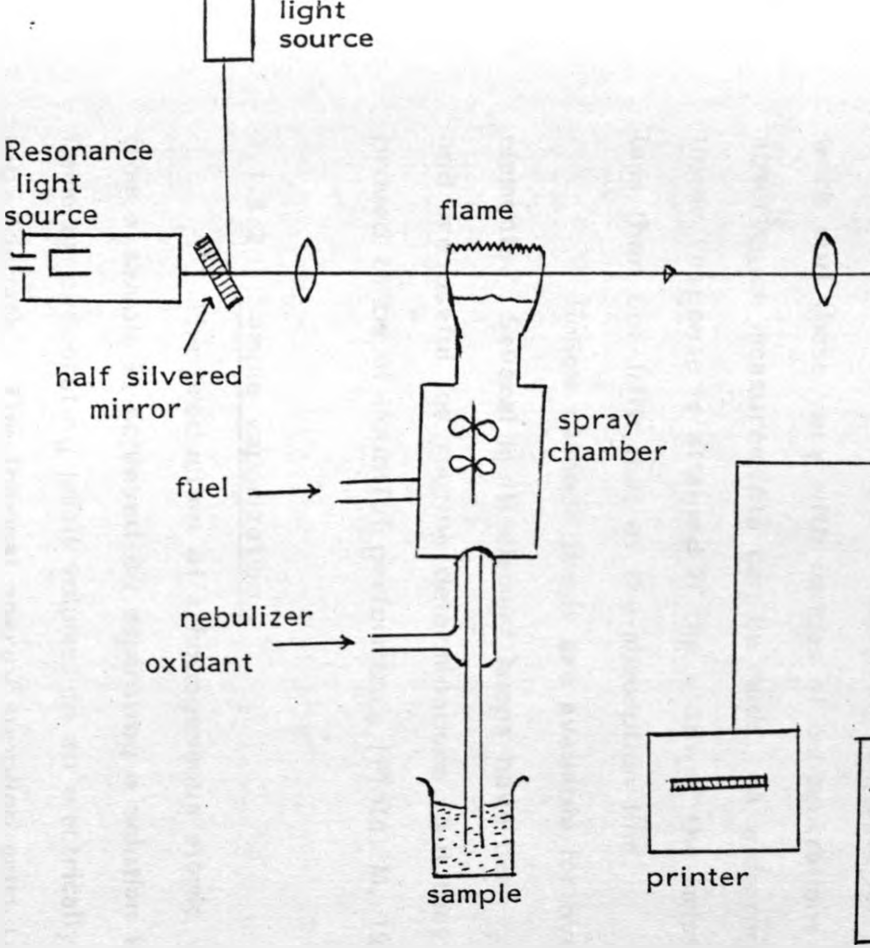

Fig. 3.1 Practical system for flame atomic absorption spectron
background corrector [M. Mariee and J. Laporte, 19

confined to the inside of the cathode and characteristic of the cathode material, is produced. The gas that fills the envelope, bombards the cathode thereby vaporising atoms from the surface. The gases commonly used in the hollow cathode are neon and argon [Russel and Walsh, 1959].

The emission spectrum of the cathode material includes a number of intense, sharp lines arising from transitions between excited states and the ground state. Only a few resonance lines per element are suitable for quantitative work and these vary with ranges of concentrations over which absorbance measurements can be made. A wide range of linear response is attained if the width of the emission line is less than one-fifth that of the absorption line.

Hollow cathode lamps are available for over sixty elements. Several multi-element lamps have been constructed and are useful for routine determinations, but they have proved to be of doubtful performance [Pinta, M. 1975].

3.1.3.2 Sample vaporization

The production of a homogeneous atomic vapour from a sample is achieved by aspirating a solution into a flame or evaporating small volumes in an electrically heated tube furnace. The thermal energy supplied must (a) evaporate the solvent and (b) dissociate the remaining solids into their constituent atoms without causing appreciable ionization.

3.1.3.3 Flame vaporization

The sample solution is drawn first into a nebulizer by the flow of support gas where it forms a mist or aerosol. Fuel gas is introduced and the mixture passed to a spray chamber where large droplets condense and run to waste.

The resulting homogeneous mixture of sample droplets and gases passes through to the burner for combustion. An equilibrium concentration of free atoms will be established in the flame. The signal in the photomultiplier varies with the concentration [Pinta M., 1969].

The burner is aligned along the optical axis of the instrument and just below the beam from the lamp so as to provide a flame of long absorption path and hence maximum sensitivity. The design of the burner coupled with the use of a separate nebulizer and spray chamber ensures the formation of a non-turbulent or laminar flame which results in stable operation of good precision, and easy choice of optimum vaporizing conditions [Pinta M., 1969].

The most generally used flame is air-acetylene, with a moderate burning velocity and a temperature of about 2,500K. The cooler air-propane and hotter nitrous oxide-acetylene flames are also used.

3.1.3.4 Quantitative measurements and interferences

Quantitative measurements may be made using a previously prepared calibration curve or by the method of standard addition. The operating conditions are first optimised

with regard to the expected concentration range of samples and linearity of response. This involves choice of appropriate resonance line, adjustment of lamp current, flame temperature, sample aspiration rate, burner alignment and monochromator slit width. The relative precision of atomic absorption measurement is good and best results are obtained where flame atomisation is used. Calibration curves invariably show curvature towards the concentration axis when absorbance exceed unity. This non-linearity is caused by unabsorbed radiation reaching the detector or when the half-width of the emission line from the lamp approaches or exceeds that of the absorption line.

Interferences in atomic absorption measurements arise from spectral, chemical and physical sources. Spectral interferences resulting from the overlap of absorption lines in rare, but broad band absorption by molecular species can lead to significant background interference. This is corrected by matrix matching of samples and standards or by use of standard addition method.

Chemical effects include stable compound formation and ionisation, both of which decrease the population of free atoms in the sample vapour and thereby lower the measured absorbance. Examples of compound formation include reactions between alkaline earth metals and oxyanions such as aluminates, silicates and phosphates, as well as formation of stable oxides of aluminium, vanadium and boron. This situation is corrected by use of releasing agents, typically strontium or lanthanum salts which themselves form stable oxysalts. Stable oxides can

sometimes be dissociated by using hotter flames. The addition of easily combusible complexing agents such as EDTA to the sample solution and use of fuel-rich flames with a low oxygen content are ways of minimising oxide formation. Ionization of sample atoms can be suppressed by adding an ionization buffer which is an easily ionizable metal such as lithium or lanthanum, in excess, particularly in the hotter flames [Pinta M., 1969].

Physical interference may result due to formation of solid solutions of one element within another. The effect of this is to modify the volatilization profile of the analyte and to make it dependent upon the matrix composition. This effect is eased by use of a releasing agent, or matrix matching methods. Variable aspiration rates due to changes in the surface tension and viscosity with solution composition can occur [Pinta 1969, Meehan 1964, Mariee and Laporte 1971].

3.1.4 Sources of error

The uncertainty in photometric measurements can conveniently be treated as arising from errors inherent in determinations at set wavelengths and those arising only in spectral scanning.

In quantitative photometric work the most generally useful indicator of errors is Beer's Law [Meehan 1964]. The evidence of failure will be the production of a non-linear curve when absorbances are plotted against concentrations, for a given wavelength. The errors generally noted are either chemical [Pinta M, 1969], instrumental [Goldring, 1953], stray

radiation [Mariee and Laporte, 1971], or pressure broadening in gases [Price W.J., 1979].

3.2 CHLORIDE ION MEASUREMENT

3.2.1 Introduction

With increasing demands on water for industrial, agricultural and domestic consumption, resources are being used more intensively than before. With each cycle of re-use, it becomes more important to check that water is sufficiently pure for the purpose for which it is intended and that the waste water returned to the common stock does not contain unacceptable levels of pollutants.

Non-specific parameters such as conductivity, pH and biological oxygen demand have largely sufficed as measures of water quality. However, the need in many circumstances for the determination of specific chemical substances is becoming more pressing.

As an analytical technique, potentiometry has the advantage of being easily adaptable to circumstances. One reason for this is the very wide range of concentrations that can be determined by the same equipment with only a minimum of procedural variations and another is the comparative ease with which measurements can be made either with battery powered instruments in the field or with automatic apparatus, for continuous monitoring inside industrial plant or in remote locations. For both applications, the robustness of many electrodes is an advantage compared with the photometric

techniques. In recent years, a wide variety of ion-selective electrodes has become available. A number of species are now commonly determined by means of such electrodes; sodium in pure water, fluoride and nitrate in potable waters, sulphide and cyanide in industrial effluents; potassium, calcium and carbon dioxide in biological fluids; chloride and ammonia in a great variety of media [Alpha, 1975].

3.2.2 Electrochemical principles

Potentiometric analysis depends on the relationship between the concentration of the determinand and the emf of an electrochemical cell in which the determinand is one of the components of an equilibrium system. The ideal relationship is the Nernst Equation

$$E = E^{\circ} + K \log c \qquad (3\text{-}5)$$

where E is the measured potential, E° is a standard emf which is constant for a given temperature, c is the concentration of the determinand, and $K = 2.303\ RT/nF$, where R is the gas constant, T the absolute temperature, F is the Faraday's constant and n is the number of electrons discharged or taken up by one mole of determinand.

3.2.2.1 Concentration and activity

The ideal relationship (3-5) is only approached as the solution approaches infinite dilution. For real solution, the relationship

$$E = E^{\circ} + K \log a \text{ , holds} \qquad (3\text{-}6)$$

where a is the activity of the species in question related to the concentration by the equation

$$a = c.f, \qquad (3\text{-}7)$$

where f is the activity coefficient.

In potentiometric analytical methods, the ionic strength is kept constant by adding to the sample an excess of indifferent electrolyte so that variations in concentrations of the determinand do not affect the activity coefficient.

The ion-selective electrodes respond only to the concentrations of the free ions in solution. The concentration c, in equations (3-5) and (3-7) refers to the free ions and does not include any associated or complex species. When an ion forms complexes and its total concentration is required, it is necessary to adjust the conditions in the sample so that the free ion is present as a constant proportion that can be related to the total.

3.2.2.2 Cell potentials and electrode potentials

Two different electrodes immersed in a solution containing species which can react at the electrode, generate a potential across the electrodes as a result of the reaction with the solution. This potential can be measured and is dependent on physico-chemical state of the electrode-solution-electrode-solution system.

The potential generated across such electrodes is given by the expression

$$E = E^{\circ} - K \log \text{(product of activities of the products)}. + K \log \text{(product of the activities of the reactants)}. \quad (3\text{-}8)$$

There is no way in which the absolute values of these electrode potentials can be determined from measurements of cell potentials and the many tabulated values are based on the convention that the standard potential of hydrogen is zero (sec. 3.7.1) [Latimer, 1952; Conway, 1952].

For concentration determination a potentiometric system uses both a reference electrode and an ion-selective electrode. This electrode arrangement is used with reference electrodes whose half-cell potentials have been characterised [Ives and Janz, 1961].

3.2.3 The electrodes

Modern ion-selective electrodes are membrane electrodes in which the current is carried by ions. The classical metallic electrodes with electronic transport are still in use for many purposes, especially as components of reference electrodes. The ion-selective electrodes have been described by Koryta [1972, 1975] and Moody and Thomas [1971].

Only a small number of metals can be used to make electrodes suitable for potentiometric analysis. Metals with negative standard potentials tend to react with water displacing hydrogen and a stable potential cannot be obtained. Some metals do not react with water because they are kinetically passive and these could be used as selective electrodes for their own ions but they have no practical application because of their susceptibility to oxidation. Amalgamating metals with mercury reduces their sensitivity to oxidation and reactivity towards water. This enables potentiometric measurements to be made in controlled conditions [Bennetto and Willmott, 1971].

If an excess of a sparingly soluble salt MpXq is added to a solution containing a concentration C mol l^{-1} of the X^{x-}, so that the solution is in equilibrium with the solid salt, the concentration of the metal ions M^{m+}, in the solution is given by the solubility product equilibrium

$$K_s = (a_m)^p (a_x)^q \qquad (3\text{-}9)$$

where a_m and a_x are the activities of M^{m+} and X^{x-} ions at equilibrium. If an electrode of metal M is immersed in the solution, its potential will be determined by a_m, which is related to a_x by the solubility product

$$E = E^{\circ}_m + \frac{K}{m} \log a_m = E^{\circ}_m + \frac{K}{p.m} \log K_s - \frac{q.K}{p.m} \log a_x . \qquad (3\text{-}10)$$

As long as there is solid M_pX_q present, the electrode potential will depend on the activity of the anion

X^{x-} and the electrode can be considered as an X-selective electrode. Equation (3-10) can be expressed as

$$E = E^{o}_{x} - \frac{K}{x} \log a_{x} \qquad (3\text{-}11)$$

where $E^{o}_{x} = E^{o}_{m} + \frac{K}{p.m} \log K_{s}$

Coating the electrode with a layer of the salt, either electrolytically or by chemical reactions provides a source of the salt and ensures that the solution near the electrode is saturated with it. Electrodes of this type include silver-silver chloride, silver-silver bromide and mercury-mercurous chloride electrodes [Midgley D., 1976].

Strong oxidising or reducing agents interfere with the electrode sensitivity because the electrodes are sensitive to redox equilibria in the same way as inert metal electrodes [Harzdolf and Keim, 1976].

The limit of detection of the electrodes is set ultimately by the solubility of the sparingly soluble salt. On immersion of the electrode, the sample solution always dissolves off the electrode so that the solubility product equilibrium is satisfied. As long as the concentration of the determinand is much greater than that gained by dissolution of the membrane, the relationship between the emf and determinand concentration is Nernstian.

In the absence of interferences, the emf in the curved part of the calibration graph may be calculated if the solubility product is known. Equation (3-11) may be written as

$$E = E^{o}_{x} - \frac{K}{x} \log fx - \frac{K}{x} \log [X]. \qquad (3\text{-}12)$$

where fx is the activity coefficient of X and [X] is the total concentration of X, which is equal to the original concentration C, of the solution and concentration arising from dissolution of the sparingly soluble salt, C_s.

3.2.4 Calibration

Except when they are applied to some titrimetric procedures, ion-selective electrodes always need some form of calibration. The relationship between the emf and the logarithm of the concentration must be found empirically. The standard potential, E°, and the calibration slope, K, in the Nernst equation

$$E = E^\circ + \frac{K}{z} \log f + \frac{K}{z} \log c, \qquad (3\text{-}13)$$

cannot be predicted with sufficient accuracy for analytical purposes, although K is generally close to the theoretical value. The activity coefficient, f, may also be difficult to predict accurately and it is generally kept constant by making measurements in a medium of constant ionic strength. An empirically determined value of E° in this medium will include activity coefficient effects and give an equation

$$E = E^\circ_{emp} + \frac{K}{z} \log C. \qquad (3\text{-}14)$$

Both E and E°_{emp} change with time and temperature. It is therefore necessary to check the value of E°_{emp} with every batch of analysis.

The best approach to calibration depends on the number of samples involved, the frequency with which the analysis is carried out, the nature of the sample and the performance of the electrode [Midgley D., 1976] (see also section 4.4).

3.2.4.1 Preparation of a permanent calibration graph [Midgley,D. 1976].

The following conditions are necessary for preparation of a permanent calibration graph:-

(1) The calibration graph should be prepared from standard solutions in conditions that are identical with those applying to the samples i.e. reagents added to the samples should also be added to the standards and the standard solutions should cover the expected concentration range of the samples.

(2) The temperature of each batch of samples must be within 1°C of the temperature at which the calibration was obtained.

(3) A precision test of the electrode should show the electrode to have no significant deviations from one batch to another.

(4) A standard solution should be introduced with each batch of samples and emf values observed with the samples should be referred to the emf observed with the standard. This procedure compensates for changes in the standard potential of the electrode.

(5) The calibration graph should be prepared with all emf values referred to in (4).

(6) A second standard solution should be analysed with each batch of samples and the results plotted in a control chart.

The results from the precision test in condition (3) can be used to form the calibration graph (fig. 3.2).

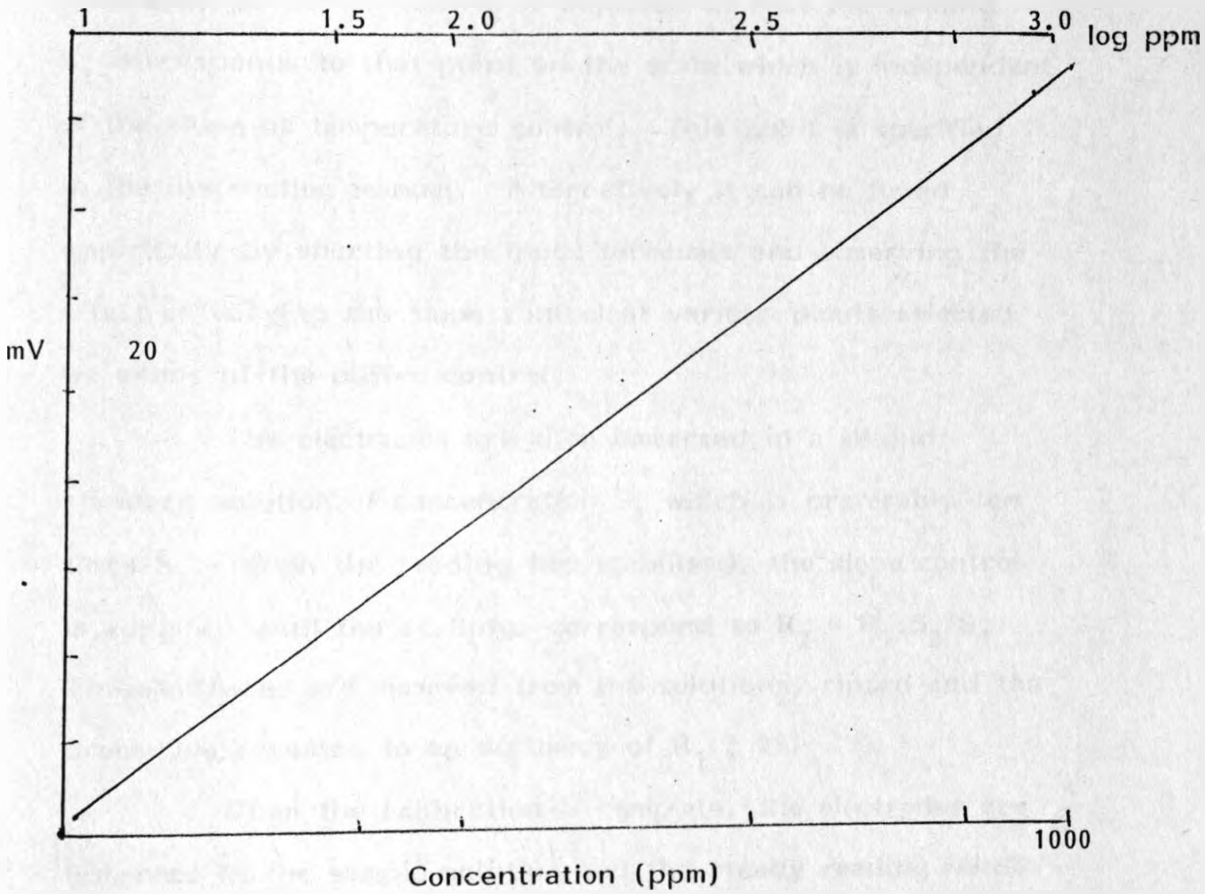

Fig. 3.2 Calibration graph for a univalent determinand [Midgley, D. 1976].

3.2.4.2 Nernstian calibration using the direct activity scale of a plon meter

Two standard solutions are used to calibrate the direct activity scale. The direct readings of concentration or activity are made from a logarithmic scale which usually spans two or three decades.

The electrodes are immersed in the first standard solution of concentration S_1. When the reading is steady the calibration or buffer control is adjusted so that the reading R_1 corresponds to that point on the scale which is independent of the slope or temperature control. This point is specified in the instruction manual. Alternatively it can be found empirically by shorting the input terminals and observing the effect of varying the slope control at various points selected by means of the buffer control.

The electrodes are then immersed in a second standard solution of concentration S_2 which is preferably ten times S_1. When the reading has stabilised, the slope control is adjusted until the readings correspond to $R_2 = R_1.S_2/S_1$. The electrodes are removed from the solutions, rinsed and the procedure repeated to an accuracy of $R_1 \pm 2\%$.

When the calibration is complete, the electrodes are immersed in the sample solution and the steady reading noted as R_x, from which the corresponding concentration can be calculated as

$$C = S_1.R_x/R_1 \qquad (3\text{-}15)$$

The reading with the first standard solution should be checked, from time to time and returned to its initial setting R_1 or S_1.

3.2.5 Sources of error

Sources of error associated with the electrode system itself usually involves faulty calibration and poor control of temperatures. The errors that originate in the sample solution are more likely to go undetected and therefore lead to an incorrect decision. If the general nature of the samples is known, it is possible to modify the procedure so as to reduce or eliminate the error.

If samples contain variable and high concentrations of background electrolyte, the ionic strength adjustment solution normally added to dilute samples may not be concentrated enough to swamp the variability of the samples and low results will be obtained. The concentration of the ionic strength adjustment solution may be increased to cope with this problem or the usual solution may be added in greater proportions. These procedures should be avoided if the determinand concentration is near the limit of response of the electrode. If the ionic strength adjustment solution contains a buffer so that it also controls the pH, the effect of the above procedures on pH control should be considered.

The presence in the sample of substances that form complexes or ion pairs with the determinand reduces the concentration of free determinand and so lowers the results. If the complex formed is weak so that the masking effect is significant only at high concentrations of the determinand, diluting the sample will remove the problem.

3.3 SULPHATE ION MEASUREMENT

3.3.1 Introduction

Most light scattering measurements were made with visual turbidimeters. An enormous variety of these exist; among the common ones are Jackson, Hellige, Dulboscq and Parr turbidimeters [Minear and Keith ,1982]. The turbidimeter generally involves a method to visually compare a turbid sample with that of some reference [Willard and Dean, 1960].

Isolated particles, whether single atoms or molecular aggregates, scatter radiation so long as their major dimension is less than 1-1½ times wavelengths. Larger particles reflect radiation. In the U.V. and visible regions of the spectrum, the scattering of these particles are those of colloidal size, i.e. from 1nm to 1μm in greater diameter.

When a beam of radiation of intensity I_o passes through a non-absorbing media that scatters light the transmitted intensity I is given by the expression

$$I = I_o \, e^{-\tau b} \qquad (3\text{-}16)$$

where τ is the turbidity and b the pathlength in the medium.

The equation can be rearranged as

$$\tau = \frac{2.303}{b} \log \frac{I_o}{I} \qquad (3\text{-}17)$$

where b is in centimeters, τ has the units of cm^{-1}. The quantities τ and I vary with concentration of the turbid sample.

Where concentrations of suspended or dissolved materials are of interest, it is sufficient to determine the intensity of scattering of the system and to read the results from calibration curves for similar systems.

3.3.2 Instrumentation

For efficient light scattering measurements, it is necessary to use sources of radiation providing high-intensity monochromatic radiation at short wavelengths. A mercury arc or laser, with appropriate filter combinations for isolating one of its emission lines is the most convenient source. However, if only a particle count or determination of concentration of a particular material is desired, a polychromatic source such as tungsten lamp is adequate. Even in this case the best results are obtained in the blue spectral region by use of a filter to block other wavelengths [Willard, Merritt and Dean, 1960].

Unless a system is unusually turbid, the intensity of scattering is small. Photomultiplier tubes are used to increase the intensity. They have the advantage of eliminating the need for an amplifier where observations are restricted to systems of moderate and high scattering power [Wells P.V. 1937; Cary and Hawes 1964; Dyre et al 1955].

Measuring the transmitted intensity allows turbidity readings over a wide range of concentrations but leads to poor sensitivity at low turbidity. It is difficult to detect the small deviations from full illuminations caused by low concentrations. Measuring the scattered light intensity gives high sensitivity at low turbidities where intensity of scattering may be compared with a dark background. However high turbidities cannot be determined by scattering because of interparticle interference. The methods are relative and data interpreted by using calibration curves.

A close control of temperature, amounts and concentrations of samples and reagents, rate of stirring and length of mixing, is essential for duplication of results. Usually, a stabilizer such as a gelatine is added to protect the colloid, to prevent coagulation beyond a certain size. Manual analyses are tedious and automatic devices have been developed for plant stream monitoring [Strobel, 1973].

3.3.3 Methods of instrumental turbidity measurement

Proper instrument operation is essential for accurate and precise turbidity measurements. A standardization material must generally possess the requirements of accuracy, stability and ease of use. Despite formazin's use as the primary calibration material, it has not been well characterised [Barnes, 1964]. The formazin suspension is very stable in its concentrated form. 4000 NTU (Normal Turbidity Units) stock suspensions retain their exact values for over one year, when

compared to freshly synthesized standards. Formazin is unstable when dilute. This instability along with the time-consuming process of continually making fresh dilutions necessitates the use of secondary standards.

Almost any type of suspension which fulfils the requirements of stability and ease of use can be used as a secondary standard. These include spherical latex and organic solvents as shown in table 3.1, as measured on a Hach 2100A.

Liquid	NTU
Carbon disulphide	1.73
Chlorobenzene	0.61
Carbon Tetrachloride	0.135
Methanol	0.061
Water	0.023

Table 3.1: Turbidities of pure liquids in NTU as measured on the Hach 2100A [Barnes, 1964].

At sufficiently high concentrations, turbidimetric measurement is in a non-linear region. The sample therefore can be diluted to a linear region and the respective measurement taken. Air bubbles in the sample should be avoided, as they often cause false high readings, especially in the low ranges. They can appear either suspended in solution or adhered to the sides of the sample cell.

3.4 REDOX POTENTIAL MEASUREMENTS

3.4.1 Introduction

Oxidation and reduction (redox) reactions play an important role in determining the behaviour of many elements in the environments. The mobilities of a large number of metals and aqueous forms of biologically important elements such as nitrogen and sulphur, are strongly dependent upon the redox potential. Sillen has referred to the redox potential as a master variable in the chemistry of the earth, oceans and atmosphere [Sillen L., 1976]. As early as 1920, Gillespie attempted to measure the redox potential of waterlogged soils [Gillespie L.T., 1920]. Zobell recognised the importance of redox potentials in marine sediments and did his pioneering work on measurements on redox potentials on that environment [Zobell, C.E. 1964]. Other investigators, Bass-Becking et al, compiled work on redox potentials measurements [Bass-Becking, Kaplan and Moor, 1960].

Properly applied, the redox potential is a very useful parameter in describing and predicting the behaviour of many elements that occur in more than one oxidation state in natural environment. Measurements of redox potential must be interpreted with full understanding of the limitations imposed by the instrument and electrode technology and the specific constraints of the system in which the measurements are made.

Chemical reactions that occur in aqueous medium can usually be characterised either by one or a combination

of the variables, redox potential E, pH and the activity of the dissolved species.

3.4.2 Theoretical framework

Every oxidation reaction is accompanied by a reduction reaction and vice versa. e.g

$$A_R \rightleftharpoons A_O + ne^- \qquad (3\text{-}18)$$

$$B_O + ne^- \rightleftharpoons B_R \qquad (3\text{-}19)$$

where the subscripts R and O refer to reduced and oxidised forms of A and B respectively.

Each of the reactions (3-18) and (3-19) is a half-cell reaction. The value of the potential of some half-cell reaction can arbitrarily be designated as zero and used as the reference half-cell reaction. By convention, hydrogen gas-hydrogen ion half-cell reaction is assigned a standard potential of zero at all temperatures. i.e.

$$H^+_{(aq)} + e^- \longrightarrow \tfrac{1}{2} H_2(g),\ E=0V \qquad (3\text{-}20)$$

The standard potential E°_R of a half-cell reaction is related to the standard Gibb's free energy ΔG°_R of the reaction by

$$E^\circ_R = -\Delta G^\circ_R/nF \qquad (3\text{-}21)$$

and to the equilibrium constant (K) of the reaction as

$$E^\circ_R = RT/nF \ln K \qquad (3\text{-}22)$$

If the reactants and products are not in their standard states, the electrode potential under experimental

conditions E_L is expressed as

$$E_L = E^\circ + \frac{2.3RT}{nF} \log \frac{a_{products}}{a_{reactants}} \qquad (3\text{-}23)$$

where a is the activity of products or reactants. Equation (3-23) can be simplified to Nernst equation

$$E_L = E^\circ + \frac{0.059}{n} \log \frac{a_{products}}{a_{reactants}} \qquad (3\text{-}24)$$

This equation expresses the thermodynamic relationship between the redox potential E_L and the solution composition for a cell without polarization.

The equilibrium redox potential for any reaction can be calculated from equation (3-24) provided that the standard potential E° for the reaction and the activities of the reactants and products are known [Clark 1960, Martell 1971].

Redox potentials can be measured electrochemically in some systems. This method has been used in the experimental determination of E°_R for reactions in which electrochemical reversibility has been demonstrated.. The redox potential is commonly expressed in volts but it is equivalent to the free energy change per mole of electrons associated with a half-cell reaction. It can then be easily expressed in terms of free energy or an electron activity, $pE = -\log a_{e^-}$ such that

$$pE = \frac{F}{2.3RT} E_L \text{ [Sille'n, 1965]} \qquad (3\text{-}25)$$

A large pE signifies a strongly oxidising system and vice versa.

3.4.3 Measurement of redox potential

The redox potential is usually measured electrometrically with an electrode pair consisting of an inert electrode with a reference electrode. The tremendous advances in solid-state electronics have made possible the development of very sensitive, accurate, and reliable electrometers for potentiometric measurements [Whitfield, 1971].

An ideal E_L electrode must be made of a material that is inert to chemical reaction in the system being measured, but must be electroactive to both reduced and oxidised species involved in the redox reaction. Because it is chemically inert, it serves only as a donor or acceptor of electrons. All of the noble metals, particularly gold and platinum as well as materials such as graphite and boron carbide have been used to make E_L electrodes [Starkey and Wight, 1945; Zobell, 1946; Ives and Janz, 1961; Back and Barnes, 1965; Hartley and Axelrod, 1968]. Electrodes made of platinum are most commonly used for redox measurements and provide the greatest reliability.

The advantage of this electrode is that the platinum surface responds to a well-behaved redox couple and, at the same time, the possibility of poisoning or attack of the platinum by other components of the system is reduced. The electrode function, however, depends upon complete equilibration between the reference solution and the system to be measured. The inherent problems associated with this type of electrode when used for redox measurements in aqueous

system has been discussed by Ben-Yaakov and Kaplan [Ben-Yaakov and Kaplan, 1973].

The ease with which electrode measurements can be made belies the complexity of the electrochemical reactions taking place in the system. The fact that redox potentials made in strongly oxidising environments are usually large and positive, whereas redox potentials made in strongly reducing environments are usually negative, have lulled some investigators into the assumption that the measured potentials represent reversible Nernst potentials. Under well-controlled conditions, this may be the case; in general, however, quantitative interpretations of the measured potentials is not possible [Bricker, 1965; Berner, 1963; Stumm, 1967; Morris and Stumm, 1967; Stumm and Morgan, 1981; Whitfield, 1974].

A brief examination of the origin of the electrode potential illustrates some of the problems associated with making electrochemically reversible electrode measurements. Consider an electrode system containing a redox couple

$$A_o + e^- \rightleftharpoons A_R \qquad (3\text{-}26)$$

When the rate of reduction of A_o to A_R is equal to the rate of oxidation of A_R to A_o, the reaction is at equilibrium, the flow of current associated with the reduction exactly counterbalances the flow of current associated with the oxidation, and the potential of the reaction is fixed.

Although the net current flow is zero, the current flow associated with either the reduction or oxidation is not zero. This unidirectional current flow is called the exchange

current and the larger the exchange current, the more stable the electrode response. If an external current is passed through the electrode, the potential is shifted from its equilibrium value, and continuous variation of the current from negative to positive or vice versa, while measuring electrode potential, defines a polarization curve for the system (fig. 3.3).

The rate of exchange of electrons at the surface of the electrode, and consequently the exchange current is directly related to the surface area of the electrode.

Major difficulties arise in the measurements of redox potential by electrode methods, particularly in natural systems. The foremost of these, is related to the characteristics of the most common elements that regulate the redox potential in the natural environments. The most abundant elements that exhibit more than one oxidation state are elements that do not generally form species which are electroactive at the surface of the platinum electrode (eg. C, O, N, S). The platinum electrode and other inert redox electrodes are usually not responsive in systems dominated by redox couples of these elements, with exception of sulphur [Berner, 1963; Boulegue and Michard, 1979].

In 1955, Merkle observed that, an inert electrode in water saturated with air did not achieve the theoretical potential predicted for the oxygen-water redox couple [Merkle, 1955]. Fig. 3.4 illustrates a schematic polarization curve for the H_2O-O_2 system. It can be seen that over a large

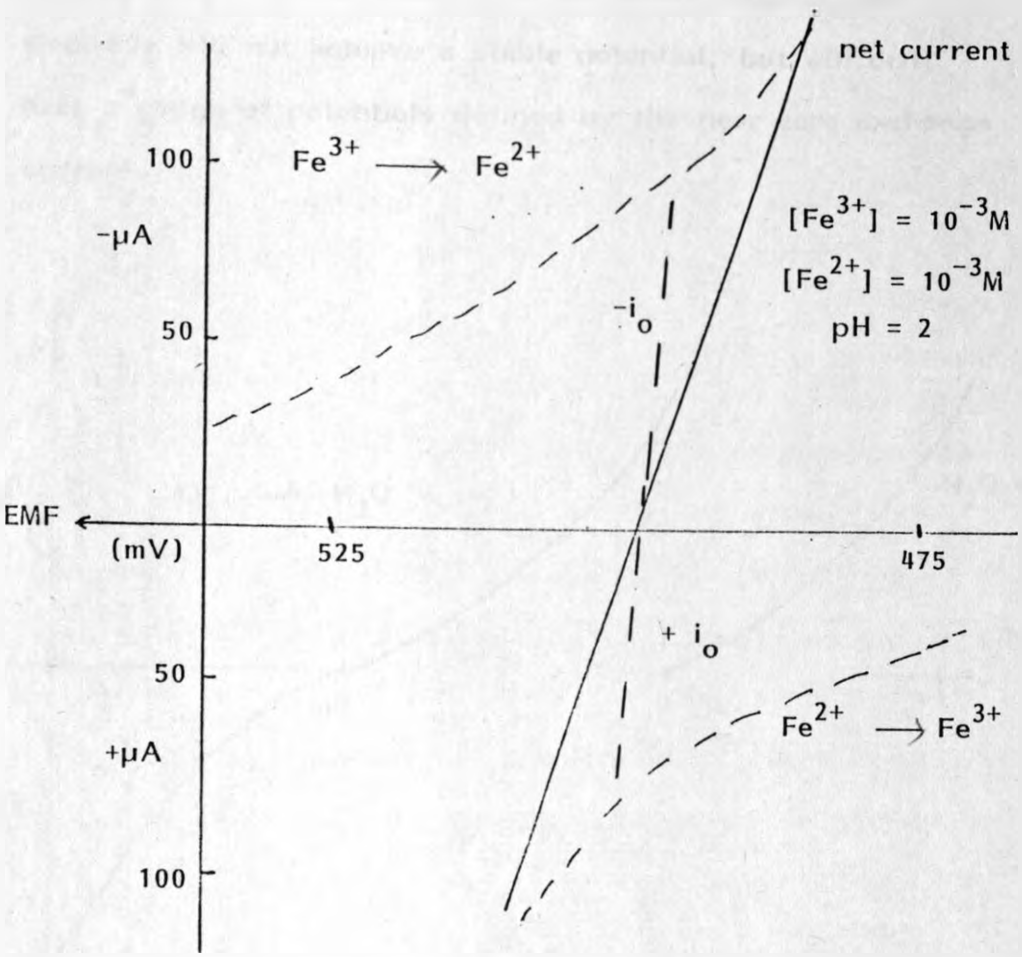

Fig. 3.3 Polarization curve for a system at a pH = 2 that contains $[Fe^{2+}] = 10^{-3}M$ and $[Fe^{3+}] = 10^{-3}M$. The solid line represents the polarization curve; lines labelled $+i_o$ and $-i_o$ represents the exchange current: lines labelled $Fe^{3+} \longrightarrow Fe^{2+}$ and $Fe^{2+} \longrightarrow Fe^{3+}$ represent the hypothetical cathodic and anodic currents [Stumm and Morgan, 1970].

range of potential, the exchange current is essentially zero. Consequently, in the absence of any other couples, the electrode will not achieve a stable potential, but will drift over a range of potentials defined by the near zero exchange current.

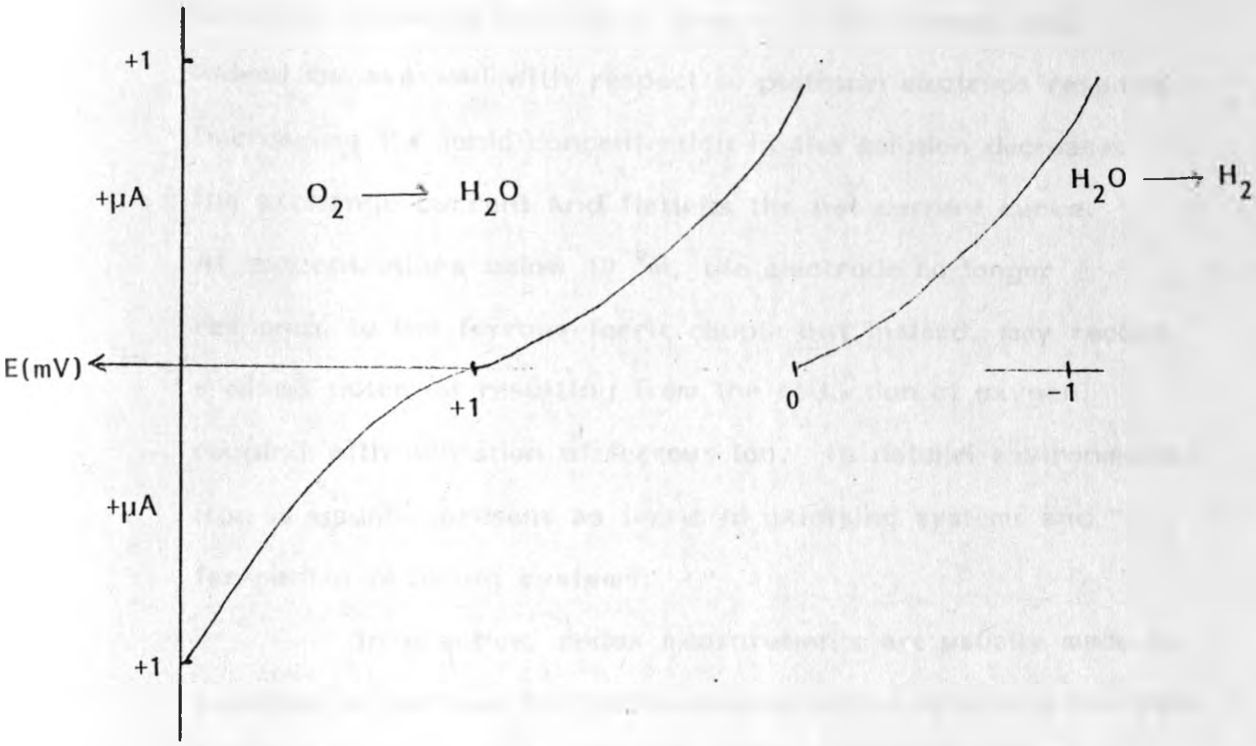

Fig. 3.4 Schematic polarization curves.

Aqueous systems containing iron and manganese are exceptions and in some environments rich in these elements, it is possible to make meaningful redox measurements [Bricker, 1965 and Nordstrom et al, 1979]. Fig. 3.3 represents an acidic system containing equimolar 10^{-3} concentrations of ferrous and ferric ions. It can be seen that the exchange current is large and this system does indeed behave well with respect to platinum electrode response. Decreasing the ionic concentration in the solution decreases the exchange current and flattens the net current curve. At concentrations below 10^{-6}M, the electrode no longer responds to the ferrous-ferric couple but instead, may record a mixed potential resulting from the reduction of oxygen coupled with oxidation of ferrous ion. In natural environments, iron is usually present as ferric in oxidising systems and ferrous in reducing systems.

In practice, redox measurements are usually made by inserting a platinum electrode coupled with a reference electrode into the system to be measured. The commonest reference electrodes used are calomel, silver-silver chloride and the standard hydrogen electrode.

The surface of the electrode must be kept clean in order to prevent deterioration of electrode response. A number of methods for cleaning have been advocated [Starkey and Wight, 1945; Callame, 1968; Ives and Janz, 1961; Edmunds, 1973].

In addition to the constraints imposed on E_L measurements by limitations of the platinum electrode (or other inert electrodes) certain precautions must be taken with the reference electrode used in the measuring system. The composition, operation and responses of reference electrodes are well detailed in text books [Zobel, 1946; Edmunds, 1973; Bates, 1964; Rock, 1967 and Nordstrom et al 1979].

3.5 CONDUCTANCE MEASUREMENT

3.5.1 Introduction

The mechanisms whereby aqueous solutions are able to conduct a current of electricity, and the various factors which affect this property of conductance, or conductivity have been actively studied by physicists and chemists for more than a century. These mechanisms can be used to make estimates of dissolved ionic concentrations based on conductivity determinations.

The specific conductance of a solution can be measured if it is introduced into a cell between two parallel plates exactly one centimeter apart, each being 1 cm^2 in area, by measuring the electrical resistance between the plates and taking its reciprocal at accurately known temperature (see section 4). The measured conductivity is expressed as

$$K = d/aR \qquad (3\text{-}27)$$

where d is the distance between the plates, in centimeters, a, the area of each plate in cm^2 and R, the measured resistance

in ohms. Solution conductivity increases with increasing temperature.

The equivalent conductance of a solute is the conductance of one gram equivalent of the material dissolved in water, and is represented as Λ, defined as follows

$$\Lambda = 1000\ K/C \qquad (3\text{-}28)$$

where K is the specific conductance, and C is the concentration of the salt in gram equivalent per litre. As the concentration decreases, the value of the equivalent conductance increases towards a limiting value, called equivalent conductance at infinite dilution.

3.5.2 Techniques and instruments

Use of electrical conductivity determinations within disciplines of natural water chemistry, studies of wastewater and pollution, and of water supply development and utilization began before the end of the 19th century [Whitney and Means, 1897; Romanoff, 1957]. The technique was adopted for analysis of soil extracts and other waters of interest in soils. At first, the conductivity measurements were used as a tool for calculating soluble salts percentages in soils.

Conductance measurements require suitable cell into which the sample is introduced for measurement, an electric power source, a resistance measuring device, usually a wheatstone bridge and a temperature compensation device.

3.5.2.1 Conductivity cells

In the design of conductivity cells, the following points are put into consideration:-

(a) Electrodes must be made of a metal that conducts electricity well and will not be chemically attacked by solutions.

(b) The electrodes should be mounted in a material that is chemically, mechanically and thermally stable.

(c) The portion of solution through which the current passes should have the same dimensions, effectively, whether the conductance of the solution is high or low.

(d) The solution should not be in motion when the measurement is made.

(e) The cell constant should be appropriate for the range of conductivities to be measured.

Platinum has been the preferred material for conductivity measurements because it is relatively inert and has a desirable electrical-thermal behaviour.

3.5.2.2 Compensation for temperature effects

The standard temperature for conductivity data is generally 25°C. A measurement made at any other temperature must be adjusted for temperature effects if it is to be compared with other measurements. The correction

is minimised by keeping the temperature of the solution, sample cell, and instrument the same and as near to 25°C as possible, by use of a constant-temperature bath.

Portable conductivity bridges and on-site units used for field measurements generally provide for temperature compensation. This is achieved by adding to the circuit, a resistor network whose effective resistance can be varied in a similar fashion to the anticipated temperature effect on the water samples to be tested. This variation can be done manually, using a variable resistor that is calibrated in terms of temperature, or it can be automated using a thermistor in the conductivity cell to provide a signal that can be interpreted in terms of temperature.

The temperature coefficient of resistance of solutions is not a constant. For solutions of mixed electrolytes it cannot be measured accurately for any substantial range of temperatures and concentration. Unless the solutions being tested are always similar in composition, a constant value for the coefficient should not be used, and automated or manual temperature compensation probably will introduce a significant error in the readings. Some natural solutions, such as sea water and soil extracts, have a composition dominated by several ions over a wide range of concentrations. Waters of some rivers and underground basins will have relatively consistent ionic composition, with variations in total concentrations that are not large enough to present serious problems in using

constant temperature-correction coefficient.

3.5.2.3 Types of measuring instruments

The standard technique for measurement of conductivity uses precisely known variable resistance which is balanced against the resistance of the conductivity cell filled with the sample being tested.

The electrical characteristics such as capacitance and impedance of the cells are taken into account during the equipment design [Wershaw and Goldberg, 1965].

A bipolar technique, used by Johnson and Enke determines the resistance by means of the current to voltage ratio, and offers advantage in design of measuring circuits [Johnson and Enke, 1970]. Another type of measuring device uses the dielectric property of the solution which is contained in a cell having two external electrodes with a high-frequency alternating-current power source. This form of conductivity measurement is useful for titrations or other operations where contact between solution and electrode would not be desirable.

3.5.3 Conductivity range of natural waters

From the limiting conductances of H^+ and OH^-, the specific conductance for pure water at pH 7.0 can be calculated as 0.05 µs/cm. In practice, it is difficult to maintain a conductance below 1.0 µs/cm in distilled water

owing to solution container-wall material and atmospheric gases [Feth et al, 1964]. Snow and rain-water may have specific conductances below 5 μs/cm in some areas where air pollution effects are minimal. Where rocks are more soluble, or solute concentrations are increased by evaporation, much higher levels are attainable, reaching tens or hundreds of thousands of microsiemens per centimeter in extreme instances.

3.5.4 Conductivity-dissolved ion relationship

The correlation between concentrations, in equivalents per litre, and specific conductances for solutions of single salts is shown graphically in fig. 3.5. For most salts, the relationship is nearly a straight line upto concentrations of 50m eq/l and except for KCl and $MgSO_4$, the concentrations multiplied by 100 would give a number rather closely approximating the specific conductance in microsiemens per cm at 25°C [Harned and Owen, 1958].

Specific conductance measurements are easy to perform and are therefore widely used in electrochemistry. Basically, electrical conductivity is a physical property, rather than a chemical property, that assists in determination of concentration of an electrolyte solution. It determines the extent to which an environment can conduct electricity and how this conduction of electricity affects the lifetime of buried pipelines, in terms of corrosion.

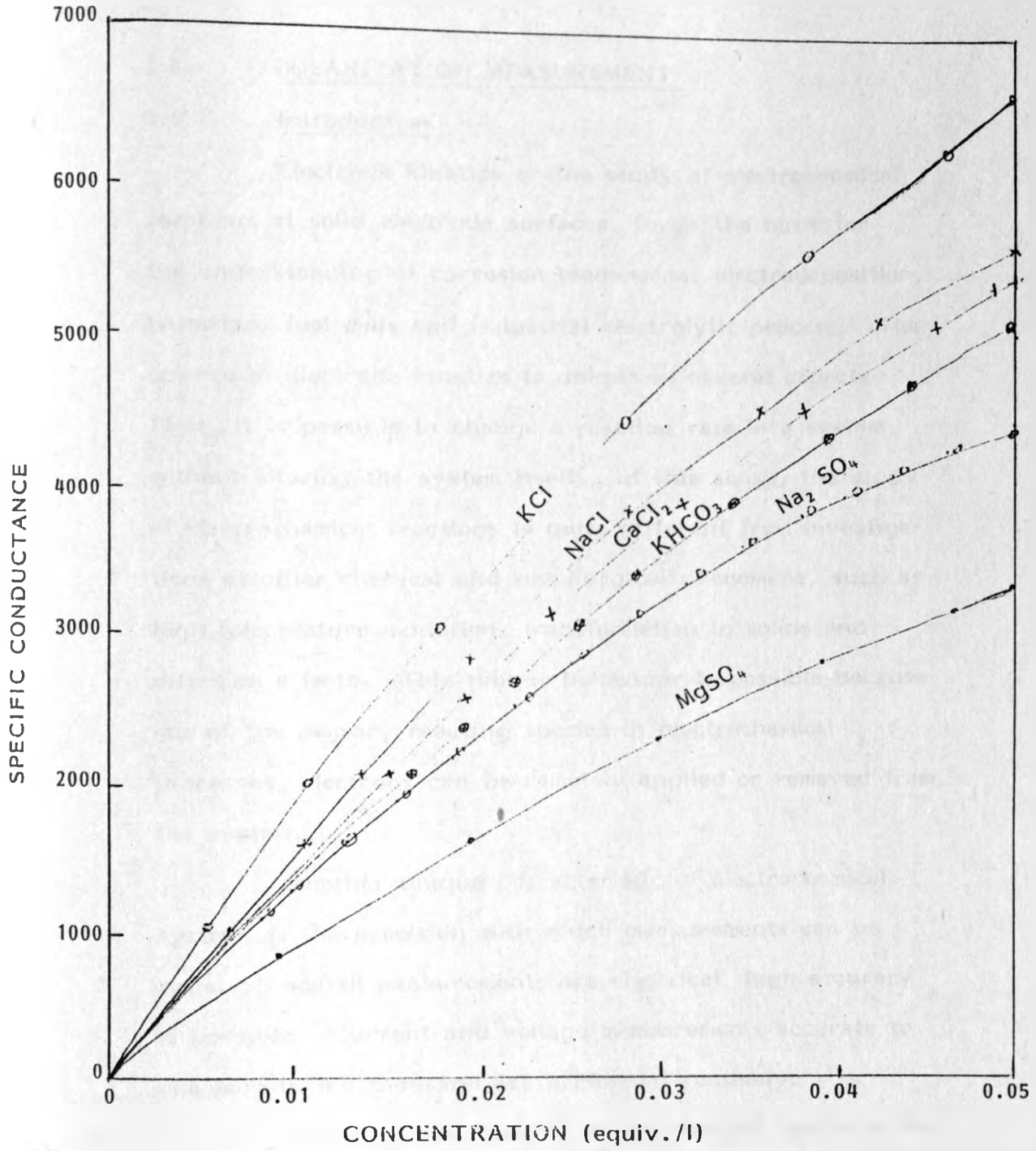

Fig. 3.5 Specific conductance of solutions of single salts at 25°C at various concentrations, in equivalent per litre [Harned and Owen, 1958].

3.6 POLARIZATION MEASUREMENT

3.6.1 Introduction

Electrode kinetics or the study of electrochemical reactions at solid electrode surfaces, forms the basis for the understanding of corrosion phenomena, electrodeposition, batteries, fuel cells and industrial electrolytic process. The science of electrode kinetics is unique in several aspects. First, it is possible to change a reaction rate in a system without altering the system itself. In this sense, the study of electrochemical reactions is quite different from investigations of other chemical and metallurgical phenomena, such as high temperature oxidation, transformation in solids and diffusion effects. This unique behaviour is possible because one of the primary reacting species in electrochemical processes, electrons can be remotely applied or removed from the system.

Another unique characteristic of electrochemical systems is the precision with which measurements can be made. Since all measurements are electrical, high accuracy is possible. Current and voltage measurements accurate to one part in ten thousand are performed routinely.

Although the study of electrochemical reactions has several unique advantages, there are certain major problems connected with this field. First, although it is the usual electrical quantities of voltage and current which are measured, the peculiar characteristics of electrochemical systems necessitate the use of highly specialised procedures for

measuring these parameters. Electrochemical systems are usually very complex. They involve a solid electrode and an electrolyte. Alterations in either electrode or electrolyte may have a pronounced effect on the behaviour of the system. Because of this complexity, the validity of analysis made from electrochemical measurements is largely dependent on how much is known about the system and the reactions which are occurring.

3.6.2 Standard polarization cell

There have been numerous polarization cells described in the literature, ranging from simple rubber-stoppered beakers to highly complex glassware assemblies. Although all of these are useful, many of them lack versitility due to the necessity of using specially shaped electrodes, lack of atmosphere control, the presence of contaminating substances such as rubber, and the inability to perform measurements at elevated temperatures.

The standard polarization cell is designed to incorporate the advantages of other polarization cells while avoiding many of their limitations. For example it can be used to study electrochemical behaviour in any media with the exceptions of concentrated caustic and hydrofluoric acid, it can be used over the temperature range of zero to over 200°C, without difficulty and it can be readily modified for a variety of electrode sizes and shapes [Stern, 1955].

The cell is a modified, multinecked, one litre round bottomed flask. The salt-bridge assembly projecting from the

left, leads to a beaker containing a saturated calomel reference electrode. There are also two auxiliary electrodes and a working electrode together with the Luggin-Haber probe tip. The multiple necks are used to introduce electrodes, gas inlet tube, thermometer and other accessories. The working electrode is mounted through an eccentric adapter, and the Luggin probe enters the cell through a clamped, ball and socket joint. The two auxiliary electrodes are used to maintain uniform current distribution within the cell. Fig. 3.6.

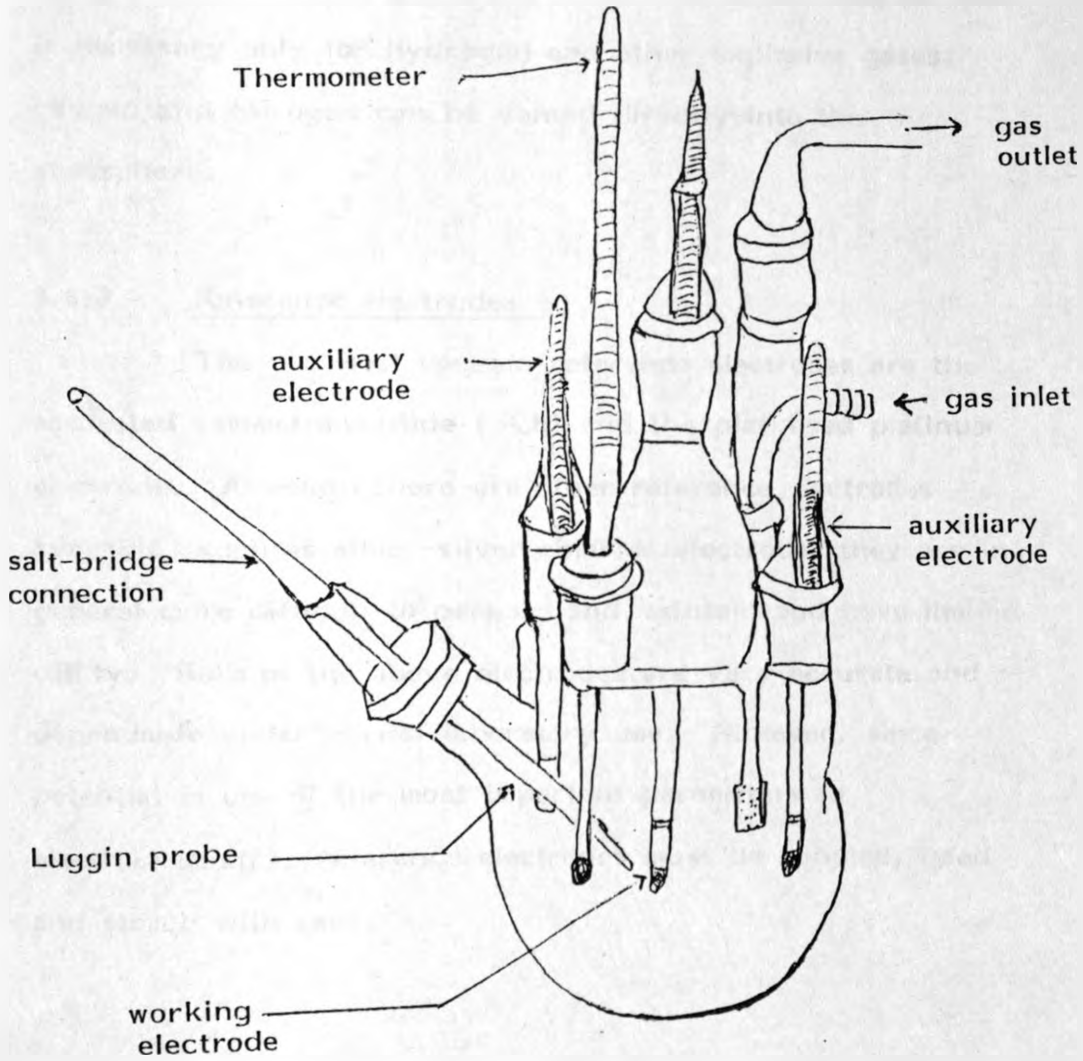

Fig. 3.6 Standard Polarization Cell (Schematic).

A quartz fibre is fused into one end of the probe to provide a slow leak, liquid junction to the calomel reference electrode. The probe tip is not sealed in this fashion to facilitate cleaning after use. The probe is filled with the cell electrolyte through the ground glass joints which are then sealed with standard taper joints [Stern and Makrides, 1955].

Cell atmosphere is controlled by the gas inlet and outlet adapter tubes. The desired gas is admitted continuously through the inlet tube and dispersed throughout the solution by means of a fritted glass cylinder. The outlet adapter tube is necessary only for hydrogen and other explosive gases, oxygen and nitrogen can be vented directly into the atmosphere.

3.6.3 Reference electrodes

The two most common reference electrodes are the saturated calomel electrode (SCE) and the platinised platinum electrode. Although there are other reference electrodes available, such as silver-silver chloride electrode, they are in general more difficult to prepare and maintain and have limited utility. Both of the above electrodes are very accurate and dependable under normal laboratory use. However, since potential is one of the most important parameters in electrochemistry, reference electrodes must be handled, used and stored with care.

3.6.3.1 Saturated calomel electrode (SCE)

This electrode is not poisoned or contaminated and is insensitive to electrolyte composition because of its design. The electrode is virtually spill-proof and very rugged. Electrical contact with the electrolyte is maintained by the small capillary at the tip of the electrode body. Cells are filled with saturated potassium chloride solution and the calomel element must not be allowed to dry. To ensure that the potassium chloride solution is saturated, a few crystals of solid potassium chloride can be introduced and should be visible all times. Excess addition of potassium chloride should be avoided as this sometimes blocks the capillary junction.

To prevent contamination of the electrode, it is important to place a salt bridge between a calomel electrode and the electrolyte under study. Calomel electrodes should not be exposed to temperatures above 50°C. Potential measurements above this temperature can be accomplished by keeping the electrode from the heated electrolyte with a salt bridge. Liquid junction potentials are usually negligible when using a saturated calomel electrode :this is one of the main advantages.

Saturated calomel electrodes should be calibrated and checked. For greatest precision, a reference electrode should be compared to a laboratory standard. A simpler technique is to compare a number of laboratory reference electrodes against each other and detect possible degradation

among one or more electrodes. Calomel electrodes are usually calibrated by immersing them in a container of saturated potassium chloride solution and measuring the potential difference between them by means of a precision potentiometer. In this manner, the possibility of excessive currents being passed through an electrode are avoided, since the relative potential difference is very small. The electrodes should have an accuracy of 0.1mV and preferably within a few tenths of a millivolt for most electrochemical and polarization measurements.

3.6.3.2 Platinised platinum

Platinum is an excellent reference electrode because of its large exchange current and its chemical resistance. Platinising increases the performance of a platinum electrode by increasing its active surface. The platinised platinum electrode is versatile because it can be directly introduced in most solutions without difficulty, it indicates the reversible hydrogen potential of acid solutions, and it can be used as a means of determining when oxygen has been completely purged from electrolytes. Also, it serves as an excellent auxiliary electrode because of its low polarization in most solutions.

After mounting the platinum electrode, it is cleaned in hot aqua regia (1 part concentrated nitric acid and 3 parts concentrated hydrochloric acid) until any black porous platinum deposit is removed. Following this operation (performed in a hood), electrodes are washed in doubly

distilled water and dried. Platinising is achieved by electrolysing in a solution containing 3% platinic chloride and 0.02% lead acetate. Lead acetate serves to produce a smooth, porous deposit of platinum. It is convenient to platinize two electrodes at the same time. The two electrodes are connected to a DC power supply or a battery or variable voltage and a current of 40 mA/cm^2 is passed through them. Electrolysis is continued for a total of four minutes and the current is reversed at the end of each minute by changing polarity. At the end of this operation, the electrodes should be covered with a black velvety deposit of platinised platinum. Electrodes are then cleaned to remove chlorine by electrolysing at a current density of 50-100 mA/cm^2 in 10% sulphuric acid for four minutes with current reversal at the end of every minute. The electrodes are rinsed in distilled water and stored in a test tube containing distilled water and never allowed to dry.

Platinum electrode is attacked in acid chloride solutions, especially when it is used as an anode electrode. For many measurements, especially hydrogen overvoltage studies, the presence of platinum ions affects the accuracy of measured data. A smooth platinum electrode produces much less contamination than a platinised electrode when used in acid chloride solutions. In any case, in chloride solutions, especially acid solutions at high temperatures, platinum should be used with caution. Platinised platinum is contaminated by trace quantities of sulphide, antimony and arsenic salts, and numerous organic compounds. It should not be used to measure

reversible potential in media containing these substances.

A platinised platinum electrode may be conveniently calibrated by measuring its potential in hydrogen-saturated, normal sulphuric acid at room temperature. Its potential should be -0.263 ± 0.002V SCE. A platinised platinum electrode has a limited life time. If an electrode requires extensive time to reach steady state potential (normal steady-state time is 1-2 minutes), the electrode should be cleaned and replatinised.

3.6.4 Electrical and electronic equipment

Since most electrochemical measurements are made with precision electronic and electrical measuring instruments, it is important that these be accurately calibrated and used correctly. Many electronic instruments show considerable drift during warm-up periods, and it is frequently advisable to leave apparatus running continuously during periods of extended use. This is particularly important in the case of electrometers and null detectors which often drift for one or two days.

Although batteries may be used as a source of direct current, it is more convenient to use variable D.C. power supplies to eliminate the battery recharging bother. An ideal power supply for galvanostatic polarization possesses the following characteristics:-

(a) variable voltage between zero and 500V,

(b) excellent A.C. filtering with an A.C ripple of no more than 100 microvolts,

(c) internal regulation which compensates for the line voltage fluctuations and current load,

(d) current output of at least 200 mA at all voltage settings. The most important consideration is the lack of A.C. ripple in the output voltage. Polarization behaviour is distorted in the presence of small superimposed alternating voltages.

The potentiometer is the most important instrument for measuring electrochemical potentials. Most potentiometers are portable with an internal battery power supply that drifts slowly with time. Potentiometers should be standardised before use and this should be repeated at one hour intervals during experiments. They should be frequently calibrated with a laboratory standard or with another potentiometer.

Electrode kinetic studies are best performed with potentiometers possessing the following characteristics:-

(a) A voltage range of at least 1.5V. For some studies such as anodization, metallic passivity and organic electrode kinetic studies, ranges extending to 5V are often needed.

(b) A sensitivity of 0.1 mV. There is no advantage gained by potentiometers with greater sensitivity, since it is unnecessary and as such potentiometers are more expensive and cumbersome to use.

(c) For greatest versatility the potentiometer should be self-contained with an internal reference cell, and possess an optical galvanometer for precision calibration.

An electrometer can be used directly to measure electrode potential or in conjunction with a potentiometer as a null indicator. The input impedance of an electrometer suitable for electrochemical studies must be 10^8 ohms or greater. This ensures that only negligible current will be drawn from the system during potential measurements, and hence does not affect the corrosion current determination. Electrometers connected to a circuit containing very high resistance ($>10^6\ \Omega$) behave erratically due to stray current pick-up. High resistance circuits are caused by loose contacts, entrained bubbles in the Luggin salt bridge, or by high resistance between the calomel electrode and the salt bridge. The erratic behaviour becomes particularly noticeable under conditions of low humidity where static electricity is prevalent. Erratic behaviour can be reduced by shortening the salt bridge and/or increasing its orifice diameter, or by increasing the conductivity between the saturated calomel electrode and the salt bridge.

For electrode kinetic studies, electrometers should possess the following characteristics:-

(a) The drift of an electrometer should not exceed 1-2 mV per day. In examining the manufacturers' published specifications, care is taken to compare zero drift data.

(b) Voltage accuracy should be 1 mV and the instrument should be capable of detecting a 0.1 mV change in potential. Most electrode potential measurements only require an accuracy of 1 mV.

(c) An electrometer should have an input impedance of 10^{12} Ω or greater and should provide means for reducing this input impedance. An input impedance of 10^{10} ohm is sufficient for most studies except those systems where either corrosion or exchange currents are very small.

The potentiostat is a device which maintains constant electrode potential. Potentiostatic techniques have found applications in electrochemical studies due to their unique characteristics. For example, the anodic dissolution kinetics of an active-passive metal can be completely characterised only by potentiostatic techniques. Further, since the potentiostat maintains electrode potential or the driving force constant, and allows current or rate to vary, the resulting data are easier to interpret. Potentiostatic polarization techniques are described for a potentiostat with the following characteristics:-

(a) It must maintain electrode potential within one millivolt or a preset value over a wide range of applied currents. Its potential range should extend from -2 to +2 volts or more.

(b) Its potential measuring circuit should possess very high input impedance (at least 10^{10} Ω or greater). This is necessary for studies of electrodes with small exchange or corrosion currents.

(c) It should possess a negligible potential drift rate. Ideally, its setting should not deviate more than 5 mV per day. Potential stability is important during long-term tests.

(d) Current output should be at least one ampere or more. This magnitude of current permits the potentiostat to be used in a variety of studies such as fuel cells, electropolishing, electro-deposition, metallographic etching and anodic protection. The versatility of potentiostats with current outputs less than 1A can be improved by utilizing small electrode areas. However, small electrode sizes decrease the convenience.

(e) Its D.C power output should be well filtered. If it has provisions for an external voltage input, it can be incorporated into automatic circuits. Also, the convenience of a potentiostat is improved if voltage can be traversed through zero without switching.

Electrochemical current measurements are commonly carried out with precision D.C meters with an accuracy of 0.5%.

There are a variety of recorders available which are useful in electrochemical studies including potentiometric recorders of the single and multipoint variety and XY recorders. The single pen potentiometric recorder is the most versatile and can be used to record a voltage or current during electrochemical studies.

Automatic polarization measuring apparatus is also available. The automatic polarization techniques possess several advantages. First, they improve reproducibility and eliminate timing errors present in manual techniques. An apparatus which is capable of automatically conducting anodic and cathodic polarization measurements under potentiostatic

conditions and automatically recording the results on semilogarithm graph paper is the best for following up corrosion processes.

3.7 pH AND ACIDITY MEASUREMENTS

In principle, any electrode reversible to hydrogen ion or hydroxyl ion can be employed to measure pH. A typical cell may be represented as follows:-

Electrode reversible to H^+ ion	Standard solution or unknown	KCl saturated	$Hg_2Cl_{2(s)}$	Hg

The emf of the above cell is given by $E_H = E_{ref} - \frac{RT}{F} . \ln a_H$ (3-29)

To avoid the problem of the liquid-junction, the assembly of the above cell is standardised by use of a standard solution of known pH to include the liquid junction potential with the measured $E_H - E_{ref}$. This is expressed as

$$pH = pH_s + \frac{(E-E_s)}{RT \ln 10} F \qquad (3-30)$$

The glass electrode, hydrogen electrode, the hydroquinone electrode and the antimony-antimonious oxide electrode find occasional use, as reversible electrodes for measurement of pH. The saturated calomel electrode is almost exclusively the reference electrode except at elevated temperatures.

3.7.1 The hydrogen electrode

It consists of a small platinum sheet or wire coated with finely divided platinum black by electrolysis of a solution of chloroplatinic acid to increase the surface area of the electrode. When placed so that it is partly in the experimental solution and partly in an atmosphere of hydrogen gas, the hydrogen electrode behaves as if it were made of hydrogen molecules and gives a reversible potential depending on the activity of the hydrogen ions in solution. For the equilibrium we have

$$H_{2(g)} \rightleftharpoons H_{2(Pt)} \rightleftharpoons 2H^{+}_{(aq)} + 2e^{-} \quad (3\text{-}31)$$

and the pH relationship

$$pH = \frac{E_{obs} - E_{ref}}{0.000198T} - \frac{RT}{2F} \cdot \log P_{H_2} \quad (3\text{-}32)$$

where E_{ref} is the potential of the reference electrode plus any liquid junction potential and P_{H_2} is the partial pressure of hydrogen gas. A stream of pure hydrogen must be passed continuously over the platinum electrode surface to ensure that the solution is representative of the bulk of the solution.

Sulphides, cyanides and compounds of arsenic, poison the hydrogen electrode. Proteins and colloidal materials are adsorbed on the platinum black coating making the electrode sluggish in response. Any organic substance susceptible of being hydrogenated or reduced by hydrogen on platinum must be absent. Strong oxidising and reducing

agents impose their own potentials at the electrode and metals more noble than hydrogen are reduced. Volatile dissolved acid or alkaline materials, or gaseous carbon dioxide may be swept out of solution by bubbling hydrogen gas. The potential of the hydrogen electrode is quite sensitive to traces of oxygen.

3.7.2 The glass electrode

Certain glasses possess the property that a thin membrane separating two solutions will show a potential difference between its surfaces that is determined by the difference in pH of the solutions. The shell of the electrode consists of a small bulb or tip of special glass sealed to a stem from ordinary pyrex glass. In this manner, the hydrogen ion response is confined entirely to the area of the special glass membrane. Inside the bulb is dilute hydrochloric acid solution, and dipping into this is an internal reference electrode, which is generally either a silver-silver chloride electrode or a calomel electrode. The dilute acid solution provides an unchanging hydrogen ion concentration and a constant chloride ion concentration. The inner cell is tightly sealed from the atmosphere by means of a wax or plastic dielectric and a metal or plastic cap.

The glass electrode assembly is dipped into the solution under examination together with an external reference electrode. The potential of the glass electrode relative to the external reference electrode is related to pH by

$$pH = \frac{E_g - E_{ref.}}{0.0591} \text{ , at } 25°C \qquad (3\text{-}33)$$

The value of E_g depends upon the nature of the particular glass membrane and the reference electrode inside the glass electrode [Perley, 1949]. It is therefore necessary to standardise each glass electrode assembly by means of a series of reference solutions of known pH.

General-purpose glass electrodes are characterised by relatively low electrical resistance, permitting construction of glass tips so thick that they are practically unbreakable. The pH response of these electrodes follows a linear relation between pH 1 and pH 11.

3.7.3 The pH meters

A direct-reading instrument has few manipulative steps and is adaptable to continuous recording or control of industrial operations. Temperature compensations can be provided by causing the feedback current flow through a temperature-sensitive resistor located in the input circuit to supply the balancing voltage. If this resistor is placed in solution to be measured, temperature compensation can be achieved automatically, pH measurements can be made within ±0.1 pH unit. When buffer standardizations are made, the meter needle is set to the pH of the buffer by standardization control knob. This control also compensates for electrode assymetry potential and instrument drift.

CHAPTER 4

EXPERIMENTAL

4.1 Preparation of soil-water extract

250g of soil was mixed with 250 cm^3 of distilled-deionised water. The mixture was stirred continuously in order to disperse the soil sample into a state of slurry. The stirring was done for thirty minutes by a low speed magnetic stirrer.

The slurry was placed in a high speed laboratory centrifuge and centrifugated in order to separate the particles from the water phase. The centrifugation period depended on the amount of colloidal materials present in the sample. This time varied between one hour and one and a half hours.

The water phase was extracted and filtered to remove any suspended particles. The sample (soil-water extract) was ready for use when the water phase was transparent.

The procedure was repeated for all the soil samples collected from all the sites under investigation. The volumes were made to one litre by repeating the above procedure. The samples were stored in one litre plastic bottles which had been thoroughly cleaned, rinsed and dried.

4.2 Preparation of soil slurry

100g of soil was added to 100 cm^3 of distilled-deionised water. The mixture was stirred as above to disperse the soil

particles into a slurry. The resulting mixture was mechanically shaken for ten minutes to form a thorough mixture. The mixture was stirred for a further ten minutes, as above, and was ready for analysis.

The slurry was used for the required analysis immediately it was made. A fresh slurry was prepared for each analysis to be performed.

4.3 Atomic absorption spectrophotometry

The soil-water extract was analysed for zinc, iron, copper, manganese and magnesium using the atomic absorption spectrophotometer model UNICAM SP90. Each element to be analysed had its analytical procedure as outlined below.

4.3.1 Iron analysis

A calibration curve, Fig. 5.1 was prepared by diluting iron stock solution BDH 1000 ppm for A.A.S. to concentrations ranging from 1.0 ppm to 20 ppm. The stock solution was diluted by the use of distilled-deionised water.

20 cm^3 of each of the standard solutions was placed in a 50 cm^3 beaker and aspirated through the above A.A.S. instrument and the absorbance read-out was recorded and the calibration curve, Fig. 5.1, was drawn.

The experiment was repeated for each sample of the soil-water extracts. The results so obtained were compared with the readings on the calibration curve and the concentration of iron in each sample was recorded in Appendix 1.

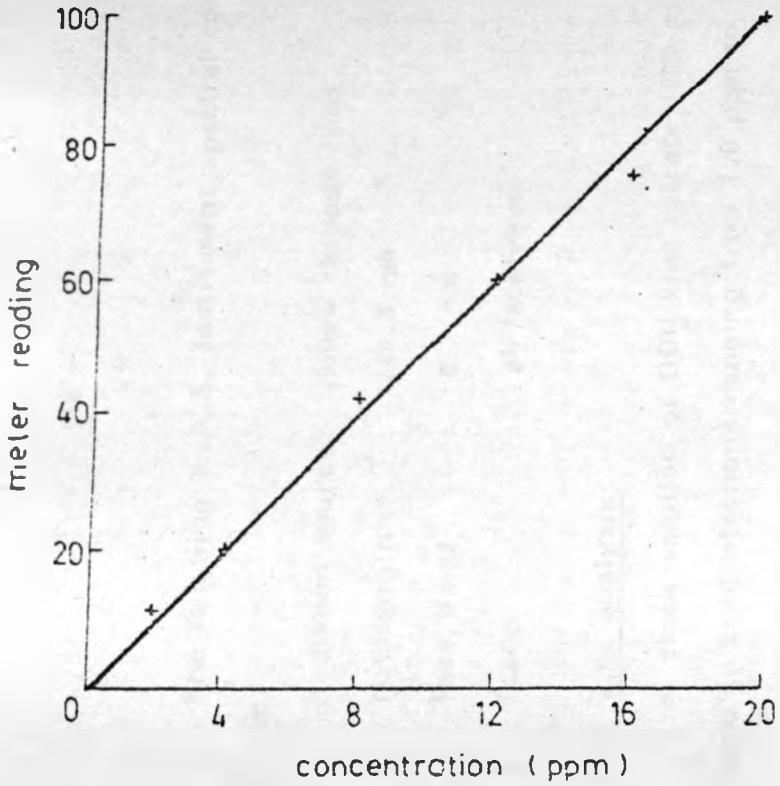

Fig. 5.1: Iron calibration curve for the analysis of soil-water extracts.

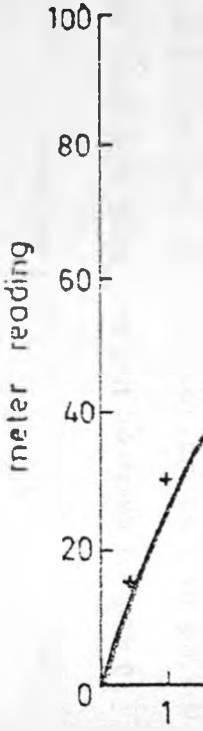

Fig. 5

The following A.A.S. instrument spectral conditions were set:-

Radiation source: hollow cathode lamp

Wavelength : 248.3 nm

Pass Band : 0.2 nm

Flame : air/acetylene

4.3.2 Zinc analysis

A stock solution of BDH zinc nitrate 1000 ppm was diluted to concentrations ranging from 1.0 ppm to 10.0 ppm.

The A.A.S. instrument spectral conditions were set as follows:-

Radiation source : Hollow cathode lamp

Wavelength : 213.9 nm

Pass band : 2 nm

Flame : air/acetylene

20 cm^3 of each of the standard solutions, made above, was placed in a 50 cm^3 beaker and inspirated into the A.A.S. as set above. Respective readings were obtained and a calibration curve, Fig. 5.2, was plotted.

The experiment was repeated with 20 cm^3 of soil-water extract to which 5 cm^3 of 5% lanthanum solution was added. The 5% lanthanum solution removes interferences during zinc absorption analysis. The results were matched with standards of the calibration curve and recorded in Appendix 1.

4.3.3 Copper analysis

A copper stock solution of 1000 ppm was made by use of 1.0g of copper metal dissolved in 100 cm^3 of conc. HCl (A.R.) and diluted to one litre by the use of distilled-deionised water.

The standard solutions ranging from 0.5 ppm to 5.0 ppm was made by diluting the above stock solution.

20 cm^3 of each standard solution were aspirated into the A.A.S. instrument and the readings so obtained were used to plot calibration curve Fig. 5.3.

The experiment was repeated with 20 cm^3 of each of the soil-water extract samples. The results were matched with the calibration curve and the copper concentration in sample is recorded in Appendix 1.

The A.A.S. instrument spectral conditions were set as follows:-

Radiation source	:	Hollow cathode lamp
Wavelength	:	324.8 nm
Pass band	:	0.7 nm
Flame	:	air/acetylene

4.3.4 Magnesium analysis

4.947g of anhydrous magnesium sulphate were dissolved in 250 cm^3 of distilled-deionised water in a one litre volumetric flask. When all the magnesium sulphate had dissolved, the volume was made to the mark by use of the distilled-deionised water. This was the magnesium stock solution 1000 ppm Mg.

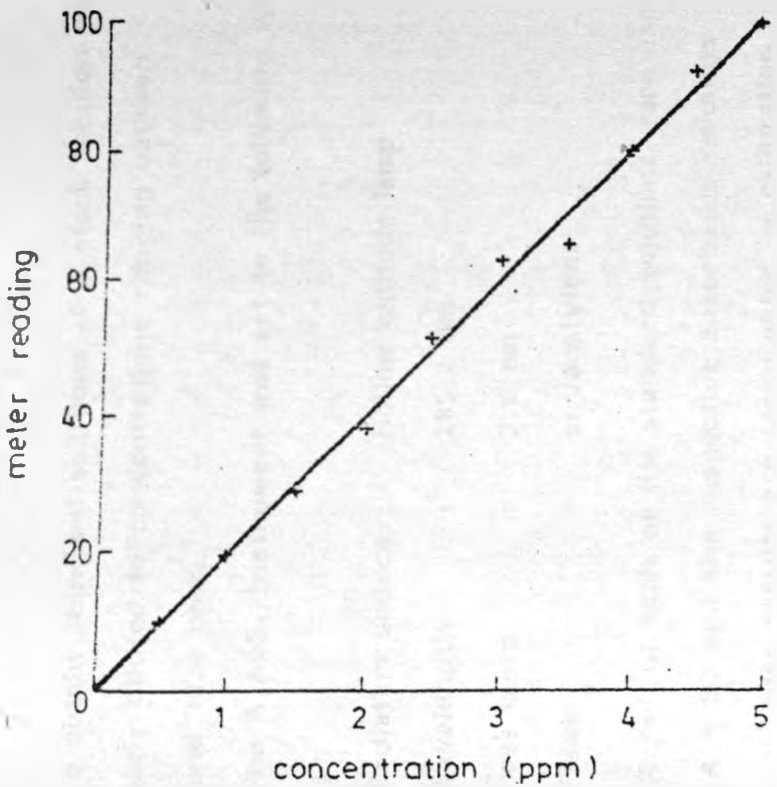

Fig. 5.3: Calibration curve for copper analysis in soil-water extracts.

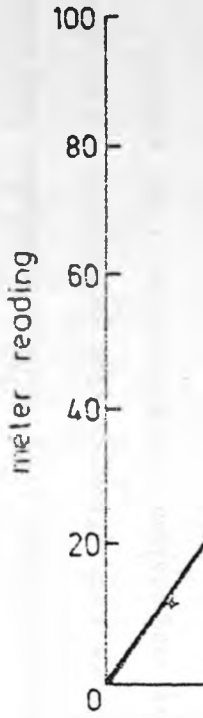

Fig. 5

To obtain standard solutions, the stock solution was appropriately diluted to concentrations ranging between 1.0 ppm and 10.0 ppm.

The A.A.S. instrument was set to the following spectral conditions:

Radiation source	:	Hollow cathode lamp
Wavelength	:	285.2 nm
Pass band	:	2.0 nm
Flame	:	air/acetylene

20 cm^3 of each of the standard solutions were aspirated into the A.A.S. and the respective absorbance readings recorded. These results are represented as calibration curve Fig. 5.4.

The experiment was repeated with 20 cm^3 of soil water extract samples to which 0.5% lanthanum solution was added. The results were compared with the calibration curve values and the respective magnesium concentrations in the samples recorded in Appendix 1.

4.3.5 Manganese analysis

1.0g of manganese powder was accurately weighed and placed in a 100 cm^3 beaker. 10 cm^3 of conc. HCl were added followed by 20 cm^3 of distilled-deionised water. The mixture was swirled until all the manganese powder had dissolved. The solution was transferred to a one litre volumetric flask with thorough washing of the dissolution beaker. The volume was made to the mark with distilled-deionised water. This was the 1000 ppm manganese stock solution.

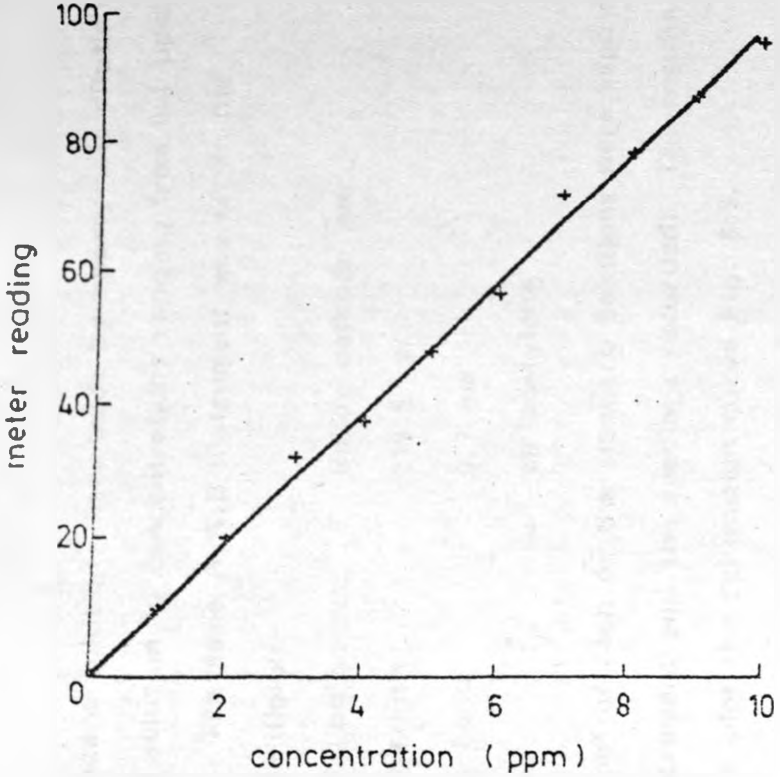

Fig. 5.5 Calibration curve for manganese analysis in soil-water extract.

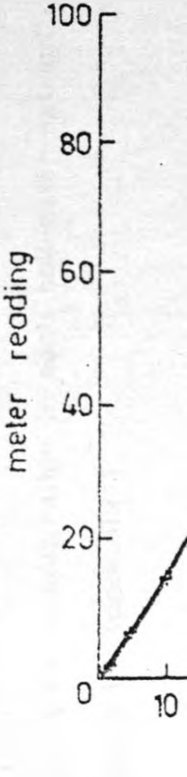

Fig.

Standard solutions were made by appropriate dilutions of the stock solution to concentrations ranging from 0.1 ppm to 5.0 ppm. The same A.A.S instrument was set to the following conditions:-

Radiation source	:	Hollow cathode lamp
Wavelength	:	279.5 nm
Pass band	:	0.7 nm
Flame	:	air/acetylene

20 cm^3 of each of the standard solutions were aspirated into the instrument and the readings recorded. The results were used to plot the calibration curve Fig. 5.5.

The experiment was repeated with 20 cm^3 of soil-water extract sample to which 5 cm^3 of 1% Lanthanum solution was added. The results were compared with the calibration curve and the manganese concentration in each soil-water extract sample recorded in Appendix 1.

4.4 CHLORIDE ION ANALYSIS BY POTENTIOMETRIC METHOD

4.4.1 Preparation of standard solutions

5.0g analytical reagent grade sodium chloride were dried in an oven at 150°C for four hours. Out of this 1.649g were accurately weighed and transferred to a one litre calibrated flask. Distilled-deionised water was added and volume made to the mark. The resulting solution of 1ml was equivalent to 1mg of chloride or 1000 ppm chloride stock solution.

Standard solutions with concentrations ranging from 10 ppm to 500 ppm were made by appropriate dilutions of the stock solution.

4.4.2 Preparation of chloride buffer solution

77.8g analytical of reagent grade ammonium acetate were dissolved in 250 cm^3 of water. 57 cm^3 of analytical reagent grade glacial acetic acid (sp.gr. 1.05) was added to the mixture. The resulting mixture was diluted with distilled-deionised water to one litre.

4.4.3 Analytical procedure

Two standard solutions of concentrations 10 ppm and 100 ppm were used for the calibration procedure. 50 cm^3 of 10 ppm solution were pipetted into a 100 cm^3 beaker containing a magnetic stirrer. 5 cm^3 of the buffer solution were pipetted into the beaker containing the 10 ppm chloride solution.

The chloride and reference electrodes were rinsed with deionised water, dried with a clean, dry tissue and immersed in the test solution. The solution was stirred at a constant moderate rate.

The Orion pH/mV meter model 801 was used and it gave digital readout of potential. The steady potential (e.m.f.) was noted and recorded as E_1.

The experiment was repeated with the second standard solution (100 ppm) and the steady reading of e.m.f. recorded as E_2.

From the emfs E_1 and E_2 the calibration slope was calculated using the formula

$$K = \frac{E_1 - E_2}{\log S_1 - \log S_2}$$

where S_1 is the concentration of the lower standard solution (10 ppm) and S_2 is the concentration of the higher standard solution (100 ppm). The value of K = -58 mV was obtained.

The experiment was repeated with the soil-water extract samples. For each sample the steady emf reading was noted and recorded as E_x.

The difference between the emf of the sample (E_x) and that of the higher concentration (E_2) was calculated as $\Delta = E_x - E_2$. This difference was used to calculate the concentration of chloride ion in the sample by use of the formula

$$C_x = S_2 \text{ X antilog } (\Delta / K)$$

The experiment was repeated for all the soil-water extract samples and the chloride ion concentrations calculated and recorded in Table 5.1.

4.5 SULPHATE ION ANALYSIS BY TURBIDIMETRIC METHOD

4.5.1 Standard sulphate solutions

Sulphate stock solution was prepared by dissolving 0.544g of analytical reagent grade potassium sulphate in 100 cm^3 of distilled-deionised water. The solution was transferred to a one litre volumetric flask and the volume made to the mark by use of distilled-deionised water. The resulting solution contained 0.1mg sulphur per cm^3 equivalent to 300 ppm sulphate. This solution was appropriately diluted to make standard solutions between 1.0 ppm and 100 ppm.

4.5.2 Analytical procedure

50 cm^3 of the standard solution were placed in a 100 cm^3 beaker to which 2.0 cm^3 of 0.5 MHCl were added. The mixture was swirled for one minute and 1.0 cm^3 of $BaCl_2$ (A.R) was added to the mixture. It was swirled again for one minute and turned turbid.

The turbid mixture was poured into a clean 50 cm^3 cylindrical cuvet and the sulphate content recorded by use of the model 2100A Turbidimeter by HACH. The procedure was repeated with all the standard solutions and a calibration curve plotted (Fig. 5.6).

The above procedure was repeated for all the soil-water extract samples. The sulphate concentrations are recorded in Table 5.2.

4.6 REDOX POTENTIAL MEASUREMENT

Field-condition soil sample was placed in a 500 cm^3 beaker. Enough distilled-deionised water was added to just wet the soil sample. A platinum and a calomel electrode were inserted into the soil sample three centimeters apart.

The potential that developed between the two electrodes was measured by use of a digital meter model 801, Orion pH/mV.

The experiment was repeated for all the soil samples and the results obtained recorded in Table 5.3. The results were compared with those recorded by the American Bureau of Standards [Romanoff, 1957] for relative corrosivity in Table 5.4.

4.7 MEASUREMENT OF MOISTURE CONTENT

20.0g of field-condition soil samples were placed on preweighed porcelain bowls. The samples were heated in an oven thermostated at 100°C. The changes in masses were recorded at intervals of half an hour until a constant mass was obtained. After the last three constant values the samples were left overnight in the oven and a final mass was read and recorded after cooling in a desiccator.

The experiment was repeated for all the collected soil samples and mass changes were recorded. The mass changes were converted to percentage mass changes or moisture content and recorded in Table 5.5.

4.8 pH AND ACIDITY/ALKALINITY MEASUREMENT

4.8.1 pH measurement

4.8.1.1 Buffer solutions

Buffer solutions with pH values 4.008, 7.413, 9.180 and 10.012 were prepared for the calibration of the pH meter. These solutions were prepared by the following procedures

(a) pH 4.008

20.0g potassium hydrogen phthalate were dried in an oven at 50°C for one hour. 10.12g of this dry salt were dissolved in distilled-deionised water and diluted to one litre in a volumetric flask.

(b) pH 7.413

1.179g potassium hydrogen phosphate and 4.302g anhydrous disodium hydrogen phosphate were dissolved in

distilled-deionised water and diluted to one litre.

(c) pH 9.180

3.80g sodium tetraborate decahydrate (Borax) were dissolved in carbon-dioxide free water and diluted to one litre.

(d) pH 10.012

3.0g sodium carbonate were heated in an oven at 270°C for one hour. It was then cooled in a desiccator. 2.640g of the dry sodium carbonate were mixed with 2.092g sodium hydrogen carbonate and dissolved in carbon dioxide free water. The solution was diluted to one litre.

4.8.1.2 Analytical procedure

30 cm^3 of each of the buffer solutions prepared above, was transferred into a 50 cm^3 beaker. A clean well rinsed and dried combined glass-calomel electrode was immersed into each buffer solution respectively. The analogue display was adjusted to coincide with the pH of the prepared buffer solution.

The combined glass-calomel electrode was immersed in a beaker containing 30g of field-condition soil, and the displayed pH was recorded, for all the field-condition soil samples under investigation.

The combined glass-calomel electrode was washed rinsed and dried. It was immersed in 50 cm^3 beaker containing 30 cm^3 soil slurry or 30 cm^3 soil-water extract. The pH displayed for each of the slurry and soil-water extract was recorded. All the pH values obtained in this experiment are recorded in Appendix 2.

4.8.2 Acidity/Alkalinity measurements

On examining the values recorded in Appendix 2, it is seen that the pH values of most soil-water extracts are acidic while a few are basic. The following methods were utilized for analysis of the acidic and/or basic nature of the soils.

4.8.2.1 Acidity measurement

50 cm^3 of soil-water extract were placed in a 100 cm^3 flask and three drops of phenolphthalein were added. The mixture was titrated against 0.02M solution of sodium hydroxide to pink colour. The experiment was repeated for all acidic samples and the acidity calculated accordingly and recorded in table 5.6.

4.8.2.2 Alkalinity measurement

50 cm^3 of soil-water extract were placed in a white porcelain dish about 12 cm in diameter. Two drops of phenolphthalein solution were added.

In the presence of free alkalis and alkali carbonates the indicator appeared pink in colour for pH<8.3. Two drops of methyl orange were added where the pink colour did not appear.

The soil-water extract was titrated against 0.02M hydrochloric acid until the colour turned orange/yellow. The amount of alkalinity was calculated from the total volume of acid required to neutralize the solution to the end point and recorded in table 5.6.

4.9 MECHANICAL ANALYSIS AND SOIL TEXTURE DETERMINATION

Mechanical analysis was performed on the soil samples and the texture was determined from the mechanical analysis.

4.9.1 Analytical procedure

(a) Preparation of calgon solution

40.0g of predried, powdered sodium hexametaphosphate were dissolved in 750 cm^3 distilled-deionised water in a one litre flask by adding it to the water while stirring. 10.0g predried anhydrous sodium carbonate was added to the mixture and the volume made to the mark by use of the distilled-deionized water.

(b) Preparation of soil sample

50.0g soil samples were transferred to 500 cm^3 shaking bottles and 30 cm^3 of calgon solution were added to each bottle and left to stand overnight. 400 cm^3 distilled-deionised water were added to each bottle and was tightly stoppered. The mixture was mechanically shaken for ten minutes.

The soil suspensions were transferred to one litre sedimentation cylinders and stirred with a plunger for one minute. The hydrometer was slowly immersed in the suspension. The hydrometer reading and the temperature were recorded after forty seconds.

The suspensions were left to settle for six and a half hours ($6\frac{1}{2}$ hrs) after which both temperature and hydrometer readings were taken.

4.9.2 Calculations

The hydrometer was calibrated at 20°C and therefore a correction factor had to be made when the temperature was higher than 20°C.

$$\% \text{ sand} = \frac{100 - [(R_1 - B_1) + 0.36(T_1 - 20)] \times 100}{W}$$

$$\% \text{ clay} = \frac{[(R_2 - B_2) + 0.36(T_2 + 20)] \times 100}{W}$$

% silt = 100% - % sand - % clay.

where:

R_1 = First reading hydrometer sample.

B_1 = First reading hydrometer blank.

R_2 = 2nd reading hydrometer sample.

B_2 = 2nd reading hydrometer blank.

T_1 = First temperature reading.

T_2 = 2nd temperature reading.

0.36 = temperature correction factor.

20 = hydrometer calibration temperature in °C.

W = weight of sample taken for analysis.

The results obtained in this analysis are shown in Appendix 3.

4.10 MEASUREMENT OF SOIL CONDUCTANCE

50 cm^3 of 0.01M potassium chloride solution were placed in a conductivity cell model PR 9510 connected to a direct reading conductivity measuring bridge model PR 9501. The resistance of the KCl solution was read directly on the meter

and since the specific conductivity of the KCl solution was known, the cell constant was calculated.

The experiment was repeated for all the soil slurry and soil-water extract samples. Using the cell constant calculated above, and from the resistance readings obtained, the conductance values were determined and recorded in table 5.7.

4.11 LOSS OF MASS MEASUREMENTS:

4.11.1 Preparation of metal pipes

Metal pipes, half an inch in diameter (11.5mm) were cut to sizes of 153mm long. They were thoroughly polished by use of very smooth emery paper to remove any oxides on the surface. The surfaces were degreased by use of acetone and left to dry. The dry pipes were weighed to the nearest milligram.

The dry pipes were buried in field-condition soils in plastic containers in the laboratory. The soil was placed half-way the 153 x 245 x 225mm plastic boxes and then three pipes laid in a horizontal position in each box. More soil was placed to cover the pipes and fill the box. The box was covered with an air-tight lid.

The pipes were unearthed three times at intervals of four months. The unearthed pipes were cleaned and checked for corrosion.

4.11.2 Cleaning the pipes

The unearthed pipes were first cleaned with water to remove the clinging soil. Further cleaning was done with a

mixture of hot water, 3.0M hydrochloric acid solution and stannous chloride solution, until all the rust stains were removed. The clean pipes were rinsed with acetone and air-dried overnight. The dry pipes were weighed and the difference in mass for the period of burial recorded in Appendix 4. The pipes were physically examined for the type and extent of corrosion that had taken place.

4.11.3 Field samples

From observations of the laboratory-buried pipes, some pipes were laid in some selected sites in the field. The samples were cut to lengths of one meter and laid in six different sites.

The field-buried pipes were prepared in the same way as the laboratory-buried pipes and buried half a meter below the ground level. The pipes were laid in a horizontal position and the pit backfilled in a manner to avoid disturbing the position of pipes.

The pipes were unearthed three times at intervals of six months. They were cleaned in the same way as the laboratory pipes and examined for the type and extent of corrosion that had taken place. The results are discussed in chapter 5.

4.12 POLARIZATION MEASUREMENTS

The rate of an electrochemical reaction is limited by various physical and chemical factors. Hence an electrochemical

reaction is polarized or retarded by these environmental factors. Polarization is divided into three main types (sec. 2.5.2). Depending on what kind of polarization is controlling the reduction reaction, environmental variables produce different effects.

A study has been made of the relationship of anode current density with electrode potential for mild steel, in dilute solutions of soil electrolytes and under conditions simulating the natural corrosion of metal buried in the soil. The results allow the estimation of the increase in corrosion rate resulting from the change in electrode potential of buried mild steel that may be caused by adjacent cathodic protection or other electrical installations.

Two electrochemical methods are used to determine the corrosion rate in the soil. These are the Tafel extrapolation and the linear polarization (also called resistance polarization) techniques.

4.12.1 Specimen (working electrode) preparation

A number of electrodes were made by cutting 10mm each of a 10mm-diameter mild steel rod, spot-welding it to a nichrome wire and covering the 10mm long electrode with epoxy resin. The electrode surface was ground and finely polished to a smooth surface by use of a smooth emery paper on a rotating disc.

The polished electrode surface was degreased by use of acetone and heat-treated in vacuum to prevent surface oxidation. The heat treatment also increased corrosion resistance which was necessary for the intended investigation. The electrode was used immediately after preparation. A new surface was prepared for every analysis to be conducted.

4.12.2 Tafel extrapolation measurements

The potentiostatic polarization technique was used to obtain the Tafel slopes for the anodic and cathodic reactions. In this technique potential was maintained constant and the current was measured. The potential was maintained constant by the use of a potentiostat which functions by monitoring the potential between a working electrode and the reference electrode and automatically altering the current between the working electrode and the auxiliary electrode.

A current meter was placed in the lead to the auxiliary electrode and a short low resistance lead was used to connect the working electrode to the potentiostat. The following steps were used for the manual potentiostatic polarization measurements.

(1) The mixed or corrosion potential of the working electrode was determined with the potentiometer-ammeter circuit with all other wires disconnected from the polarization cell.

(2) After waiting for ten minutes to allow the mixed potential to become constant, the potentiostatic circuit (sec. 3) was connected to the polarization cell.

(3) Potentiostatic measurements were conducted by increasing or decreasing potential in 50 mV steps and waiting for five minutes for each potential to stabilize (sec. 4.12.4).

4.12.3 Linear polarization (resistance polarization) measurements

The term "polarization resistance" is now familiar with those interested in monitoring corrosion rate. The term was originally coined to describe the ratio between the applied potential and the current for an electrode [Callow L.M. et al, 1976] The first theoretical analysis of the likely relationship between resistance and corrosion current was developed by Stern and Geary (1957). They considered the rate equations for the anodic and cathodic processes comprising a simple electrochemical equilibrium, on the basis that both processes are activation controlled and that the activation energy barrier at the electrode/solution interface is symmetrical. It was established that, close to the reversible (mixed or corrosion) potential, the applied potential and current density were linearly related to a close approximation. Their ratio "linear polarization", R_p was related to the corrosion current density (corrosion rate) in terms of Tafel slopes βa and βc for anodic and cathodic processes as follows:-

$$i_{corr} = \frac{\beta a \, \beta c}{2.3(\beta a + \beta c)} \cdot \frac{1}{R_p}$$

The same circuit used for the Tafel extrapolation technique was used in the present investigation for the

resistance polarization. The first step (sec. 4.12.2) was used to record the corrosion potential. The working electrode was then cathodically or anodically polarised by manually selecting the respective potentials at 10 mV steps.

4.12.4 Preparation of trial runs solutions

It was found necessary to run some trial analysis to establish the position of the luggin probe that gives the optimum readings. The following solutions were prepared for the said purpose in the polarization measurements.

(a) 0.001M Na_2SO_4 + 0.0001M KCl

(b) 0.001M $FeSO_4$ + 0.0001M KCl

(c) 0.001M NaCl

(d) 0.001M KCl

The chemicals used were all A.R. quality and dissolved in distilled deionised water. 300 cm^3 of each of the above solutions were used in the polarization cell.

The potential between the working electrode and the reference electrode was kept constant by placing the luggin probe as close to the working electrode as possible. The potential between the working electrode and the auxiliary electrode was varied "potentiostatically" and the current that flowed recorded. The potential was manually varied at steps of 50 mV for five minutes. The position of the luggin probe was varied and the position of maximum current output noted and the probe fixed.

The experiment was repeated for all the above solutions and the soil water extract samples as prepared in section 4.1. Polarization curves for the soil-water extracts were drawn (Figs. 1-24), from which corrosion currents and potentials were deduced by the Tafel slopes and linear polarization analysis. The respective Tafel slopes, corrosion currents and corrosion potentials were calculated and recorded in Appendix 5.

The solutions were bubbled with a stream of nitrogen for deaeration, for a period of one hour per sample. The polarization measurements were repeated for the deaerated soil-water extracts and the respective curves are shown in figures 1-24.

4.12.5 The corrosion cell maintenance

The corrosion cell (sec. 3.6.2) was cleaned and degreased by use of the chromic-sulphuric acid cleaning solution. It was then rinsed with distilled deionised water followed by acetone and allowed to dry.

The cell cleaning procedure was repeated for every solution to be tested to eliminate contamination from the previous solution. All the components of the cell including the luggin probe, thermometer and the auxiliary electrode were properly rinsed at the beginning of a new experiment.

CHAPTER 5

RESULTS AND DISCUSSIONS

A number of analytical techniques and procedures have been described in chapters 3 and 4. From these, results have been obtained and represented in form of tables, graphs and appendices. In this chapter the relevance of these results to the underground pipeline corrosion is being analysed and determined. By the end of the data analysis, the extent and rate, type and nature of corrosion shall be identified and a number of recommendations made for the corrosion resistance or prevention to the underground pipeline.

5.1 ATOMIC ABSORPTION SPECTROPHOTOMETRIC ANALYSIS

This technique was used to analyse the amount of iron, zinc, copper, manganese and magnesium in the soil-water extracts of the sites under investigation. The results obtained are recorded in Appendix 1.

From the appendix, it is noted that the ions are found in quantities increasing in the following order.

$$Mg > Fe > Cu > Mn > Zn$$

This order indicates that, in the sites under investigation, the magnesium salts were the most soluble in water while those of zinc were the least soluble. The solubilities of copper and manganese salts were about the same in a few sites although their differences were not large in other sites.

Since metallic corrosion is an electrochemical process, the dissolved ions have a marked effect if present in the soil where the underground pipeline is laid.

Examination of table 5.7 and Appendix 1 shows that the soils that have high concentrations of the above ions have high electrical conductivity (low resistivity). This indicates that the presence of these ions determines the electrical conductivity, expressed as electrical resistivity, of the soil electrolyte.

The comparison between table 5.3 and Appendix 1 shows that the sites with high concentrations of the above ions, have low redox potentials. In this case, it is observed that the soil corrosivity in these sites is expected to be high. However examination of the unearthed pipes shows high corrosion at the beginning but slows down with time.

The mass changes recorded for the first four months were relatively higher than those recorded for the following months. This indicates that the corrosion was very fast forming corrosion products that formed a protective layer on the surface of the pipe.

Examination of Appendices 1 and 3 shows that most of the ions determined above were found in either sandy-clay or clay soils. These soils have high water contents and it is possible to form hydrated ions which would form a protective layer on the surface of the buried pipe.

In general, the corrosive soils contain large amounts of soluble salts which result in low electrical resistivity values.

The least corrosive soils, as a group, have high electrical resistivity and low salt concentrations. If metal ions are present in the electrolyte, they combine with oxygen, hydroxide or even water to form respective insoluble products on the surface of the buried pipeline, thereby protecting the pipe from corroding.

5.2 CHLORIDE ION ANALYSIS

Chloride ion is an important constituent of the soil during the process of underground corrosion. The presence of chloride ions in the soils results in pitting type of corrosion of metals due to destruction of passive films on the surface of the metal.

The amount of chloride in each of the sites under investigation was determined and recorded in Table 5.1.

Site	Chloride Concentration (ppm) ± 0.1	Site	Chloride Concentration (ppm) ± 0.1
1	49.7	14	85.2
2	17.8	15	35.3
3	39.1	16	38.3
4	17.8	17	26.6
5	85.2	18	16.0
6	28.4	19	21.3
7	24.9	20	35.9
8	24.9	21	36.1
9	14.2	22	30.2
10	17.8	23	33.0
11	14.2	24	28.4
12	17.8	25	23.1
13	32.0	26	28.4

Table 5.1: Chloride ion concentration (ppm) for the sites under investigation.

From Table 5.1 it is observed that the chloride ion concentrations range between 10 ppm and 90 ppm. It is observed that most of the sites had chloride concentrations between 20-40 ppm.

By examination of the physical appearance of the buried pipes it was noted that those pipes buried in higher-

chloride concentration soils had many small spots indicating that localized corrosion had taken place. This was even more marked on the pipes buried in soils with 80-100 ppm chloride ions.

It was however noted that very few dark spots of localized corrosion, were noted on the pipes buried in soils with chloride ion concentration below 20 ppm. In this case uniform corrosion was realised. However, some pipes in the lower chloride ion concentration showed strong aspects of corrosion. This indicated that it was not only the chloride ion that was responsible for the corrosion of the pipes in the respective soil sample.

By examination of Appendix 4, the loss of mass, it is noted that there is some loss of mass on every unearthed pipe. It is generally observed that there was higher loss of mass recorded in soils where the chloride ion concentration was high and vice versa. It is however difficult to assign a mathematical relationship between the amount of mass loss and the chloride ion concentration.

It was also generally observed that for the first eight months of burial, the loss of mass in the soils with high chloride ion concentration, was higher than in the lower chloride ion concentration samples for the same period of time. After this period, the loss of mass was generally observed to be lower in the higher chloride ion concentration samples. It was also noted that some sites showed mixed results; i.e. some low-chloride sites showed high mass losses and vice versa.

In these it was difficult to associate the mass loss to the chloride content only.

By examination of the unearthed pipes, it was noted that the localised corrosion was on the upper side of the pipe. The uniform corrosion was observed all over the surface of the pipe. It was also noticed that the pits of the localized corrosion could not be measured because they were not deep enough. However, with a longer duration, the pits would develop to measurable dimensions.

Chloride is often taken as an index of the corrosiveness in water. It varies from very wide trace limits found in unpolluted waters to high concentrations in sea water. Some of the purest land water have chloride contents below 5 ppm and most public water supplies contain less than 20 ppm of chloride [Butler and Ison, 1978].

Chloride ion interferes with the development of protective films and also breaks any passive films more readily. Although under certain conditions the overall amount of metal lost is not markedly influenced by the concentration of the chloride, the attack differs from that in distilled water. The attack by chloride is more localised and results in deep pits.

Corrosion is drastically increased by the presence of chloride ions which activate the anodic process. Riggs, Sudbury and Hutchinson reported that pits usually grow in the direction of gravity, mostly downwards from horizontal surfaces [Riggs, Sudbury, Hutchinson, 1960]. They found

that as pH increases, the corrosion progresses from general to highly localized pitting. Beginning at pH 4 the pits are covered by a cap of corrosion products and at pH 12, the corrosion products assume an unusual tubular shape. In most cases the corrosion pits are covered by corrosion products and are difficult to see, and sometimes they take a long time before they show up.

In the crevice or pitting corrosion, the overall reaction involves the dissolution of the metal M and the reduction of oxygen to hydroxide ions. In the oxidation process we have

$$Fe_{(s)} \longrightarrow Fe^{2+}_{(aq)} + 2e^{-}$$

In the reduction process we have

$$O_{2(g)} + 2H_2O_{(\ell)} + 4e^{-} \longrightarrow 4OH^{-}_{(aq)}$$

Initially these reactions occur uniformly over the entire surface of the metal. After a short interval oxygen on one part of the pipe may be depleted due to restricted convection. Oxygen reduction ceases in this area. However metal dissolution continues and this tends to produce excess positive charges in the electrolyte. This excess charge is necessarily balanced by the migration of chloride ions. This increases the concentration of the metal chloride within this area. These metal chlorides are soluble in water leading to the reaction

$$(M^{+}\ Cl^{-})_{(s)} + H_2O_{(\ell)} \longrightarrow MOH_{(s)} + H^{+}_{(aq)} + Cl^{-}_{(aq)}$$

In case of iron and steel the reaction is

$$FeCl_{2(s)} + 2H_2O_{(\ell)} \longrightarrow Fe(OH)_{2(s)} + 2H^{+}_{(aq)} + 2Cl^{-}_{(aq)}$$

The aqueous metal chloride dissociates into a hydroxide and a free acid. Both the chloride and hydrogen ions accelerate the dissolution rate in this section of the metal leading to pitting or even crevice corrosion. This chloride attack is infact possible because the chloride ion has a specific adsorption on the metal as compared to that of the hydroxyl ion. The presence of the above aqueous acid explains why the pits are found on the top side of the buried pipe.

The iron hydroxide formed above migrates to the cathodic sites and prevents the metal from further corrosion. However in presence of chloride ions the hydroxide is displaced by the chloride to form the soluble iron chloride.

$$Fe(OH)_{2(s)} + 2Cl^-_{(aq)} \longrightarrow FeCl_{2(s)} + 2OH^-_{(aq)}$$

whereby with the presence of hydrogen ions the hydroxyl ions combine to form water molecules and the reaction above is propagated. The reaction goes on as a chain reaction and would only stop when either water or the chloride ion is depleted. Thus the higher the chloride ion concentration the longer the reaction goes on and hence the more the corrosion will be effected.

In the soil the corrosion is further complicated by the presence of other ions that would either increase or decrease the rate of corrosion. The pattern is governed by the combination of many factors and may vary with time.

5.3 SULPHATE ION MEASUREMENT

The soil-soluble salts involved testing for the presence of chloride and sulphate ions in the soil-water extracts. From the work of Nthurima [I. Nthurima, 1979] it has been reported that these ions are involved in corrosion of metals buried in the soil in Norway. Other investigators (sec. 2.3.8) have shown the effect of sulphates in the underground corrosion. The present investigation involved soil sampling and analysis of soluble sulphates. The results obtained were recorded in table 5.2.

Site	Sulphate Concentration (ppm) ± 0.1	Site	Sulphate Concentration (ppm) ± 0.1
1	25.4	14	25.0
2	20.3	15	41.0
3	22.6	16	16.5
4	13.4	17	7.0
5	31.9	18	9.5
6	22.7	19	10.0
7	19.8	20	3.5
8	29.9	21	10.0
9	16.0	22	11.0
10	17.7	23	17.2
11	19.7	24	17.5
12	27.3	25	9.0
13	9.5	26	46.0

Table 5.2: Sulphate ion concentration (ppm) in soil-water extract samples under investigation.

From this table, it is observed that 19.2% of the sites have sulphate concentrations below 10 ppm, 42.3% between 11-20 ppm, 26.9% between 20-30 ppm while only 11.5% have sulphate concentrations above 30 ppm. This analysis shows that the sulphate concentrations were not very different for the sites under investigation.

Visual examination of the unearthed pipes showed that the pipes had black spots spread all over the pipes. It was noted that these spots were difficult to clean because the corrosion products stuck firmly on the pipe. This was largely observed on the pipes laid in soils with high sulphate concentrations.

On examination of Appendix 4, it was noted that higher mass losses were recorded in pipes buried in soils of higher sulphate concentration. However, the mass losses in soils with sulphate concentrations above 20 ppm were about the same for the sites under investigation. The sites with sulphate concentrations below 20 ppm showed lower mass losses, but were all about the same values.

Some sites with medium sulphate concentrations showed high mass losses. This showed that, although the presence of sulphate in the soil increased corrosion of buried pipes, it was not the only parameter responsible for the mass loss of the buried pipe.

It has been reported that the sulphate in acid solutions does not attack both steel and iron to any appreciable extents.

The major effect is the acid attack [Greene and Fontana, 1978]. However, the sulphate in the soil acts as an oxidiser and can be reduced by bacteria to sulphide which is corrosive.

Sulphate reducing bacteria known as vibrio desulfuricans can flourish only in anaerobic soils like water-logged clay containing sulphate and organic matter. Soils containing no free oxygen are non-corrosive but the sulphate-reducing bacteria enable sulphates to act as hydrogen acceptors with reduction to sulphides.

The sulphate reduction takes place in soils with little or no acid which contain no free oxygen for the oxygen-reduction process. Instead of a green or brown rust, a black one is observed due to the formation of iron sulphide. The attack is localised and sometimes very rapid.

The oxygen of the sulphate ions (present in the soil) becomes available for the cathodic reaction, taking the form

$$SO_{4(aq)}^{2-} + 8H_{(aq)}^{+} + 8e^{-} \longrightarrow S_{(aq)}^{2-} + 4H_2O_{(\ell)}$$

The sulphide ions produced combine with Fe^{2+} ions produced in the anodic reaction to give iron sulphide (FeS) which is black in colour.

Research at Manchester [1976 vol. 2 p.173] has shown that chemically prepared iron sulfide can set up corrosion of iron. The iron sulphide above acts as a cathodic surface. Hydrogen sulphide produced by bacterial processes move upto areas where oxygen is available and is converted to sulphuric acid which is very corrosive. If on the other hand, iron

bacteria are present, the Fe^{2+} is oxidized to Fe^{3+}, producing clogging.

Aerobic sulphur-oxidising bacteria, such as thiobacillus thio-oxidans are capable of oxidising elemental sulphur or sulphur-bearing compounds such as FeS, in presence of oxygen, to sulphuric acid.

$FeS_{(s)} \longrightarrow Fe^{2+}_{(aq)} + S^{2-}_{(aq)}$ followed by
$S^{2-}_{(aq)} \xrightarrow{\text{bacteria}} S_{(s)} + 2e^-$, the two electrons are used in the reduction of Fe^{2+}

$$Fe^{2+}_{(aq)} + 2e^- \longrightarrow Fe(s)$$

The atomic sulphur is then oxidized in presence of oxygen to form sulphuric acid

$$2S_{(s)} + 3O_{2(g)} + 2H_2O_{(\ell)} \longrightarrow 2H_2SO_4$$

These organisms thrive best in environments of low pH and can produce localised H_2SO_4. They are found in sewage and domestic wastes which contain sulphur and sulphur compounds.

Sulphate-reducing bacteria and sulphur-oxidising bacteria can operate in a cyclic fashion when soil conditions change. That is sulphate-reducing bacteria grow rapidly during rainy seasons when the soil is wet and air is excluded, and sulphur-oxidizing bacteria grow rapidly during dry seasons when air permeates the soil. Under these conditions, the buried pipelines corrode all the year round and very fast.

5.4 REDOX POTENTIAL MEASUREMENTS

The behaviour of some of the more important and common elements in the earth such as N, C, S, Fe, Mn and other trace metal elements, is strongly dependent upon the redox potential of the environment in which they occur [Garrels and Christ, 1965; Stum and Morgan, 1981]. Redox potential is recorded as the potential measured at an inert metal surface using a recommended reference electrode (eg. hydrogen, calomel etc.).

Redox potential measurement was conducted for twenty six soil samples under this investigation (sec. 4.6). The results obtained were recorded in Table 5.3.

Site	Redox Potential (mV) ± 0.1	Site	Redox Potential (mV) ± 0.1
1	497.0	14	302.0
2	346.6	15	346.6
3	594.0	16	295.0
4	271.0	17	214.0
5	277.0	18	256.0
6	280.0	19	175.0
7	366.0	20	325.6
8	258.5	21	375.0
9	316.3	22	274.0
10	302.0	23	291.0
11	252.0	24	258.0
12	198.0	25	215.0
13	325.2	26	273.1

Table 5.3: Redox potential measurements for soil samples under investigation using SCE.

From Table 5.3 it is noted that the redox potentials vary between 200 mV and 500 mV and can be classified as follows:

Redox potential (mV)	No. of samples
Below 200	2
201-300	13
301-400	9
401-500	1
Above 500	1

It is seen from this classification that majority of the samples have redox potentials upto and below 400 mV.

From the physical appearance of the pipes, it was noted that there was higher corrosion on pipes buried in soils with redox potentials below 300 mV. It was generally observed that the corrosion in the higher redox potential soils was less than in the low redox potential soils.

From Appendix 4, the mass loss by the pipes in the low-redox potential soils was higher than that recorded in the high redox potential soils. The highest mass losses were recorded for pipes buried in soils whose redox potentials are well below 200 mV. It was also noted that in some soils with low redox potentials there was low mass loss. This meant that the reaction involved may have resulted in pitting type of corrosion in which very little mass is lost but the metal losses both mechanical and tensile strength.

Soils of low redox potential may be expected to provide a suitable environment for the proliferation of sulphate-reducing

bacteria. This supports microbiological corrosion and provides localized anodic zone for corrosion due to the differential aeration.

In 1945, Starkey and Wight measured redox potentials in many soils along pipeline distribution systems in U.S.A. They correlated the redox potentials with the severity of soil corrosion as follows [Starkey and Wight, 1945].

Redox potential (mV) NHE	Corrosivity (description)
Below 100	Severe corrosion
100-200	Moderate corrosion
200-400	Slight corrosion
Above 400	Non-corrosive

The Starkey-Wight findings tabulated above agree to some extent with the present investigation. However, their findings fail to explicitly describe the moderate and slight terms in their description of corrosivity. The reference provided also fails to provide details of other soil properties that would influence soil redox potentials, such as pH, acidity/alkalinity, conductivity/resistivity, soluble salts and water content.

In this investigation it has been found the soils which have low chloride ion, high sulphate concentration, high acidity, low electrical conductivity and low moisture retention have low redox potentials. These soils are either sandy or sandy-clay soils which also permit free diffusion of air. In

this case, the parameters named above are responsible for the corrosivity of soils recorded in this investigation.

5.5 SOIL-MOISTURE CONTENT

The soil samples under investigation were analysed for the moisture content. This was done by the constant-mass method and the moisture content calculated as a percentage by mass (Table 5.5).

Site	% Moisture ± 0.1	Site	% Moisture ± 0.1
1	15.2	14	10.7
2	12.5	15	7.6
3	17.2	16	13.9
4	20.4	17	15.8
5	21.6	18	17.4
6	14.7	19	23.6
7	19.8	20	14.7
8	14.6	21	19.3
9	8.3	22	13.9
10	24.3	23	12.9
11	12.9	24	23.7
12	14.2	25	17.8
13	12.6	26	14.9

Table 5.5: Percent moisture content of soil samples under investigation.

From this table, it is observed that the moisture content varies between 10% and 24% with 80% of the samples having moisture content below 20%.

Examination of the corrosion pattern on the buried pipes shows that severe corrosion had taken place in soils with moisture contents above 13%. The corrosion between 13% and 24% moisture, ranged between uniform to pitting type of corrosion. Below 13% moisture content the corrosion was moderate for most of the soils under investigation.

It was also noted that there was a direct relationship between the percent moisture content and the loss in mass of buried pipes. It was generally observed that the higher the moisture content the higher was the mass loss of pipes buried underground.

It was therefore concluded that soil-moisture content was a property of the soil that influenced the corrosion of buried pipe. The same results were observed by Markovic on unprotected buried pipes [T. Markovic, 1956]. He indicated that iron was greatly influenced by the water content of the soil. He noted that the attack increased from negligible value in perfectly dry soil to a maximum where soil was saturated with water (Fig. 2.5).

Gupta also investigated the relationship between soil moisture content and corrosivity and found the same results as above. He incorporated water content and electrical resistivity and his results are graphically represented in Fig. 2.5 [Gupta and Gupta, 1978].

The corrosion of iron and metals in the underground surface at normal or moderate temperatures is as a result of an electrochemical reaction. In this case water is the medium and solvent for the reaction. The overall electrochemical reaction is divided into the anodic processes and cathodic processes.

The anodic process involves the transfer of metal into solution as hydrated ions with an equivalent number of electrons left in the metal.

$$M_{(s)} \longrightarrow M^{n+}.xH_2O_{(aq)} + ne^-$$

For iron we have

$$Fe_{(s)} \longrightarrow Fe^{2+}.6H_2O_{(aq)} + 2e^-$$

The cathodic processes involve assimilation of the excess electrons in the metal by depolarizers (atoms, molecules or ions in the solution that can be reduced at the cathode). eg

$$O_{2(g)} + 4H^+_{(aq)} + 4e^- \longrightarrow 2H_2O_{(\ell)} \quad \text{(acid soils)}$$

$$O_{2(g)} + 2H_2O_{(\ell)} + 4e^- \longrightarrow 4OH^-_{(aq)} \quad \text{(neutral soils)}$$

It is noted from these reactions that water is necessary as a reaction solvent during the corrosion of metals. Water also reacts with the iron forming the hydrated iron complex which is an intermediate product in the corrosion process.

The water is necessary as a solvent of the soluble salts such as chlorides and sulphates that take part in the corrosion process. Water is essential because the oxygen that is dissolved in the water helps in the study of corrosion

of metals immersed in aerated waters. Water helps in the study of redox potentials and electrical resistivity since water is not a good conductor of electricity. It is found that the redox potentials and electric resistivity are directly proportional to the soil-moisture content (secs. 5.4 and 5.8).

5.6 pH, ACIDITY AND ALKALINITY MEASUREMENTS

The pH of soils is of great importance in the determination of soil corrosivity towards underground pipes. Deep mineral soils are less acid than are the humus-rich surface soils. A strongly acid reaction is occasionally found in mineral soils containing pyrite or sulphurous mud or slate as a result of bacterial oxidation.

At pH values low enough for soil water to dissolve the surface oxides, total acidity, as determined by titration, would seem more relevant than pH for judging the corrosivity of the soil.

In the soils under this investigation, titration method was used to determine the acidity and/or alkalinity of the soil-water extracts. The pH of the field-condition, soil-slurry and soil-water extract samples were obtained and recorded in Appendix 2. The acidity and basicity values were recorded in Table 5.6.

Site	Hydrogen ion x 10^{-5} Concentration (m/l)	Site	Hydrogen ion x 10^{-5} Concentration (m/l)
1	1.8	14	3.1
2	1.9	15	2.5
3	2.9	16	3.6
4	1.7	17	2.0
5	5.0	18	3.9
6	1.8	19	1.6
7	2.0	20	10.0
8	9.7	21	10.8
9	3.7	22	9.0
10	4.1	23	2.9
11	0.5	24	7.6
12	3.4	25	2.3
13	2.1	26	1.9

Table 5.6: Acidity/ (mol/l) of soil-water extract samples under investigation.

Examination of both Appendix 2 and Table 5.6 shows that about 90% of the soils under investigation were acidic and only 10% were either neutral or basic. The difference in pH values between the field-condition, soil-slurry and soil-water extract samples was due to the respective dilutions with water.

After determining the pH values, respective titrations were carried out to determine the acidity/alkalinity of the soil-water extract samples. The results showed that majority of the soil-water extract samples were weak acidic solutions.

After unearthing the pipes it was found that corrosion had taken place on the surface of the pipes to varying degrees. It was generally noted that there was a higher attack in

stronger acid soils than in weaker ones.

On examination of Appendix 4, it was noted that those pipes buried in high acid soils had lost more mass than the pipes buried in weaker acid soils. However there are a few cases of high acidity and the corrosion is mild. This showed that even if acidity influences corrosion of pipes it was not the only factor that effects the corrosion of the buried pipes.

In the corrosion process both cathodic and anodic reactions take place. The anodic reaction involves the dissolution of the metal to ions and the cathodic reaction involves the hydrogen evolution. In presence of oxygen hydrated iron(II) is formed in the acid soils. The following are the postulated cathodic reactions

(1) $2H^{+}_{(aq)} + 2e^{-} \longrightarrow H_{2(g)}$

(2) $4H^{+}_{(aq)} + 4e^{-} + O_{2(g)} \longrightarrow 2H_2O_{(\ell)}$ (acid soils)

(3) $2H_2O_{(\ell)} + 4e^{-} + O_{2(g)} \longrightarrow 4OH^{-}_{(aq)}$ (neutral or alkali soils).

In the latter case the water acts as a weak acid. The iron ions released in the anodic reaction combine with the cathodic reaction products to form $Fe(OH)_2$ and $Fe(H_2O)_2$.

In general the cathodic reaction will take place at any point of especially low overpotential where molecular hydrogen can be formed more easily (Fig. 2.1).

Bondurant found in his investigation in the U.S.A. that, for most metals and alloys under his investigation their underground corrosion increased with decreasing pH value of

the soil [Bondurant, 1971]. In strongly acid soils (pH<4.5) corrosion was significantly high even for the more resistant materials such as copper. In 1976, Gerhoold and Cann reported that, except for amphoteric metals like aluminium which are subjected to high corrosion rates in alkaline soils, most alkaline soils are less corrosive. They found that steel corrodes more rapidly in acid soils than in neutral and alkaline soils [Gerhoold and Cann, 1976]. However, these investigators fail to furnish the other conditions of soils under their investigation which could have affected their results.

In this investigation it has been found that the soil corrosivity cannot always be attributed to change in pH because, the electrical conductivity, soluble salts and gases, together with moisture content have also been identified as factors influencing corrosion of underground pipes.

5.7 SOIL TEXTURE ANALYSIS

Among the factors that govern corrosivity of a given soil are (1) porosity (or aeration), (2) electrical conductivity (or resistivity), (3) dissolved salts including depolarizers or inhibitors, (4) moisture content and (5) alkalinity or acidity. Each of these variables may affect the anodic or cathodic polarization characteristics of a metal in the soil. These variables depend very much on the individual soil texture.

Mechanical tests were performed on the soils used in this investigation and the soil texture deduced for each of the soils. Three broad categories were arrived at, for all the

soils; namely sand, silt and clay. The particle sizes increased in the order sand > silt > clay. These categories (respective percentages per soil) were tabulated in Appendix 3.

From this appendix it is observed that the soil textures are not pure sand, silt or clay but each exists as a major while the other two exist as minor constituents. In some cases two constituents form a mixed texture and in all cases the silt forms the lowest composition.

Three soils under investigation were classified as having sandy texture. Visual observation of the unearthed pipes showed that the pipes buried in these soils suffered little but localized corrosion. One of these soils was very corrosive to the pipes buried in it. However, the loss of mass in this case was lower than that observed for the pipes buried in the other two soils in this category.

Considering that sandy soil is porous and permits free diffusion of oxygen, the corrosion in these two sites could be due to the reaction between the oxygen and the buried metal pipe. From the high localized corrosion and the differential aeration effect the chloride ion attack could be associated with the observed corrosion.

The Table 5.6 shows that these three sites had low acid contents which was confirmed by the pH value of Appendix 2. There was no acid reaction and therefore the reaction was the oxide formation on the surface of the pipe. The following reactions were postulated:

Anodic Process

$$Fe_{(s)} \longrightarrow Fe^{2+}_{(aq)} + 2e^-$$

Cathodic Process

$$O_{2(g)} + 2H_2O_{(\ell)} + 4e^- \longrightarrow 4OH^-_{(aq)}$$

followed by the reaction

$$2Fe^{2+}_{(aq)} + 4OH^-_{(aq)} \longrightarrow 2Fe(OH)_{2(s)}$$

followed by

$$Fe(OH)_{2(s)} + \tfrac{1}{2}O_{2(g)} \longrightarrow FeO_{(s)} + 2H_2O_{(\ell)},$$

with a possibility of forming higher oxides such as Fe_2O_3 and F_3O_4. According to Pourbix (1956) E-pH diagrams, the oxides are more stable than the hydroxides at the potentials and pH values under this investigation.

From the unearthed pipes, it was noted that the mass loss was decreasing with time exposure. This meant that the oxide film formed on the metal formed a protective coating preventing further reaction with the metal pipe.

Table 5.1 showed that the chloride content in these soils was low (<20 ppm) and therefore the observed pits could have been due to differential aeration effect only. In general, the visual observation and mass losses showed that these sites had lower corrosion than the other sites under investigation.

Table 5.5 shows that the soil-moisture content was low for the sites under investigation. However, some degree of electrochemical corrosion could be associated with the amount of soil-moisture content present in the soils. Table 5.7 shows

that electrical conductivities were relatively low and could not be associated much with the corrosion observed. However, the presence of differential aeration currents, due to presence of air pockets, could have led to the pitting corrosion of pipes buried in these soils.

From Appendix 3, it is observed that five sites under investigation had mixed texture of sand and clay. In all these cases, sand is the major constituent with a sand to clay ratio between 1.5:1.0 to 2.5:1.0.

The soil-moisture contents are about 15% for all the sites in this category. In this case corrosion would be expected due to water-soluble salts present in the soils. However, the sulphate and chloride ions concentrations were relatively low and could not be fully responsible for the amount of corrosion observed.

Table 5.6 and Appendix 2 showed that the pH values for these sites were average (between 4 and 6) and the soils were acidic. Corrosion of pipes buried in these sites was therefore associated with the high acidity of the soils. This leads to metal dissolution at the anode with hydrogen evolution as the cathodic process.

The presence of high sand content shows that the soil is porous to air and hence to oxygen. Oxygen reaction was also expected with the formation of an oxide film on the buried pipe. The following cathodic processes are expected

$$2H^{+}_{(aq)} + 2e^{-} \longrightarrow H_{2(g)}$$

$$O_{2(g)} + 4H^{+}_{(aq)} + 4e^{-} \longrightarrow 2H_2O_{(\ell)}.$$

while on depleting the hydrogen ions of the acid, further oxidation forms the hydroxyl and oxide films observed above.

Electrical conductivity in these soils was low and the corrosion could be mainly controlled by the presence of high acidity and circulation of oxygen. This resulted in highly localized corrosion due to the differential aeration current flowing between the anodic (no oxygen) sites and cathodic (oxygen-rich) sites.

The other sites under investigation had clay soils whose moisture content varied from one site to another. Most of these soils had moisture content between 15% and 24%. This amount was found to be very favourable for the corrosion process [Romanoff, 1957].

Both Appendix 2 and Table 5.6 showed that these soils were quite acidic. Tables 5.1 and 5.2 showed that both the sulphate and chloride ion concentrations were very high in these soils. Electrical conductivity measurements (Table 5.7) showed that there were high local currents leading to localized corrosion on the buried pipes.

Visual observations of the unearthed pipes from these sites showed either moderate or severe localized corrosion. Results of mass losses showed that mass losses in pipes buried in these sites varied from one site to another. The mass losses were generally higher than those observed for pipes buried in sandy or the sandy-clay soils.

It was generally observed that the corrosion in this category of soils was due to (1) high soil acidity, (2) high salt

(chloride and sulphate) concentrations and (3) differential aeration currents.

Irrespective of the chemical composition of certain earth types, the physical and chemical properties and hence the corrosive properties are strongly dependent on the grain size. The smaller the grain the larger its surface area. The water capacity of the material increases since this depends partly on the wettable surface and partly on the capillarity.

Soil as a corrosive medium is considered as a porous body, formed by more or less solid, partly colloidal, soluble and hygroscopic constituents and living organisms and containing water and air in the pores.

In soils of coarse texture (sands and gravel) there is free air circulation and corrosion approaches the atmospheric type. Soils free of clay and silt have been found to have high placiticity, low-water retention and are not affected by changes in moisture content.

Clay and silt soils are characterised by fine texture, high-water holding capacity, poor aeration and poor drainage. Clay soils shrink and crack when dry and swell on wetting.

Both day and night temperatures and the barometric pressure variations affect air diffusion into the soils. Biological activity in the soil decreases the oxygen content and replace it with gases from metabolic activity such as carbon dioxide and hydrogen sulphide. These gases increase the acidity of the soil and consequently the corrosivity of the soil towards buried metals.

The effect of soil aeration was summarised by Romanoff (1957). In well-aerated soils the rate of pitting, although initially high, falls off rapidly with time because in the presence of an abundant supply of oxygen, oxidation and precipitation of iron as ferric hydroxide occur on the surface of the metal. The protective membrane formed in this manner tends to decrease the rate of pitting with time. In poorly-aerated soils, the initial rate of pitting decreases slowly with time under such conditions the corrosion products remaining in the de-oxidised state tend to diffuse outward into the soil, offering little or no protection to the corroding metal. Even in a well aerated soil an excessive concentration of soluble salt would prevent the precipitation of protective layers of corrosion products and the rate of corrosion would not be decreased with time.

5.8 SOIL CONDUCTIVITY (RESISTIVITY) MEASUREMENTS

Soil electrical conductivity is used as an indicator of soil corrosivity to underground pipes. Twenty six soil samples collected at random from different sites were used in this investigation and the results obtained were recorded in Table 5.7.

Site	Slurry	Soil-water Extract
1	500	650
2	225	300
3	250	320
4	350	400
5	900	1200
6	250	310
7	450	630
8	400	460
9	250	300
10	130	170
11	145	195
12	205	225
13	350	350
14	1000	1200
15	500	550
16	260	350
17	300	350
18	270	250
19	245	300
20	200	205
21	600	800
22	650	950
23	500	850
24	300	550
25	450	750
26	1000	1050

Table 5.7: Electrical conductivity ($\Omega^{-1}cm^{-1}$) of soil slurry and soil-water extracts samples under investigation.

From the Table 5.7 it is observed that about 80% of the soil conductivity values are below 500 $\Omega^{-1}cm^{-1}$;two samples are above 1000 $\Omega^{-1}cm^{-1}$ while the others have conductivity values between 500-1000 $\Omega^{-1}\ cm^{-1}$.

Examination of the unearthed pipes showed that those pipes buried in soils with low resistivity have suffered a large degree of corrosion. This covered about 80% of the sites, according to Table 5.7.

It was also noted from Appendix 4 that there was a higher mass loss on pipes buried in soils with low electrical resistivity.

From these observations, it was noted that soil-electrical resistivity is a factor or a property of the soil that influences corrosion of the underground metal pipes.

Examination of Table 5.5 shows that there is an inverse variation between the soil moisture content and the electrical conductance. That is as the resistivity increases, the moisture content decreases to a limiting factor below which no electrical conductivity is noticed. This shows that the two properties, soil-water content and electrical resistance influence soil corrosivity of underground pipes at the same time but of different magnitudes.

This relationship was also found by Gupta that soil corrosivity increases with decrease in the electrical resistivity value in water, upto a point when maximum resistivity was reached [Gupta S.K. and Gupta B.K., 1979]. As a general

indicator of corrosivity, Gupta came up with the following table showing the relationship between electrical resistivity and corrosivity.

Resistivity (Ω-cm^{-1})	Corrosivity (description)
Below 500	Very corrosive
500 - 1000	Corrosive
1000 - 2000	Moderately corrosive
2000 - 10,000	Mildly corrosive
Above 10,000	Progressively less corrosive

The soil resistivity/conductivity is a measurement of the amount of current circulating within the particular soil type. This current may be a result of the electrolyte of the water-soluble salts in the soil, or the stray currents in the soil. The current could also result between the charge transfer reactions between the metal ions, already present in the soil, and the buried pipe (sec. 5.1).

It should be noted that although soil electrical resistivity is a measure of corrosivity, there are many other factors or properties that influence the corrosion of the underground pipes. These factors work in combination with the soil-moisture content and electrical resistivity because there is no way of isolating any one of them in the soil [Bondurant, 1971; Nace 1971]. The

presence of chloride may result in localized corrosion whereby no noticeable mass loss is recorded on the underground pipe.

However, the amount of electricity measured will depend on the soil-water content and the dissolved salts in the soil.

5.9 POLARIZATION MEASUREMENT

An electrode is no longer at equilibrium when a net current flows to or from its surface. The measured potential of such an electrode is altered to an extent that depends on the magnitude of the external current and its direction. The direction of the potential change always opposes the shift from equilibrium and hence opposes the flow of current, whether the current is impressed or is of galvanic origin. When current flows in a galvanic cell, the anode always becomes more cathodic in potential and the cathode becomes more anodic, the difference of potential becoming smaller.

The science of electrode kinetics has made possible many advances in understanding of corrosion and practical measurement of corrosion rates. The interpretation of corrosion processes by superimposing electrochemical partial processes was developed by Wagner and Traud (1938). They introduced the concepts of electrode potential such as corrosion potential (also called mixed potential or rest potential), corrosion current density, exchange current density and the Tafel slope.

The mixed-potential theory forms the basis for the two electrochemical techniques used to determine corrosion rate.

These are Tafel extrapolation and the linear polarization (resistance polarization) techniques.

5.9.1 Tafel extrapolation

The Tafel extrapolation method for determining corrosion rate was used by Wagner and Traud to verify the mixed potential. This method uses data obtained from cathodic or anodic polarization measurements. A schematic diagram for the polarization measurements is shown in Fig. 3.4.

Prior to application of current (change in potential) the voltameter indicates the corrosion potential (ϕ_{corr}) of the specimen with respect to the reference electrode in the particular solution. After plotting the electrode potential against the logarithm of the applied current figures similar to Fig. 2.18 were obtained and marked as Figs. 1-24.

The anodic and cathodic curves are non-linear at low currents but become linear at higher currents, on a semilogarithmic plot. Applied cathodic current is equal to the difference between the current corresponding to the reduction process and that corresponding to the oxidation or dissolution process. Referring to Figures 1-24 it is apparent that at relatively high applied current densities, the applied current begins to approach total actual cathodic currents since the corresponding total anodic current becomes negligible. The region of linearity is Tafel region. In these figures, the total anodic and cathodic polarization curves (the Tafel slopes)

correspond to hydrogen evolution and metal dissolution. At the corrosion potential (potential at which the Tafel slopes intersect) the rate of hydrogen evolution is equal to the rate of metal dissolution. This point corresponds to the corrosion rate of the system in terms of current density. The accuracy of this method is limited due to interferences from concentration polarization. This method is also applicable to systems with only one reduction process since Tafel region is usually distorted by presence of more than one reduction process.

5.9.2 Linear polarization

Linear polarization analysis is used to overcome the disadvantages of the Tafel extrapolation. Within 20 mV more noble or more active than the corrosion potential, it is observed that the applied current is a linear function of the electrode potential. This is illustrated by the lower figures 1_b-24_b. In these figures the corrosion potential is used as an overvoltage reference point and a plot of overvoltage versus applied anodic and cathodic current shown on a linear relationship. The slope R_P of each of these linear polarization curves is related to the kinetic parameters as follows [Stern and Geary, 1957].

$$R_P = \frac{\Delta E}{\Delta i_{app}} = \frac{\beta a \, \beta c}{2.3(\beta a + \beta c)(i_{corr})}$$

where βa and βc are the Tafel slopes of the anodic and cathodic reactions respectively. The term $\Delta E / \Delta i_{app} = R_P$

is given in ohms (volts/amphere) and can be calculated from the graph. If βa and βc are known, from the previous work, then i_{corr}, the corrosion current density, and hence the corrosion rate, can be calculated.

It was found that within 20 mV of the corrosion potential, either anodic or cathodic, there was a linear relationship. This showed that the electrodes and solutions in this investigation agreed well with the Stern-Geary Equation, above.

Examination of the corrosion rates (corrosion currents) obtained by use of the two techniques shows that the corrosion current for the linear polarization is higher than that obtained in the Tafel extrapolation. The difference is explained by the fact that the Tafel extrapolation is effective for solutions with only one reduction (cathodic) reaction which is not possible in the soil-water extracts. Also the Tafel extrapolation technique gives a lower value due to interferences from concentration activation in the soil-water extracts due to the presence of soluble salts.

It can be concluded that the linear polarization method was a better technique for measuring the corrosion rate in the present investigation.

5.9.3 Polarization measurements of de-aerated solutions

Tomashov described soil as a stationary electrolyte where oxygen diffusion is a rate determining step [Tomashov, 1966]. Aeration has a pronounced effect on underground corrosion since oxygen reduction is the principle cathodic

reaction in soils. Oxygen, either from the atmospheric sources or from oxidizing salts or compounds, stimulates corrosion by combining with the metal ions to form oxides, or hydroxides of the metal.

In this investigation the effect of dissolved air (oxygen) in the soil-water extracts was studied. A vigorous stream of oxygen-free nitrogen was passed through each of the soil-water extract under investigation and polarization measurements carried out as described above. The results so obtained were used to draw the second polarization curves in the Figures 1-24.

It is generally noticed that on the anodic curve the corrosion currents are higher for the de-aerated than for the aerated solutions. The cathodic curve is always lower for the de-aerated solution than for the non-deaerated solution. In the de-aerated solutions the cathodic curve is perfectly linear on the semilogarithmic scale.

From these figures, it is noticed that the removal of oxygen has a marked effect on the shape of the curves. This shows that oxygen is a vital component during the corrosion of the metal immersed in these solutions. The absence of rust on the immersed mild steel electrode showed that almost all the oxygen was removed by bubbling the oxygen-free nitrogen through the solutions under investigation.

The shift of the curve in the de-aerated solution showed that the retardation due to the formation of oxide film

on the working electrode was removed by the oxygen-free nitrogen. In this case other ions in the solutions, including the hydrogen ion, had a better access to the metal surface than when oxygen was present. The linearity of the cathodic curve shows that the principle reduction reaction was eliminated from the solution during de-aeration.

From this experiment it was concluded that corrosion rates were lower in well aerated soils than in poorly aerated soils and these differences can give rise to galvanic corrosion on the buried pipes (sec. 2.3.1). It is possible for the cells of the type

metal | poorly aerated soil | well aerated soil | metal

to be formed where the metal is a pipeline and the same soil covers the metal in both cases but the soil differs in aeration due to drainage or other factors.

When the working electrode was anodically polarized, hydrogen bubbles were observed on the platinum auxiliary electrode. As the potential was reduced the evolution of hydrogen decreased and finally ceased. On further reduction of potential the solution became slightly coloured brown and at the corrosion potential the current was literally zero. Beyond this point, cathodic polarization rendered the solution more coloured and deposits were observed on the working electrode. A point was attained when the change in current was very small for any change in potential resulting in a linear section of the cathodic polarization curve.

The following reactions are postulated to be taking place during the polarization measurement.

Anodic processes:

Metal dissolution: $Fe_{(s)} \longrightarrow Fe^{2+}_{(aq)} + 2e^-$

Metal ion oxidation: $Fe^{2+}_{(aq)} \longrightarrow Fe^{3+}_{(aq)} + e^-$

Cathodic processes:

Hydrogen gas evolution: $2H^+_{(aq)} + 2e^- \longrightarrow H_{2(g)}$

Oxygen reduction (acidic solution): $O_{2(g)} + 4H^+_{(aq)} + 4e^- \longrightarrow 2H_2O_{(\ell)}$

Oxygen reduction (neutral or basic): $O_{2(g)} + 2H_2O_{(\ell)} + 4e^- \longrightarrow 4OH^-_{(aq)}$

Metal ion reduction: $Fe^{3+}_{(aq)} + e^- \longrightarrow Fe^{2+}_{(aq)}$

Metal deposition: $Fe^{2+}_{(aq)} + 2e^- \longrightarrow Fe_{(s)}$

During the rusting of iron, the iron is oxidised to ions which react with oxygen in presence of water to form the unstable iron(II) hydroxide which is further oxidised to the rust, Fe_2O_3. The possible reactions during the rust formation are

$$Fe_{(s)} \longrightarrow Fe^{2+}_{(aq)} + 2e^-$$

$$O_{2(g)} + H_2O_{(\ell)} + 4e^- \longrightarrow 4OH^-_{(aq)}$$

$$2Fe^{2+}_{(aq)} + 4OH^-_{(aq)} \longrightarrow 2Fe(OH)_{2(s)} \text{ (unstable)}$$

$$2Fe(OH)_{2(s)} + H_2O_{(\ell)} + \tfrac{1}{2}O_{2(g)} \longrightarrow 2Fe(OH)_{3(s)} \longrightarrow$$

$$Fe_2O_{3(s)} + 3H_2O_{(\ell)}$$

According to Fig. 2.1 (Pourbaix diagram) the metal ion oxidation and reduction reactions occur to a small extent in the solutions under investigation with pH values between 5-7.5 and potentials considered between +0.5V and -1.0V.

When the solution was de-aerated the other cathodic reactions could have taken place, i.e. the hydrogen ion evolution, metal ion reduction and the metal deposition, since these reactions do not depend on the presence of oxygen. Since the soil-water extracts were slightly acidic (sec. 4.8.2.1), the hydrogen evolution was a possible cathodic reaction which was actually noticed in all cases. In two cases, where the acidity was high, the hydrogen evolution was observed on the working electrode.

On the other hand, if sulphur reducing bacteria was present, the sulphates present in the soil-water extract (sec. 4.5) could be reduced to sulphide in the presence of hydrogen. The hydrogen atoms produced during the cathodic reaction are adsorbed on the iron surface. This hydrogen is then available for the reduction of the sulphate by bacteria. For each equivalent of hydrogen atoms they consume, one equivalent of Fe^{2+} ions enters the solution to form rust and FeS. The possible reactions are:

Anodic process

$$4Fe_{(s)} \longrightarrow 4Fe^{2+}_{(aq)} + 8e^{-}$$

Cathodic processes

$$H^{+}_{(aq)} + e^{-} \longrightarrow H \text{ atom (adsorbed on Fe)}$$

$$2H^{+}_{(aq)} + 2e^{-} \longrightarrow H_{2(g)}$$

Also from the neutral solution we have

$$8H_2O_{(\ell)} \longrightarrow 8H \text{ (adsorbed on Fe)} + 8OH^-_{(aq)} - 8e^-$$

$$Fe_{(s)} + 8H_{ads.} + SO^{2-}_{4(aq)} \xrightarrow{\text{bacteria}} 4H_2O_{(\ell)} + FeS$$

$$FeS_{(s)} + 2H^+_{(aq)} \longrightarrow H_2S_{(g)} + Fe^{2+}_{(aq)}$$

$$Fe^{2+}_{(aq)} + 2OH^-_{(aq)} \longrightarrow Fe(OH)_{2(s)}$$

The anaerobic bacteria thrive well under conditions of pH 5.5-8.5 and certain varieties of bacteria multiply in soils and fresh waters containing sulphates even at temperatures between 60-80°C. These are the conditions of the soil-water extracts under investigations and the presence of bacteria could not be ruled out.

5.9.4 General discussion

From the pH measurements (Appendix 2), it was found that most of the soil-water extract solutions were slightly acidic, pH between 6.0 and 7.6. From the polarization measurements it was observed that the corrosion current was highest for the solution with the lowest pH value. This indicated a metal acid reaction resulting in metal dissolution and hydrogen evolution. This was pronounced on the anodic curve with visible hydrogen bubbles on the auxiliary electrode. In some cases hydrogen bubbles were observed on the working electrode, and this was particularly more noticeable for the de-aerated solutions.

Examination of Table 5.3 (Redox potentials) and the polarization curve shows that those solutions with lower redox potentials showed higher corrosion currents. This showed that the soluble salts in the soil-water extracts were responsible for the flow of current in the solution and particularly responsible for the cathodic reactions.

The soil-water extracts that had high sulphate contents showed high corrosion currents, and particularly so for the de-aerated solutions. This showed that the sulphur-reducing bacteria were present in the solutions under investigation and were responsible for the reduction reaction in absence of oxygen.

It was generally observed that the soil-water extracts that showed high mass loss of metal buried in respective soils, also showed high corrosion currents and vice versa. This shows that the polarization curve measurement technique is a fast way of determining corrosion of such materials whose mass loss would be difficult to measure. These include buried pipes, ship hauls, aeroplanes and chemical plants, to name only a few.

It was noted that other factors which are important in underground corrosion could not be interpreted in terms of corrosion current. These include moisture content, chloride ion concentration and the electrical conductivity.

The free corrosion potentials were noted for both normal and de-aerated soil-water extracts. It was generally observed that the free corrosion potential for de-aerated solutions was lower than that of the aerated solutions.

This difference in potential could be used as a relative measure of the amount of oxygen in the solutions, assuming that the one hour deaeration process removes all the oxygen from the solution. It was generally seen that the solutions which showed high relative oxygen contents had higher loss of mass (Appendices 4 and 5).

The polarization measurement techniques used in this investigation are concluded to have achieved the following:

(1) Rapid method for determining corrosion rate. The techniques can be used to monitor corrosion rates in various process streams.

(2) The technique may be used to measure very low currents which are both difficult and tedious to perform with conventional methods of weight loss or chemical analytical techniques. The measurements of low corrosion rates are especially important in nuclear pharmaceutical, and food processing industries where trace impurities and contamination are problems.

(3) Electrochemical corrosion rate measurements may be used to measure corrosion rate of structures which cannot be visually inspected or subjected to weight loss tests. Underground pipes and tanks and large chemical plant components are examples.

(4) The techniques could also be used to estimate the amount of oxygen in a solution for an electrochemical polarization measurement.

5.10 CONCLUSIONS AND RECOMMENDATIONS

This investigation has found that the corrosivity of soils, under investigation, to the buried steel pipes depends on the following factors (1) acidity or alkalinity, (2) electrical conductivity/resistivity, (3) redox potential, (4) soluble salts including sulphates and chlorides, (5) aeration and (6) soil-moisture content. These factors depend on the chemical and physical properties as well as the texture of the respective soils.

The corrosivity of each soil was determined by the mass loss method and the corrosion current determination techniques. Two techniques were employed for the corrosion current determination. These are the Tafel extrapolation and the linear polarization techniques.

It was found that the corrosivity of the soil increased as the acidity increased and vice versa. In this case the corrosion current measured was higher for high acid content of the soil. It was also found that the mass loss for the pipes buried in high acid soils was higher than those measured for the low-acid soils.

The electrical properties were analysed in terms of electrical resistivity. It was found that where the said resistivity was low, the recorded mass losses were higher than in the high-resistivity soils. The corrosion current observed in the polarization measurements were higher for soils with lower-electrical resistivity than those with higher electrical resistivity.

Soils with high redox potentials showed high mass losses and high corrosion currents.

High chloride and sulphate concentrations in the soils reflected high corrosion currents and respective high mass losses observed on the pipes buried in these soils. However the mass loss observed in chloride soils was lower than those observed for the sulphate soils.

Lower corrosion currents were observed for aerated soils than the de-aerated soils. This was mainly due to the formation of an oxide film on the surface of the metal reducing metal dissolution reaction, in the aerated soils. Higher mass losses were observed on the pipes buried in aerated soils, in presence of moisture, but decreased with time due to the formation of the protective oxide film on the metal surface. However the mass loss continued to increase in cases where both the chloride and oxygen were present at the same time.

It has been observed that the soil samples differed in moisture content. The mass loss for the pipes buried in the soils varied with moisture content. It was found that the soils with higher moisture content showed higher mass losses and vice versa, to pipes buried therein.

The soils were generally classified into three broad classes (1) clay, (2) sandy-clay and (3) sandy soils. The sandy soil was found to have little water-retention capacity and high diffusion of air. In this case, the soils were found to have little corrosive effect. The mass changes and corrosion currents observe

in this class were low. In sandy-clay soils, there was some degree of water-retention and air diffusion was lower than in the sandy soils. The mass changes of pipes and the corrosion currents in this case were observed to be higher than in sandy soils. Therefore these soils were more corrosive to buried pipes than the sandy soils.

In the clay soils, there was high moisture content, high chloride and sulphate concentrations, than in above two classes of soils. Higher acidity was recorded in clay soils than in either sandy or sandy-clay soils. In most of the clay soils, the mass losses of buried pipes was higher than in the sandy or the sandy-clay soils.

It is therefore recommended that soils with higher diffusion of air or soil porous in nature is best for the underground water pipes buried in Nairobi. These soils should be free from cinders or pieces of wood touching the laid pipe directly. It is possible to increase the life of the pipe by thoroughly coating it with a metal or organic coating including bitumen, before burial [Butler and Ison, 1978]. All the wrench and vice marks should be well coated before burial as these form the anodic sites to uncoated pipes. The whole pipe should be changed instead of changing the corroded portion of the pipe. The changed pipe should be properly coated on all parts including the wrench and vice marks.

The soils suggested above should be analysed for the presence of chloride and acid concentrations. High chloride

soil should not be used in the underground pipelines. The acid soils can be avoided by choosing soils low in humus and moisture content or collected away from industrial activities.

Polarization techniques are quick methods of studying corrosion rates. The two methods used in this investigation (sec. 5.9) showed that the linear polarization is favoured to the Tafel extrapolation technique. It is therefore recommended that for determination of corrosion currents of underground pipes, the linear polarization is preferred to the Tafel extrapolation. However, the two methods go hand-in-hand because according to Stern and Geary equations, the anodic and cathodic Tafel slopes are used to calculate corrosion currents [Stern and Geary, 1958], in the linear polarization technique.

REFERENCES

1. Alpha; Standard methods for the examination of water and waste water. 14th Ed. American Public Health Association, Washington D.C. (1975).

2. Back, W. and Barnes, I.; Relation of Electrochemical potentials and iron content to ground water flow patterns. U.S. Geol. Survey. Prof. Paper 498c (1965).

3. Barnes, I.; Field measurement of alkalinity and pH. U.S. Geol. Survey. J. Water Supply paper 1535-H (1964).

4. Bass-Becking, L.G.M., Kaplan, I.R. and Moore, D.; Limits of natural environments in terms of pH and oxidation reduction potentials. J. Geol. 68, 243-284 (1960).

5. Bates, R.G.; "Determination of pH, theory and practice". Wiley N.Y. (1964).

6. Bates, R.G.; Definition of pH scales. Chem. Reviews 42, 1-61 (1948).

7. Beckman, O.A. and Stickney, M.E.; "Anomalies in extinction coefficient measurements". J. Anal. Chem. 25, 869 (1953).

8. Ben-Yaakov, B. and Kaplan, I.R.; Comments on redox potentials by equilibration J. Marine Res. 31, 79-82 (1973).

9. Bennetto, H.P. and Wilmont, A.R.; Electrochemical measurements with amalgam electrodes, Quart. Rev. 25, 501 (1971).

10. Berner, R.A.; Electrode studies of hydrogen sulphide in marine sediments. Geochim. Cosmochim. Acta 27, 563-575 (1963).

11. Bockris, J.M. and Reddy, A.K.N.; Modern electrochemistry Vol. 2. pp880. Plenum Press (1970).

12. Bondurant, D.M.; Proceedings of the 10th Annual Appalachian Underground Corrosion. A short course in West Virginia University, Bull. 103 (1971).

13. Booth, G.H., Cooper, P.M., Cooper, A.W. and Wakerley, D.S.; Criteria of aggressiveness towards buried metals. British Corr. J. 2, 2(3) 104-118 (1967).

14. Boulegue, J. and Michard, G.; Sulphur specifications and redox processes in reducing environments. E.A. Jenne Ed. A.C.S. Symp. Ser. 93, 25-50 (1979).

15. Bricker, O.P.; Some stability relations in the $Mn-O_2-H_2O$ at 25°C and one atmosphere total pressure. Amer. Mineral. 50, 1296-1354 (1965).

16. Butler, G. and Ison, H.C.K.; Corrosion and its protection in waters p. 65. Wiley International N.Y. (1965).

17. Byers, M.G.; General chemistry of the soil. p.119 U.S.A. Govt. Printing Office (1938).

18. Callow, L.M.; Richardson, J.A. and Dawson, J.L.; Accelerated methods of corrosion rate determination. British Corr. J. 11, 123 (1976).

19. Cary, H., Hawes, R.C.; Hooper, P.B.; Duffield, J.J. and George, K.P.; A recording spectropolarimeter. Appl. Opt. 3, 329 (1964).

20. Clark, W.M.; Oxidation-Reduction potentials of organic systems. Williams and Wilkens, Baltimore, Maryland (1960).

21. Conway, B.E.; Electrochemical Data. Elsevier, Amsterdam (1952).

22. Crumpler, T.B., Dyre, W.H. and Spell, A. Simple photoelectric polarimeter . Anal. Chem. J. 27, 1645 (1955).

23. Edmunds, W.M.; Trace elements variations across an oxidation-reduction barrier in a limestone acquifier. Proc. Symp. Hydrogeochem. Biogeochem. Tokyo, 1970 p.500-527 (1973).

24. Evans, U.R.; The corrosion and oxidation of metals. Edward Anold, London (1961).

25. Feth, J.H., Rogers, S.M. and Robertson, C.E.; Chemical composition of snow in Northern Sierra Nevada and other areas. U.S. Geol. Survey; Water supply Pap. 1535J, 6-19 (1964).

26. Fifield, F.W. and Kealey, D.; Principles and Practice of Analytical Chemistry. 2nd Edition p. 276-288, Academic Press (1983).

27. Fontana, M.G. and Greene, N.D.; "Corrosion Engineering". McGrawhill, N.Y. 225 (1978).

28. Garrels, R.M. and Christ, C.L.; Solutions, minerals and Equilibria. Harper, N.Y. (1965).

29. Gerhoold, F.W. and McCann, J.P.; "Corrosion Evaluation of underground telephone cable sheathing materials". Paper No. 31 presented at the NACE Annual conference, Houston, Texas (1976).

30. Gillespie, L.J.; Reduction potentials of bacterial cultures and waterlogged soils. Soil Sci. 9, 199-216 (1920).

31. Goldring, L.S., Hawes, R.C., Hare, G.H., Beckman,O.A. and Stickney, M.E.; Anomalies in extinction coefficient measurements.. Anal. Chem. J. 25, 869 (1953).

32. Gupta, S.K. and Gupta, B.K.; Critical soil moisture content in the underground corrosion of mild steel. Corr. Sc. J. 19, 171-178 (1978).

33. Harned, H.S. and Owen, B.B.; The physical chemistry of electrolytic solutions. Van Nostrand Reinhold, N.Y. (1958).

34. Hartley, A.M. and Axelrod, H.D.; Observations of a boron carbide electrode. J. Electroanal. Chem. 18, 115-121 (1968).

35. Harzdorf, C. and Keim, H.; "Uber Selectivitat-skonstanten von Halogenidelektroden, Zweiter Art. Z. Anal. Chem. 279, 263 (1976).

36. Ives, D.J.G. and Janz, G.J. "Reference Electrodes" Academic Press, N.Y. (1961).

37. Johnson, D.E. and Enke, C.G.; Bipolar pulse technique for fast conductance measurements. Anal. Chem. J. 42, 329-335 (1970).

38. Koryta, J.; Ion-selective electrodes. Cambridge University Press (1975).

39. Koryta, J.; Theory and Application of ion-selective electrodes. Anal. Chem. Acta 61, 329 (1972).

40. Latima, W.J.; Oxidation potentials; 2nd Edition. Prentice-Hall Engle-wood Cliffs N.Y. (1952).

41. Logan, K.H.; "Underground Corrosion". U.S. National Bureau of Standards circular C450; U.S. Govt. Printing Press (1945).

42. Markovic, T.; "Cathodic protection in underground corrosion. J. Underground Corr. 77, 566 (1956).

43. Martell, A.E. and Sillen, L.G.; Stability constants of metal-ion complexes. Supplement 1, Chem. Soc. (1971).

44. McWilliam, I.G.; Modern methods of chemical analysis. 2nd Ed. p.400-431. Wiley International N.Y. (1968).

45. Meehan, E.J. "Optical methods. Emission and Absorption of Radiant Energy and Fundamentals of Spectrophotometry" in the treatise on analytical Chem. I.M. Kolthoff and J.P. Elving, N.Y. Interscience (1964).

46. Midgley, D. and Torrace, K.; An assessment of various types of reference electrodes for use in continuous potentiometric analysis with particular application to highly pure water. Analyst 10, 833 (1976).

47. Minear, R.A. and Keith, L.H.; Water Analysis Vol. 1. Inorganic species Part I, pp.187-190. Academic Press, London (1982).

48. Moody, G.J. and Thomas, J.D.R.; Selective ion-sensitive electrodes, Merrow, Watford (1971).

49. Morris, J.C. and Stumm, W.; Redox equilibria and measurements of potentials in the aquatic environment. Adv. Chem. Ser. 67, 270-285 (1967).

50. Nordstrom, D.K., Jenne, E.A. and Ball, J.B.; Redox equilibria of iron in acid mine waters; A.C.S. Symp. Ser. 93, 51-79 (1979).

51. Nthurima, I.; "Underground corrosion" an MSc. Thesis, University of Nairobi, Kenya (1979).

52. Pearlstein, F. and Teitell, L. ; Material performance 13, 81:22 (1974).

53. Pecsok, L.R., Shield, L.D., Cairns, T. and McWilliams, I.G.; Modern methods of chemical analysis. 2nd Ed. p.400-431 (1968).

54. Perley, G.A.; Composition of pH-Responsive glasses. Anal. Chem. 21, 391-94, 559 (1949).

55. Piper, C.S.; Soil and plant analysis. Interscience Publishers Inc. N.Y. (1947).

56. Price, W.J.; Atomic Absorption Spectrometry. Wiley Heyden Pub. p. 768-770 (1979).

57. Pourbaix, M.; Potential-pH curves. J. Electrochem. Soc. 101, 217c (1954).

58. Pourbaix, M.: Electrochemical equilibrium atlas. Paris (1963).

59. Riggs, O.L., Sudbury, J.D. and Hutchinson, M.; Corrosion analysis of underground systems. Corrosion 16, 94-98 (1960).

60. Rock, P.A.; The use of Henderson equation to eliminate the emf difference between cells with and without liquid junction. Electrochem. Acta 12, 1531-1535 (1967).

61. Romanoff, M.; Underground corrosion. U.S. National Bureau of Standards. Washington D.C. (1957).

62. Schaschl, E. and Marsh, G.A.; "Some new views on soil corrosion". Material Protection J. 2, 11, 8-17 (1963).

63. Scott, G.N.; The use and behaviour of protective coatings on underground pipes. Proc. Amer. Petroleum Inst. 1, 10:78 (1929).

64. Sillen, L.G.; Master variables and activity scales. Adv. Chem. Ser. 67, 45-56 (1967).

65. Sillen, L.G. ; Oxidation state of earth's ocean, and atmosphere. 1. A model calculation on earlier states. Ark kemi 24, 431-456 (1965).

66. Starkey, R.L. and Wight, K.M.; Anaerobic corrosion in soil. Tech. Rept. Amer. Gag. Assoc. (1945).

67. Stern, M. and Geary, A.L.; Polarization resistance measurements in near-neutral waters. J. Electrochem. Soc. 104, 56 (1957).

68. Stern, M. and Makrides, A.C.; Polarization resistance curves. J. Electrochem. Soc. 107, 782 (1960).

69. Stern, M.; Electrochemical methods of corrosion current determination. J. Electrochem. Soc. 102, 609 (1955).

70. Strobell, H.A.; Chemical Instrumentation. 2nd Edition p. 581-585. Interscience (1973).

71. Stumm, W. and Morgan, J.J.; Aquatic chemistry. p583 Wiley Interscience, N.Y. (1970).

72. Stumm, W. and Morgan, J.J.; Aquatic chemistry. 2nd Ed. "Corrosion of iron in near-neutral water solutions". Wiley Interscience N.Y. (1981).

73. Tomashov, N.D.; "Theory of corrosion and protection of metals". The Science of corrosion. MacMillan Co. N.Y. (1966).

74. Tomashov, N.D. and Chernova, G.P.; "Passivity and Protection of metals against corrosion". Plenum Press, N.Y. (1967).

75. Uhlig, H.H. and Review, R.W.; Corrosion and corrosion control. 3rd Ed. Wiley Interscience. p. 2-3 (1985).

76. Uhlig, H.H.; "The cost of corrosion in the United States of America." Chem. Eng. News 2, 2764 (1949).

77. Uhlig, H.H. and Review, R.W.; An introduction to corrosion science and engineering. Wiley Interscience p.27 (1985).

78. Vetter, K.J.; "Electrochemical kinetics" (theoretical aspects). Academic Press, N.Y. London p.107-110 (1967).

79. Van Slyke, D.D.; Measurement of Buffer values and their relationship to the dissociation constant of the buffer and the concentration and reaction of buffer solutions. J. Biol. Chem. 52, 525 (1922).

80. Wanatabe, W. and Devanathan, M.A.; Reversible oxygen electrodes. J. Electrochem. Soc. 111, 615 (1964).

81. Wagner, C. and Traud, W.; Mixed potential determination in water. J. Electrochem. 44, 391 (1938).

82. Wershaw, R.L. and Goldberg, M.C.; High precision conductivity bridge. Anal. Chem. 42, 1180-1181 (1965).

83. Whitfield, M.; Thermodynamic limitations on the use of the platinum electrode in redox potential measurements. Limnol. Oceanogr. 19, 857-865 (1974).

84. Whitfield, M.; "Ion-Selective electrodes for the analysis of natural waters". A.M.S.A. Handbook No.2. The Australian Marine Sciences Association, Sydney (1970).

85. Whitney, M. and Means, T.H.; An electrical method of determining soluble salt content of soils. U.S. Dept. Agric. Division. Soils, Bull. 8, (1987).

86. Zobell, C.E.; Studies on redox potential of marine sediments. Amer. Assoc. Petroleum Geol. 30, 447-513 (1946).

Appendix 1: Concentrations of iron, zinc, copper, magnesium and manganese (in ppm) in the soil-water extracts.

Site	Zinc	Copper	Iron	Manganese	Magnesium
1	0.10	0.80	0.60	1.00	4.00
2	0.55	0.80	0.50	0.10	1.50
3	0.20	0.60	0.05	0.01	4.90
4	0.15	0.80	0.20	0.01	2.20
5	0.20	0.10	1.00	0.20	22.00
6	0.10	0.20	0.20	0.50	1.30
7	0.10	0.60	1.80	0.05	2.20
8	0.50	1.20	7.80	0.60	0.90
9	0.10	0.60	0.05	0.05	0.80
10	0.15	0.40	7.60	0.03	0.35
11	0.10	0.40	2.40	0.05	0.80
12	0.10	0.40	0.01	0.02	1.20
13	0.01	0.20	0.40	1.00	2.90
14	0.01	0.08	0.80	0.70	3.50
15	0.01	0.08	0.20	0.10	4.20
16	0.01	0.04	0.20	1.00	2.20
17	0.01	0.06	0.01	0.20	1.30
18	0.01	0.08	0.60	0.40	4.80
19	0.01	0.04	0.01	0.05	3.50
20	0.02	0.20	0.20	0.05	1.60
21	0.01	0.60	0.01	0.05	1.60
22	0.02	0.40	0.01	0.01	3.70
23	0.01	0.20	0.20	0.05	2.90
24	0.02	0.60	0.40	0.05	4.20
25	0.02	0.40	0.40	0.04	11.30
26	0.02	0.20	0.20	0.01	14.10

Appendix 2: pH values of soil slurry, field condition soil and soil-water extracts of the samples under investigation.

Site	Field Sample	Soil Slurry	Soil-Water Extract
1	6.3	6.5	6.9
2	5.8	6.1	6.3
3	6.0	6.1	6.4
4	4.4	6.8	7.0
5	3.4	4.0	6.2
6	7.4	7.8	7.9
7	5.9	6.4	6.6
8	5.0	6.0	6.4
9	6.0	6.8	6.9
10	5.2	5.6	6.2
11	7.0	7.0	7.2
12	6.4	6.6	6.8
13	6.2	6.9	7.0
14	5.6	6.4	6.6
15	5.4	5.9	6.3
16	5.7	6.2	6.2
17	6.2	7.2	7.6
18	5.4	6.1	6.9
19	6.2	6.6	6.9
20	5.7	6.3	6.4
21	5.6	6.2	6.4
22	4.6	5.8	6.2
23	5.8	6.9	7.0
24	5.3	5.8	6.6
25	5.4	6.5	6.8
26	6.4	6.6	7.0

Appendix 3: Mechanical analysis and soil texture determination of soil samples under investigation.

Site	% Sand	% Silt	% Clay	Texture
1	30	26	44	C
2	26	22	52	C
3	30	16	54	C
4	72	12	16	S_L
5	36	18	46	C
6	70	14	16	S_L
7	16	12	72	C
8	56	12	32	SC_L
9	32	20	48	C
10	24	14	62	C
11	50	18	32	SC_L
12	62	10	28	SC_L
13	36	18	46	C
14	22	20	58	C
15	15	14	54	C
16	32	14	54	C
17	52	14	34	SC_L
18	36	14	50	C
19	80	8	12	S_L
20	26	20	54	C
21	30	10	60	C
22	32	14	54	C
23	32	20	48	C
24	66	10	24	SC_L

Appendix 4 : Loss in metallic mass of laboratory pipe samples (in grams).

Site	Code	4 Months	Code	8 Months	Code	12 Months
1	Y_3	1.06	Y_2	3.04	Y_1	4.02
	B_2	1.72	B_1	1.06	B_3	0.32
	R_1	1.41	R_1	0.53	R_3	0.20
2	Y_3	2.85	Y_2	5.45	Y_1	7.17
	B_1	2.34	B_2	0.86	B_3	0.45
	R_3	3.96	R_2	3.30	R_1	2.17
3	Y_2	2.46	Y_1	3.02	Y_3	3.49
	B_1	1.08	B_2	0.22	B_3	0.28
	R_1	1.66	R_2	0.26	R_3	0.20
4	Y_3	1.64	Y_2	2.16	Y_1	4.57
	B_1	0.91	B_2	0.50	B_3	0.34
	R_3	1.84	R_2	1.58	R_1	0.99
5	Y_3	1.62	Y_1	2.57	Y_2	4.32
	B_1	1.86	B_2	0.50	B_3	0.12
	R_3	0.98	R_2	0.88	R_1	0.44
6	Y_2	0.76	Y_3	3.00	Y_1	3.52
	B_1	1.03	B_3	0.26	B_2	0.13
	R_1	2.78	R_2	1.08	R_3	0.89

Appendix 4: Continued

Site	Code	4 Months	Code	8 Months	Code	12 Months
7	Y_2	2.74	Y_3	3.95	Y_1	3.96
	B_1	0.93	B_3	0.34	B_2	0.22
	R_1	0.12	R_2	0.45	R_3	0.31
8	Y_1	2.74	Y_2	3.26	Y_3	3.93
	B_3	0.76	B_2	0.66	B_1	0.45
	R_3	0.28	R_3	0.26	R_1	0.07
9	Y_3	2.54	Y_1	2.78	Y_2	2.88
	B_2	0.71	B_1	0.65	B_3	0.51
	R_3	1.98	R_1	1.16	R_2	0.26
10	Y_1	2.49	Y_3	3.04	Y_2	3.63
	B_1	0.64	B_2	0.18	B_3	0.16
	R_3	0.45	R_2	0.11	R_1	0.04
11	Y_1	4.95	Y_3	3.97	Y_2	4.93
	B_1	0.88	B_2	1.04	B_3	1.97
	R_3	0.58	R_1	0.30	R_2	0.19
12	Y_3	3.37	Y_1	3.98	Y_2	4.34
	B_3	1.92	B_2	0.57	B_1	0.31
	R_2	0.54	R_3	0.38	R_1	0.14

Appendix 4: Continued

Site	Code	4 Months	Code	8 Months	Code	12 Months
13	Y_1	0.70	Y_3	2.74	Y_2	3.06
	B_3	1.10	B_1	0.46	B_2	0.28
	R_1	1.90	R_3	1.70	R_2	0.88
14	Y_3	1.60	Y_2	1.82	Y_1	2.00
	B_3	2.75	B_2	1.84	B_1	2.75
	R_1	0.88	R_2	0.48	R_3	0.65
15	Y_1	2.12	Y_2	3.56	Y_3	5.10
	B_3	3.03	B_1	2.92	B_2	2.14
	R_1	1.73	R_2	0.25	R_3	0.30
16	Y_1	3.56	Y_2	3.90	Y_3	4.45
	B_1	1.86	B_3	1.08	B_2	0.90
	R_2	1.36	R_1	1.54	R_3	2.78
17	Y_3	1.04	Y_2	2.26	Y_1	3.77
	B_3	1.07	B_1	0.26	B_2	0.37
	R_1	1.42	R_3	0.24	R_2	0.13
18	Y_3	1.72	Y_1	2.09	Y_2	3.78
	B_1	1.32	B_3	0.76	B_2	0.42
	R_1	1.11	R_3	0.65	R_2	0.29

Appendix 4: Continued

Site	Code	4 Months	Code	8 Months	Code	12 Months
19	Y_3	1.80	Y_1	2.94	Y_2	3.10
	B_3	0.10	B_1	0.05	B_2	0.02
	R_1	1.12	R_3	0.76	R_2	0.68
20	Y_1	1.01	Y_2	1.72	Y_3	3.08
	B_2	0.36	B_1	0.86	B_3	0.96
	R_1	1.36	R_3	0.20	R_2	0.17
21	Y_2	0.94	Y_3	1.68	Y_1	3.12
	B_1	1.35	B_3	0.48	B_2	0.22
	R_3	0.65	R_1	0.59	R_2	0.14
22	Y_2	0.68	Y_3	1.56	Y_1	2.98
	B_2	0.27	B_3	0.36	B_1	0.04
	R_2	0.73	R_1	0.32	R_3	0.60
23	Y_2	1.50	Y_3	2.58	Y_1	2.74
	B_3	0.52	B_2	0.36	B_1	0.37
	R_1	0.29	R_3	0.33	R_2	0.20
24	Y_2	1.02	Y_3	1.39	Y_1	3.26
	B_3	0.18	B_1	0.38	B_2	0.14
	R_2	0.32	R_1	0.28	R_3	0.35

Appendix 4: Continued

Site	Code	4 Months	Code	8 Months	Code	12 Months
Diffe-rent Soils	Y_2	0.52	Y_1	1.49	Y_3	1.69
	B_3	0.82	B_1	1.15	B_2	0.84
	R_1	0.82	R_3	1.05	R_2	1.06

Appendix 5: Corrosion parameters obtained from electrochemical polarization measurements.

Sample No.	Tafel slopes β/mV		Corrosion Currents (μA)		Corrosion potential		
	βa (mV	βc (mV)	Tafel Extra-polation (μA)	Linear Polari-zation (μA)	Before de-aera-tion (μA)	De-aerated (mV)	Difference (mV
1	75	900	9.5	17.2	655	705	50
2	70.6	1300	13.4	18.1	665	765	100
3	94	1120	9.5	13.2	655	765	110
4	89	550	8.4	10.4	745	805	60
5	109	1200	5.8	16.9	725	755	30
6	145	1000	11.5	17.7	730	785	55
7	133	4600	17.9	18.7	705	765	60
8	66.7	400	6.3	7.25	765	785	20
9	80	667	7.9	8.9	745	785	40
10	156	1200	12.2	13.8	675	770	95
11	140	640	8.0	11.7	755	785	30
12	109	2000	15.8	21.8	665	715	50
13	108	700	9.5	10.9	725	780	55
14	111	977	16.0	19.3	680	745	65
15	114	2200	13.1	16.6	690	760	70
16	120	1455	18.9	24.8	690	770	80

Appendix 5 Continued

Sample No.	Tafel slopes β/mV		Corrosion currents (μA)		Corrosion potential		
	βa (mV)	β c (mV)	Tafel Extra-polation (μA)	Linear Polari-zation (μA)	Before de-aera-tion (μV)	de-aerated (mV)	Difference (mV)
17	109	1200	10.0	11.0	735	775	40
18	169	875	17.0	26.3	630	775	145
19	114	600	7.5	13.8	715	785	70
20	140	1067	14.2	13.1	705	760	55
21	140	1400	14.1	17.9	705	770	65
22	80	1267	11.5	22.2	625	755	130
23	133	1334	17.0	29.0	655	780	125
24	133	1818	10.5	16.1	695	780	85

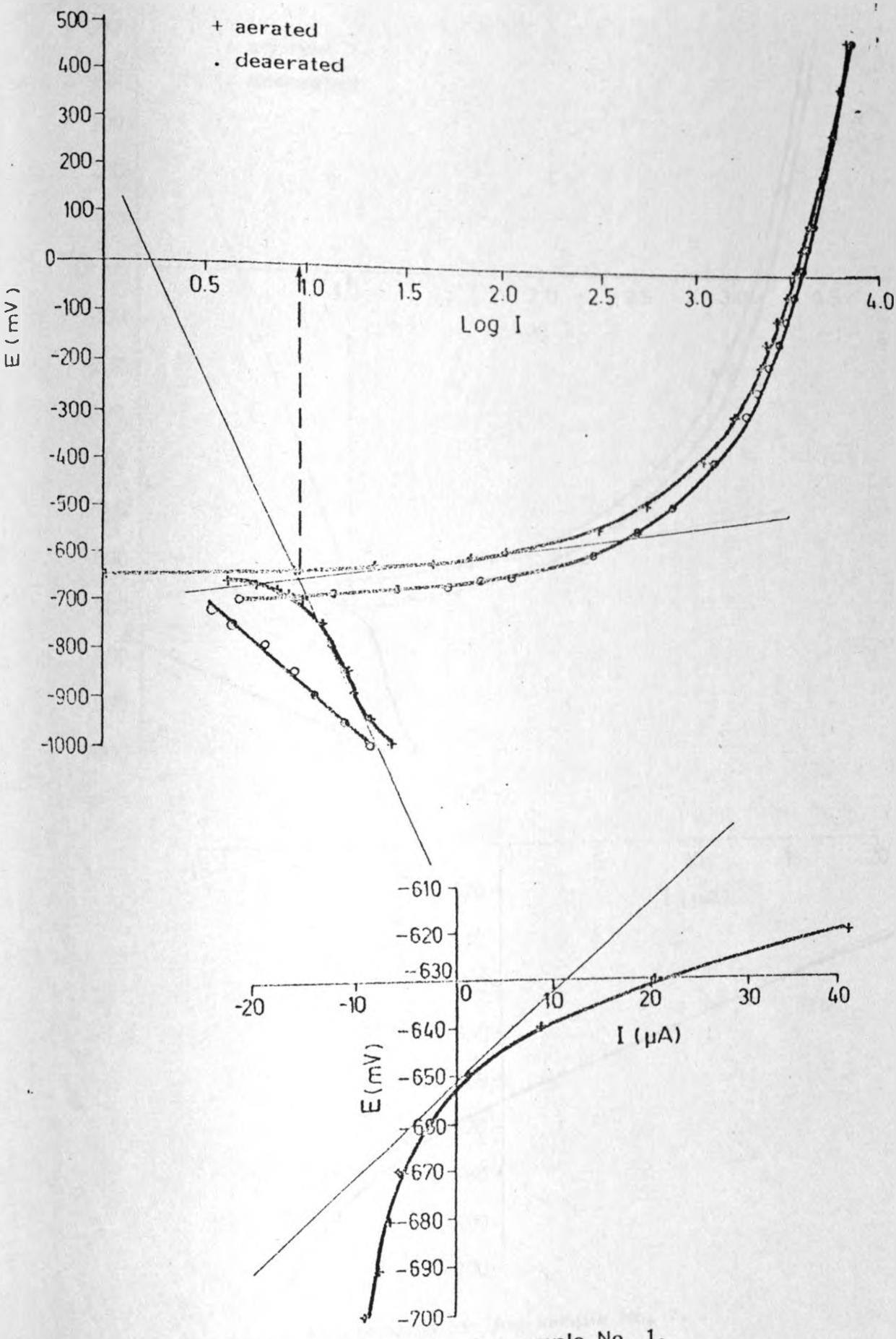

Fig. 1: Corrosion current determination for sample No. 1.

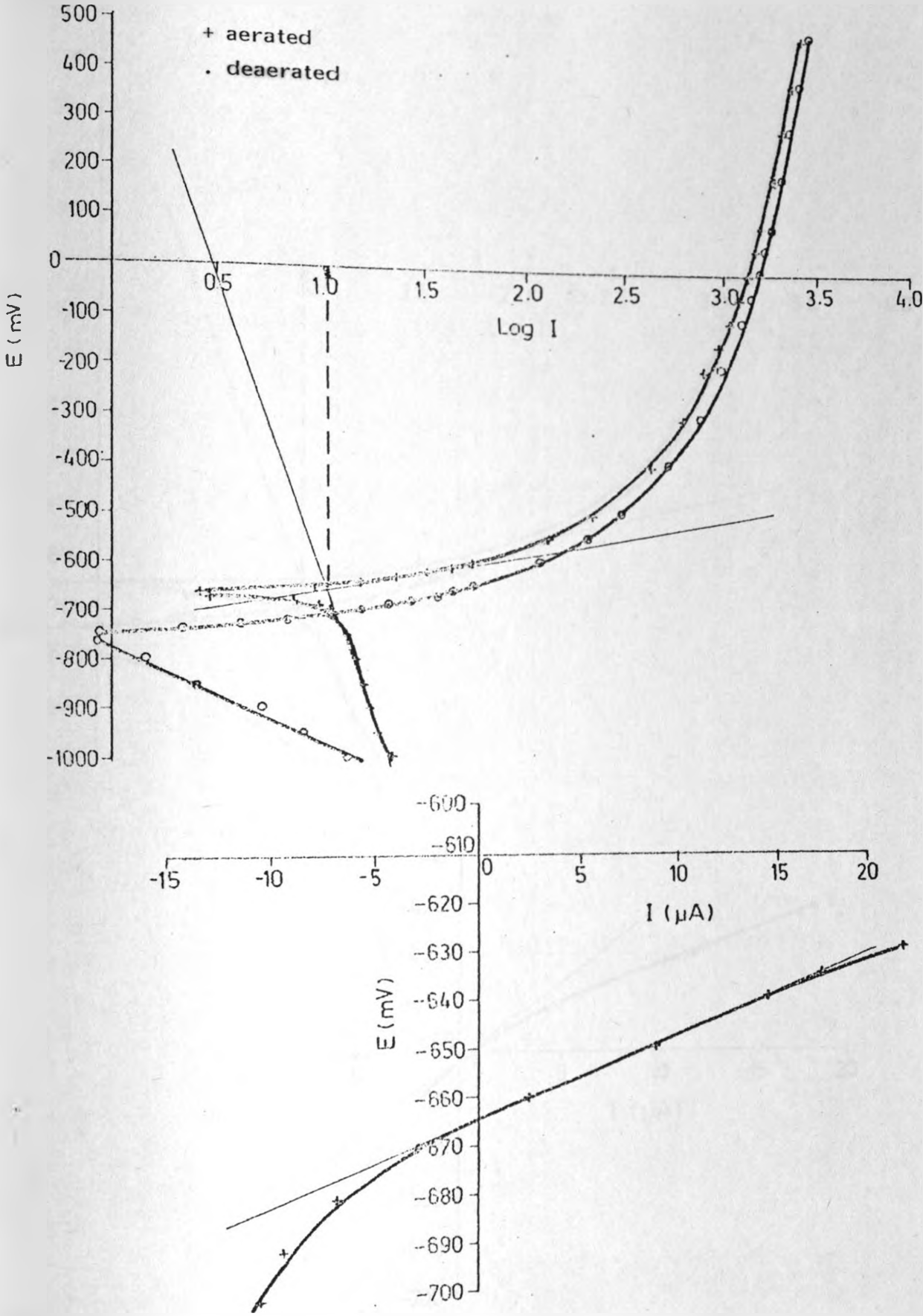

Fig. 2: Corrosion current determination for sample No. 2.

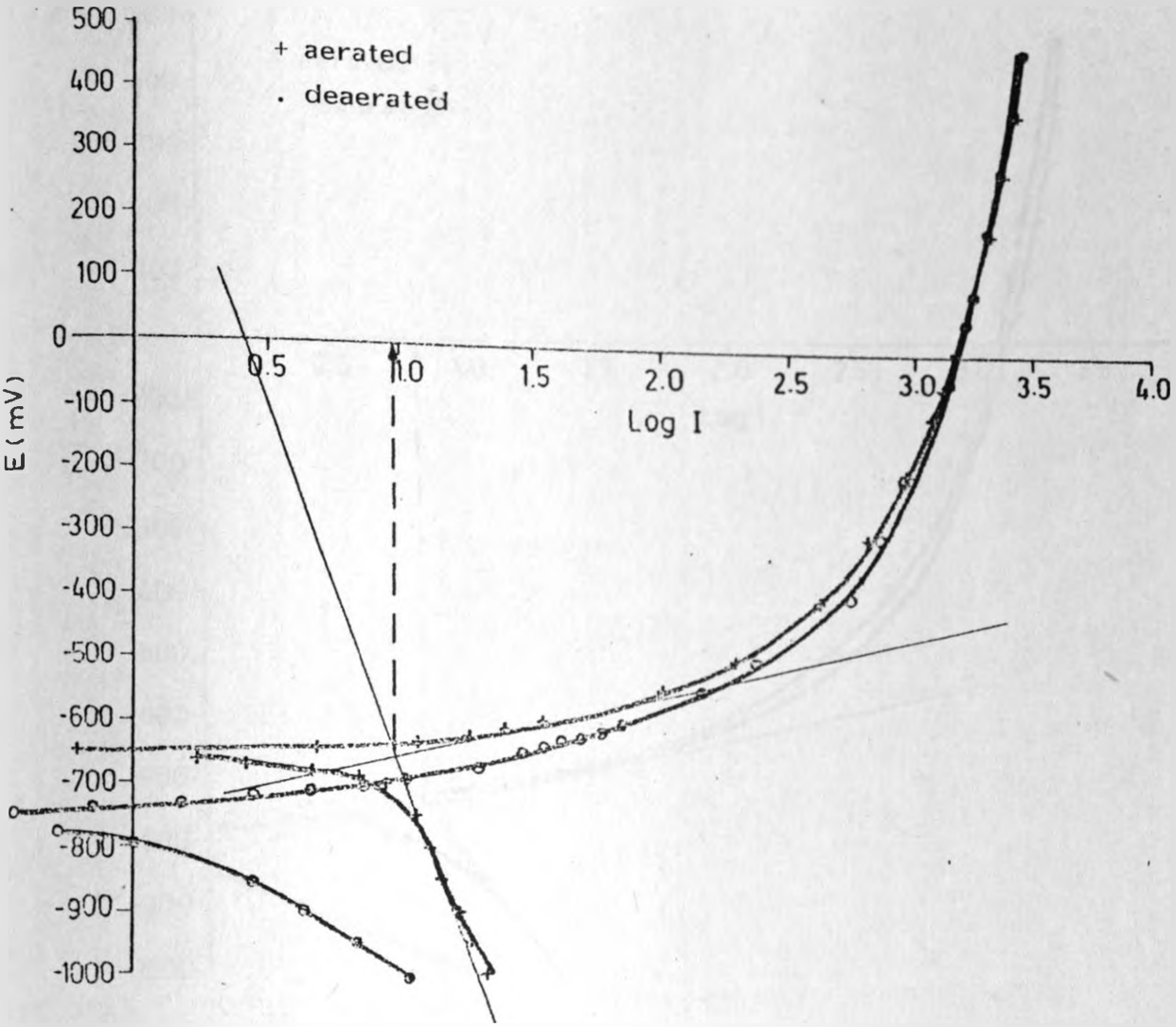

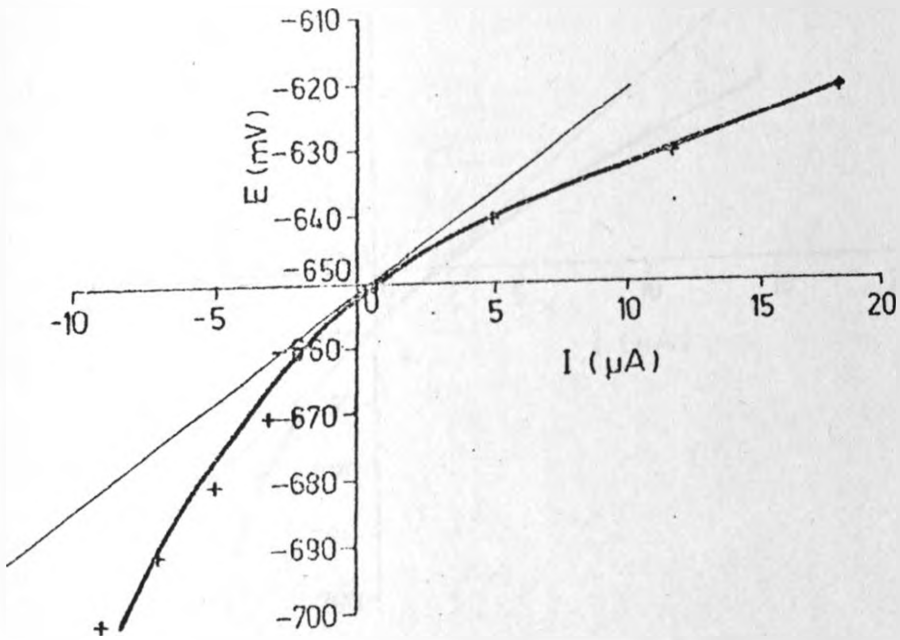

Fig. 3: Corrosion current determination for sample No. 3.

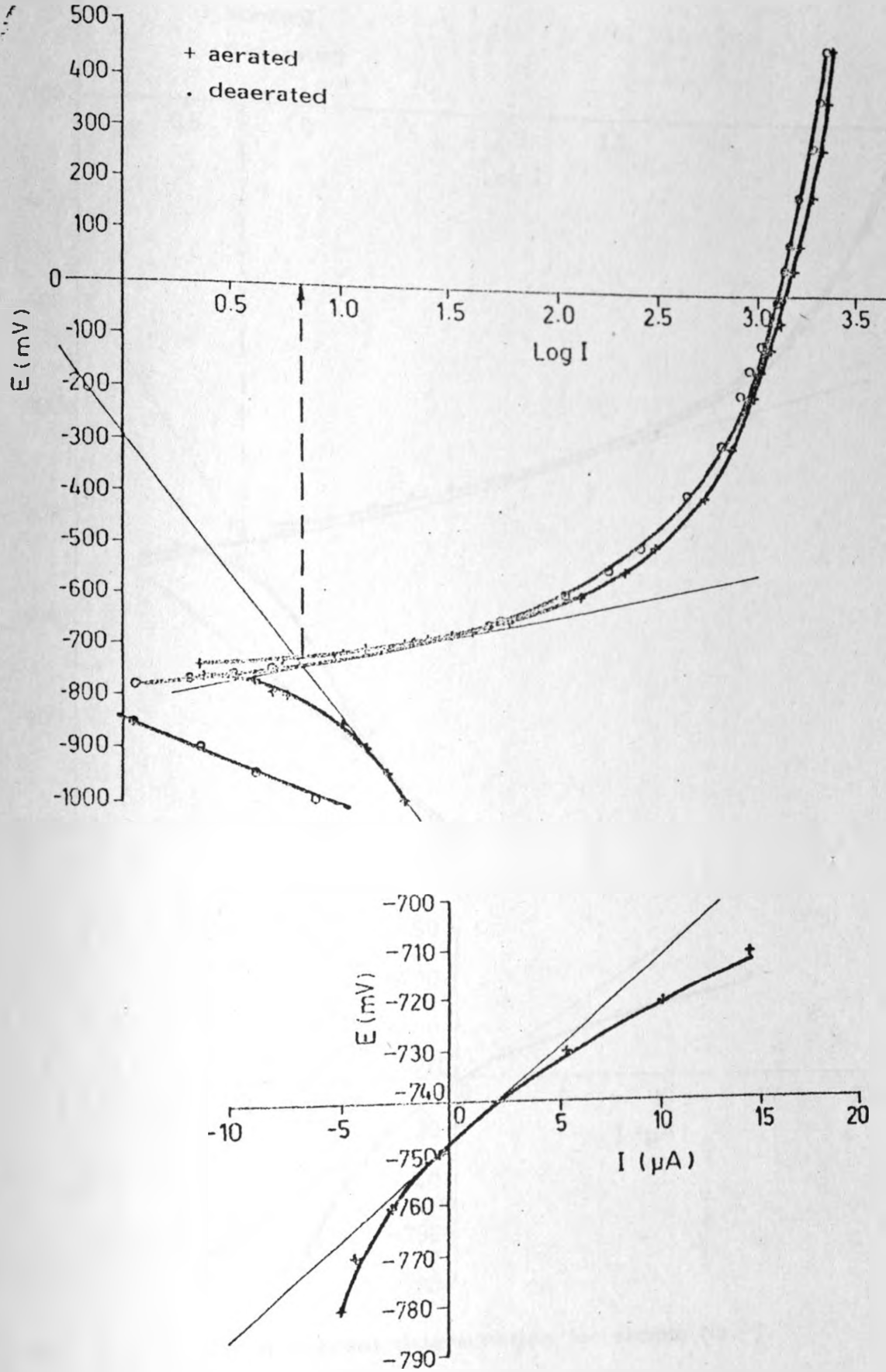

Fig. 4: Corrosion current determination for sample No. 4.

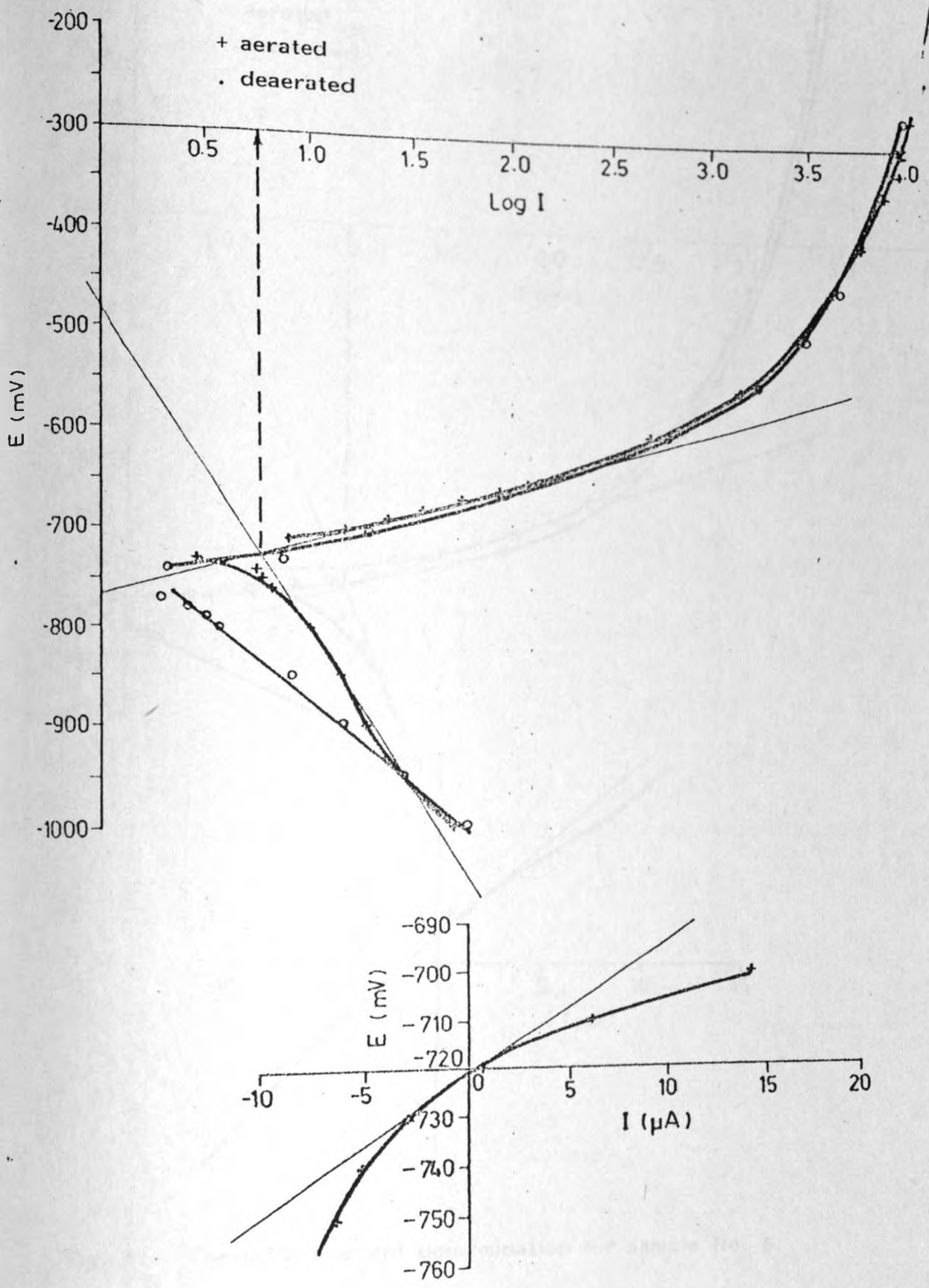

Fig. 5: Corrosion current determination for sample No. 5.

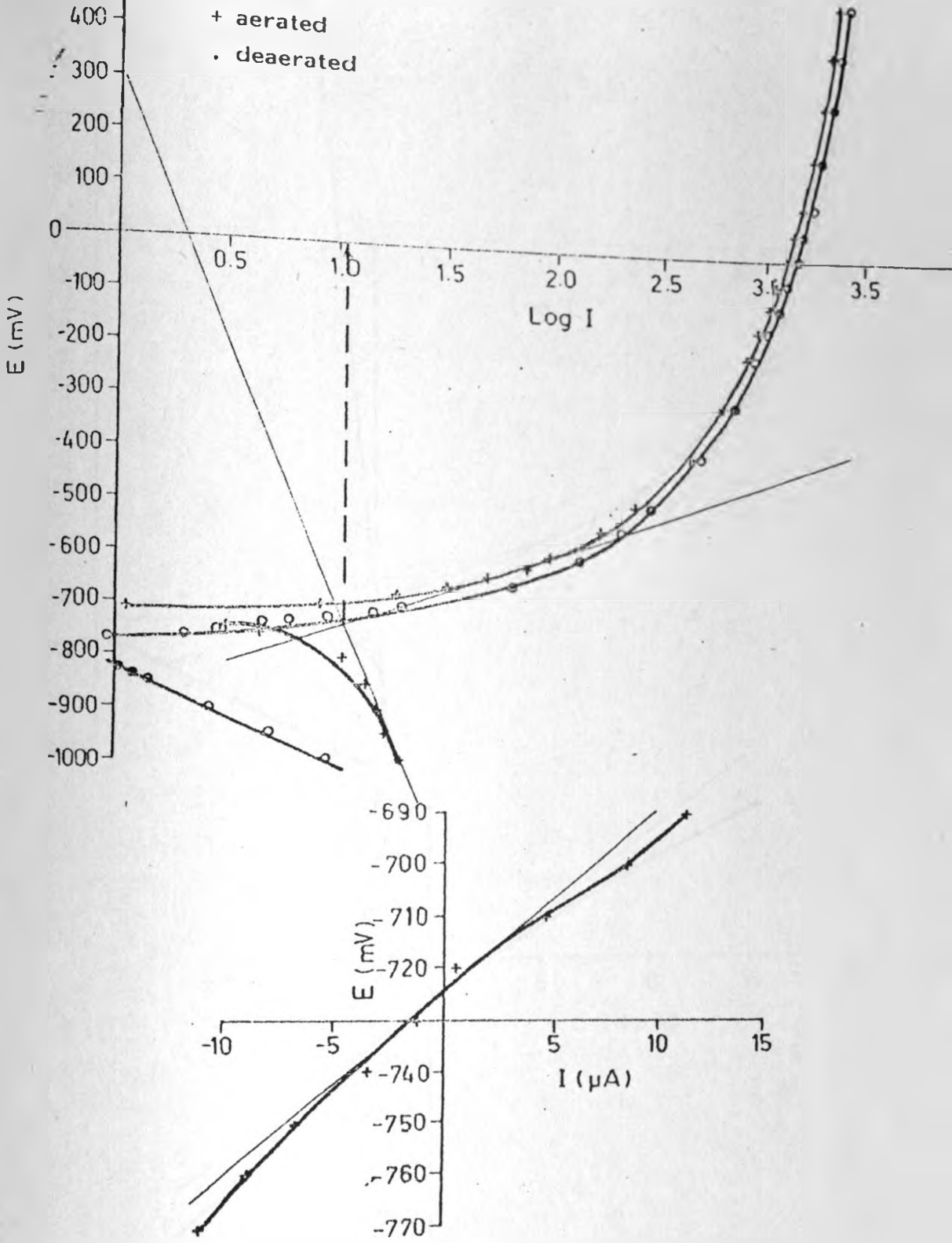

Fig. 6: Corrosion current determination for sample No. 6.

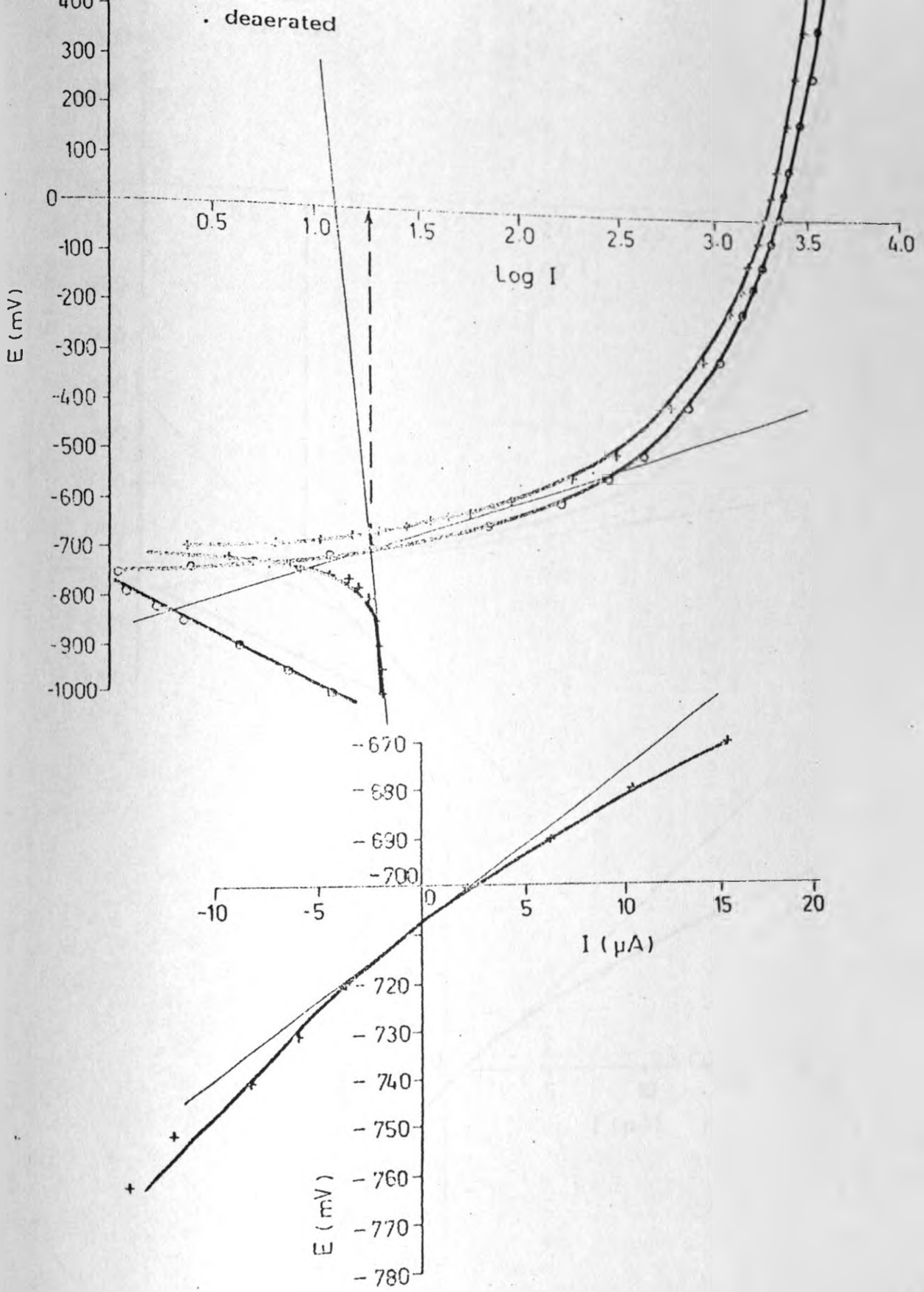

Fig. 7: Corrosion current determination for sample No. 7.

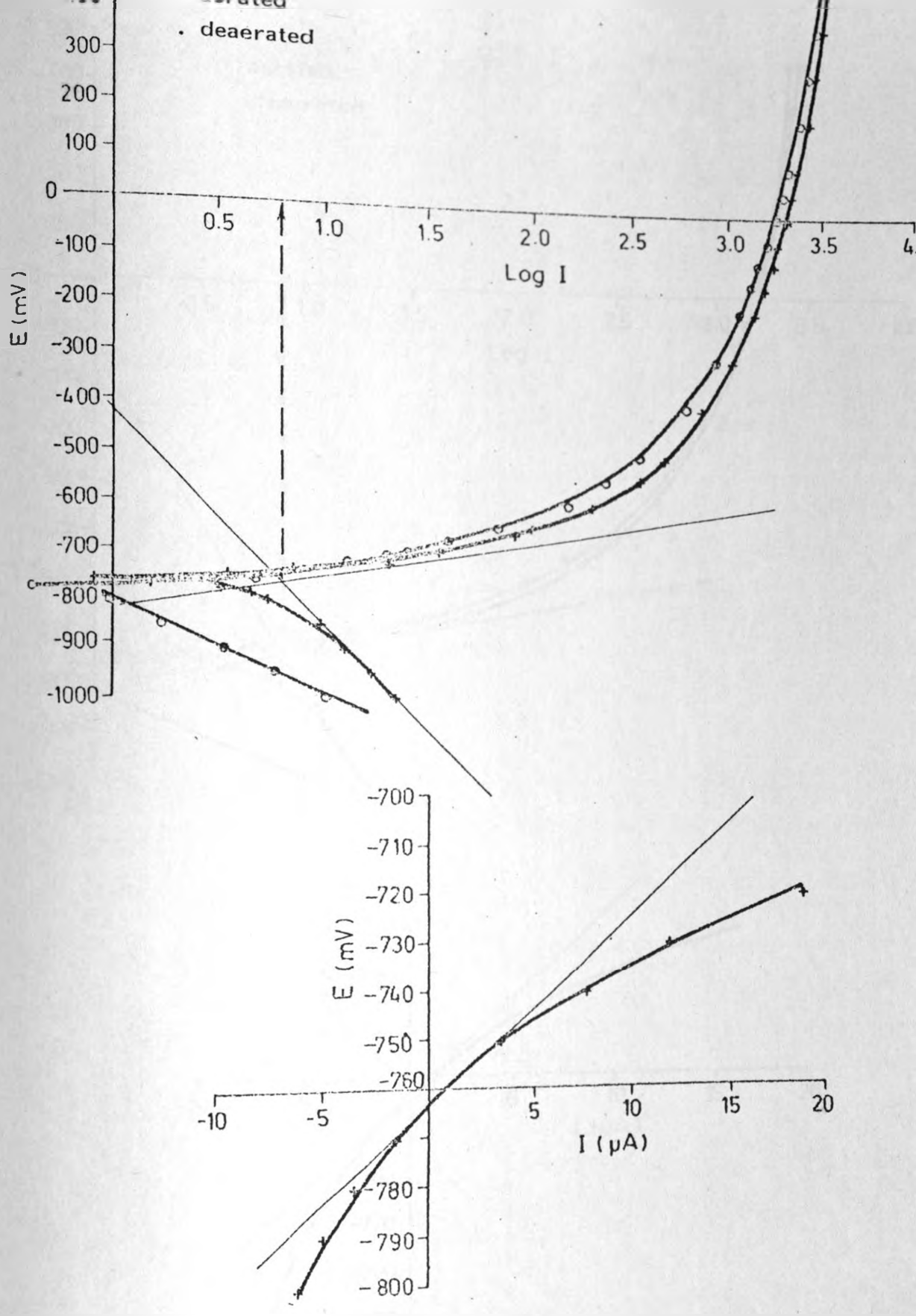

Fig. 8: Corrosion current determination for sample No. 8.

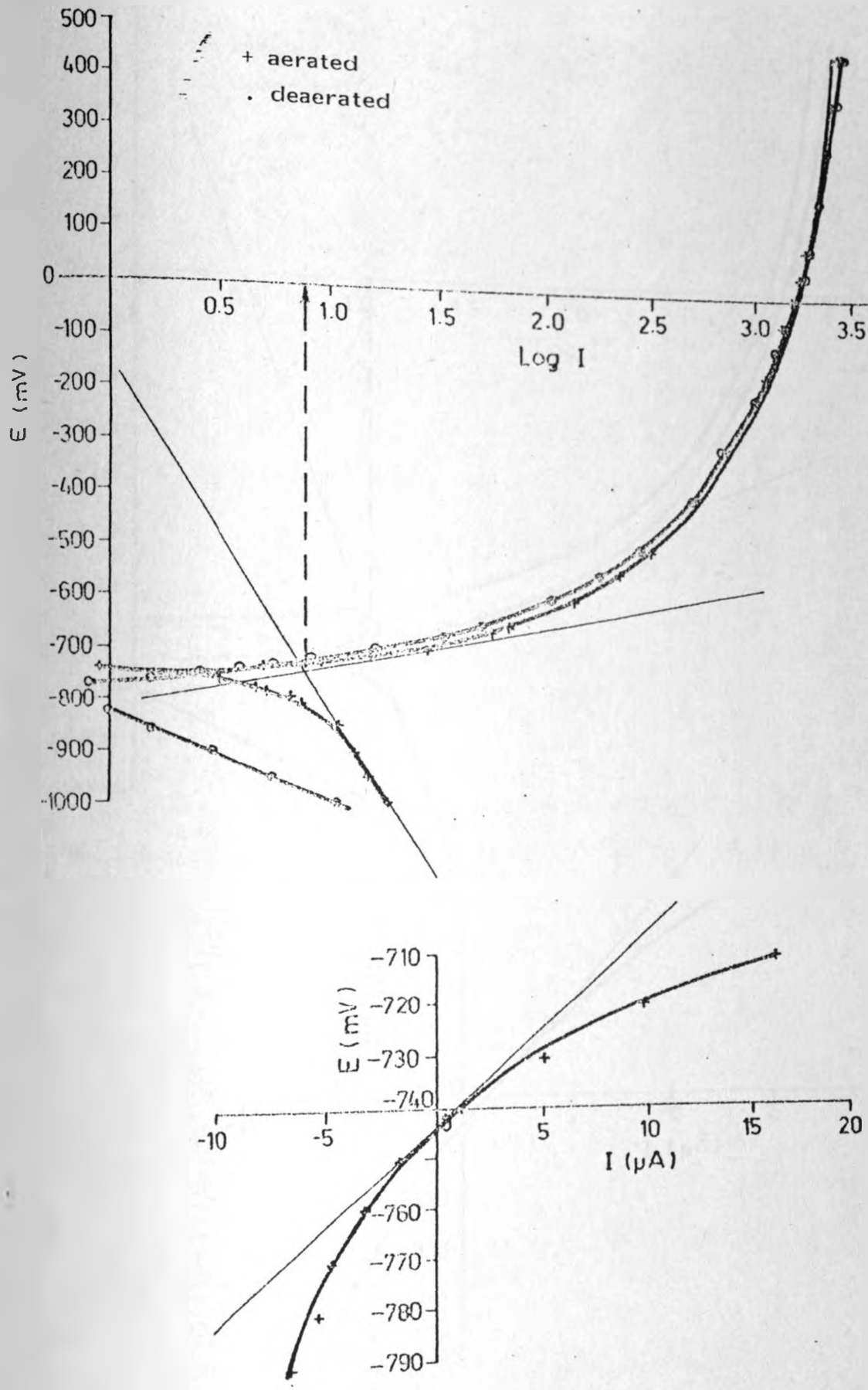

Fig. 9: Corrosion current determination for sample No. 9.

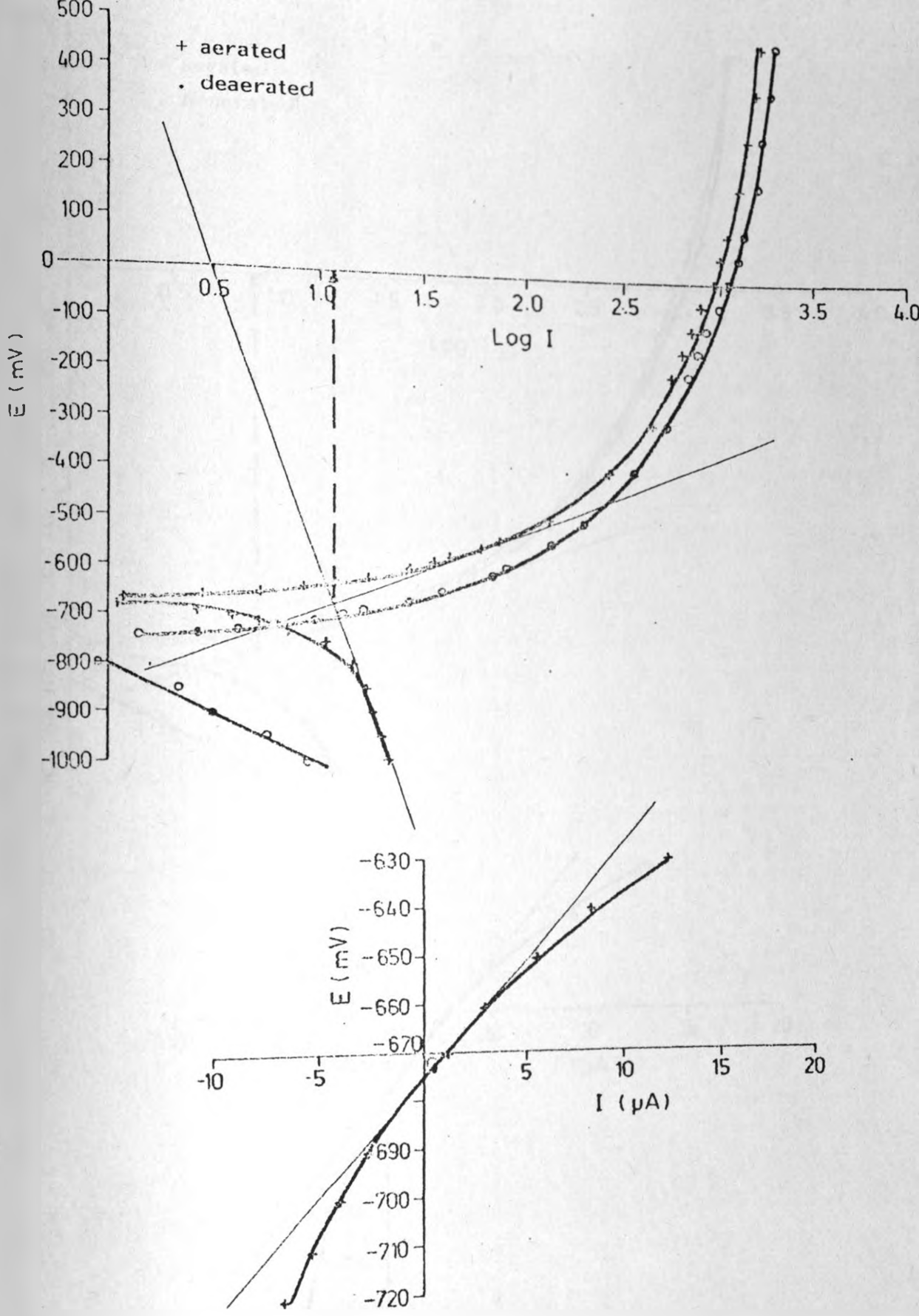

Fig. 10: Corrosion current determination for sample No. 10.

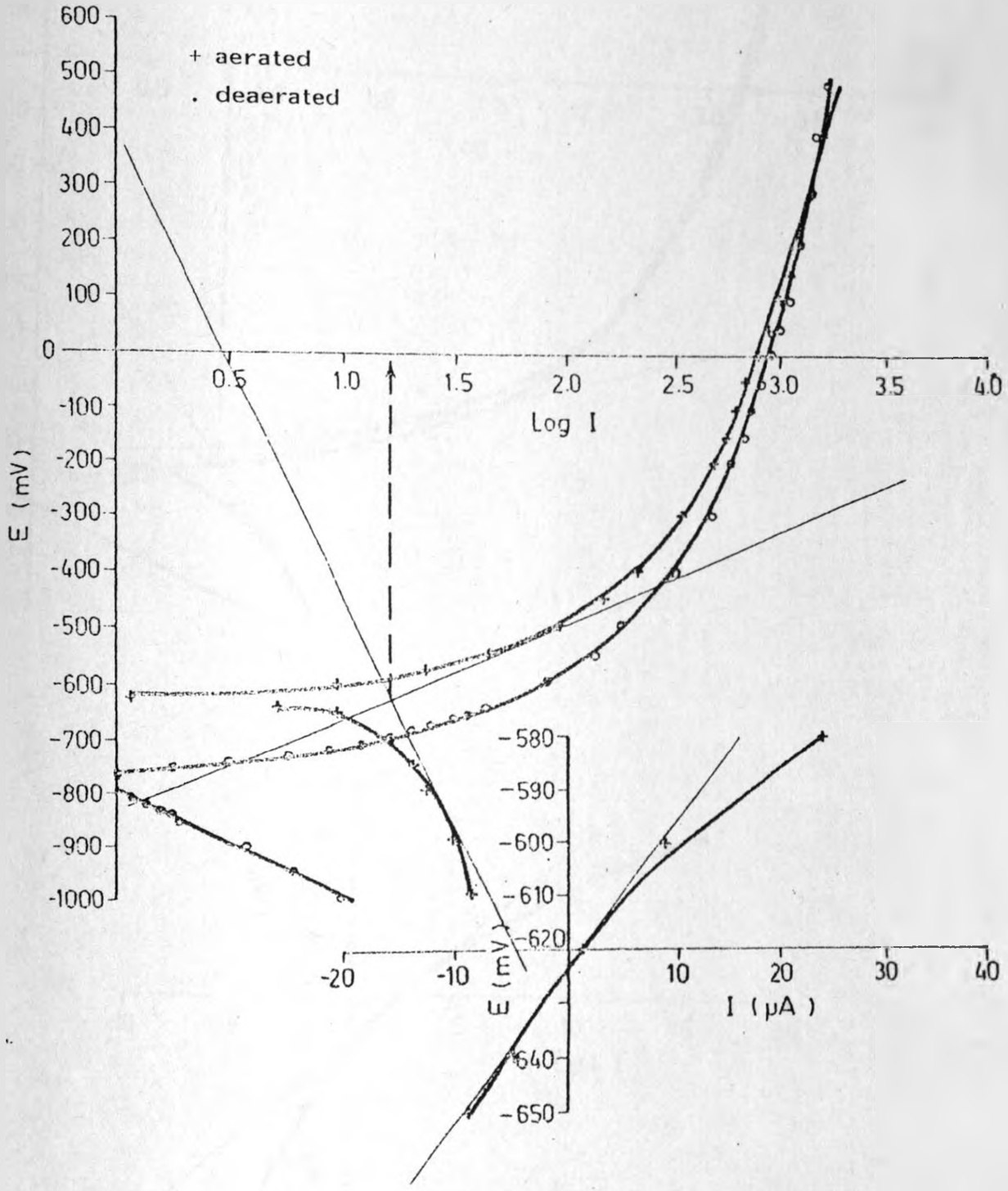

Fig. 18: Corrosion current determination for sample No. 18.

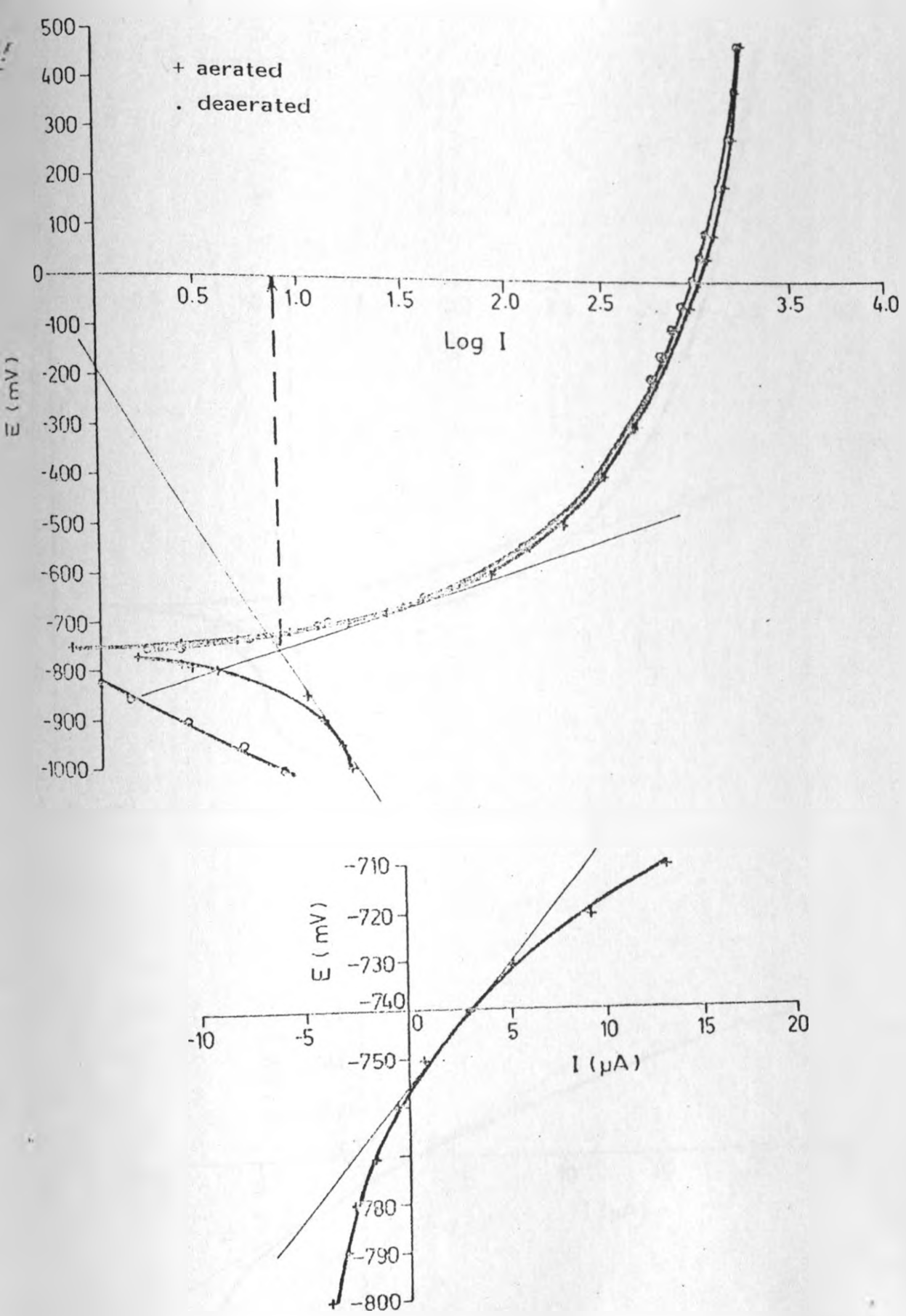

Fig. 11: Corrosion current determination for sample No. 11.

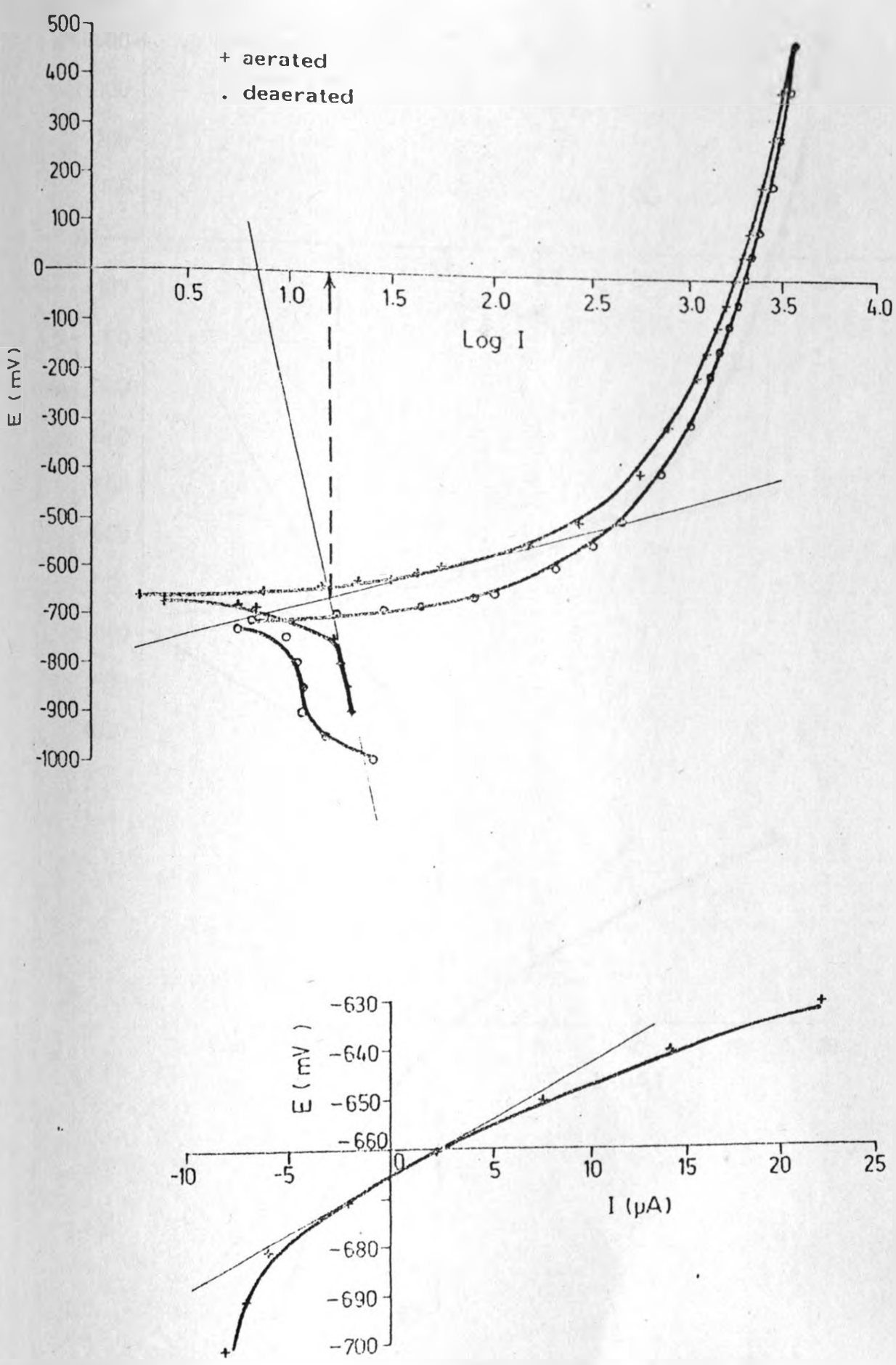

Fig. 12 Corrosion current determination for sample No. 12.

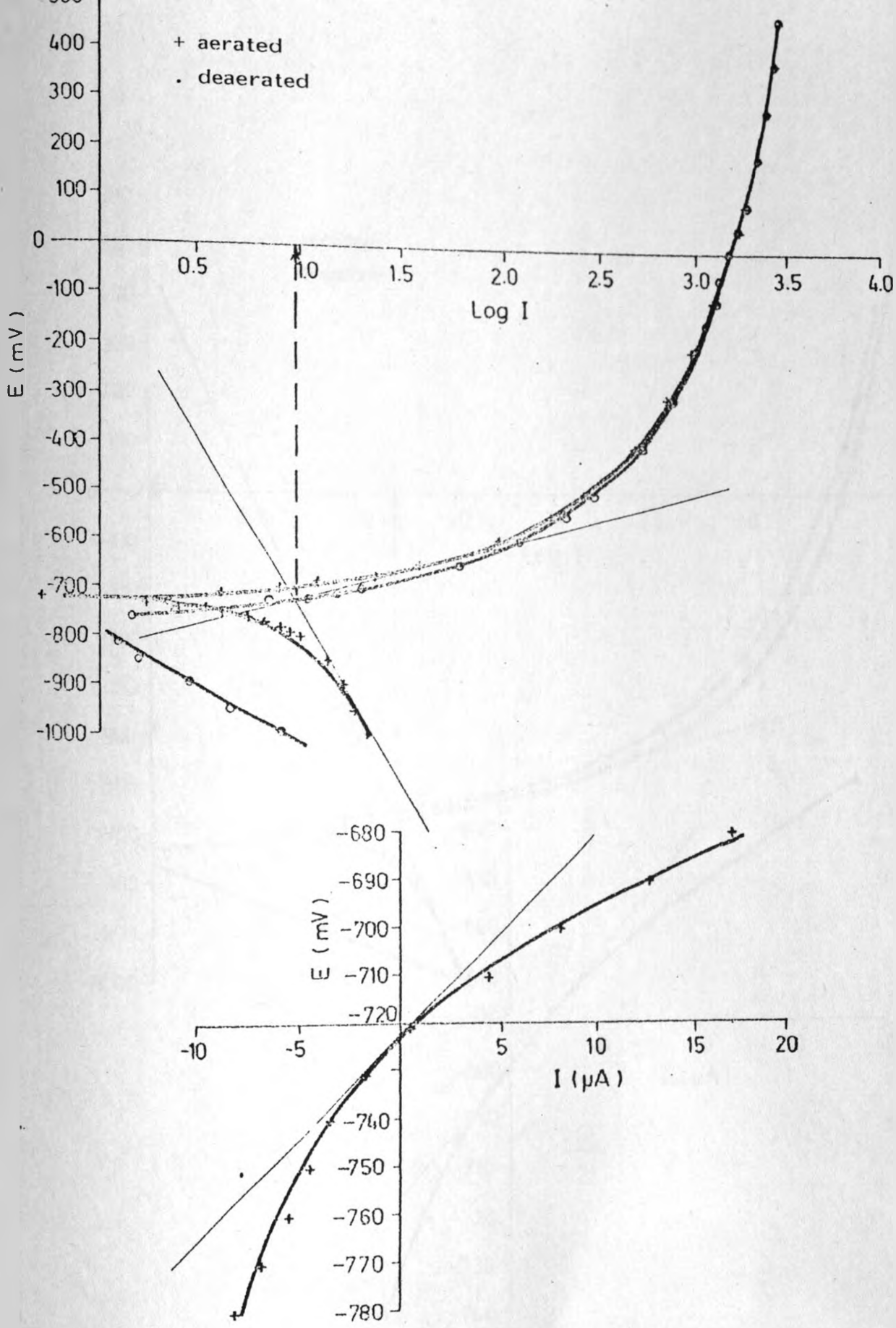

Fig. 13: Corrosion current determination for sample No. 13.

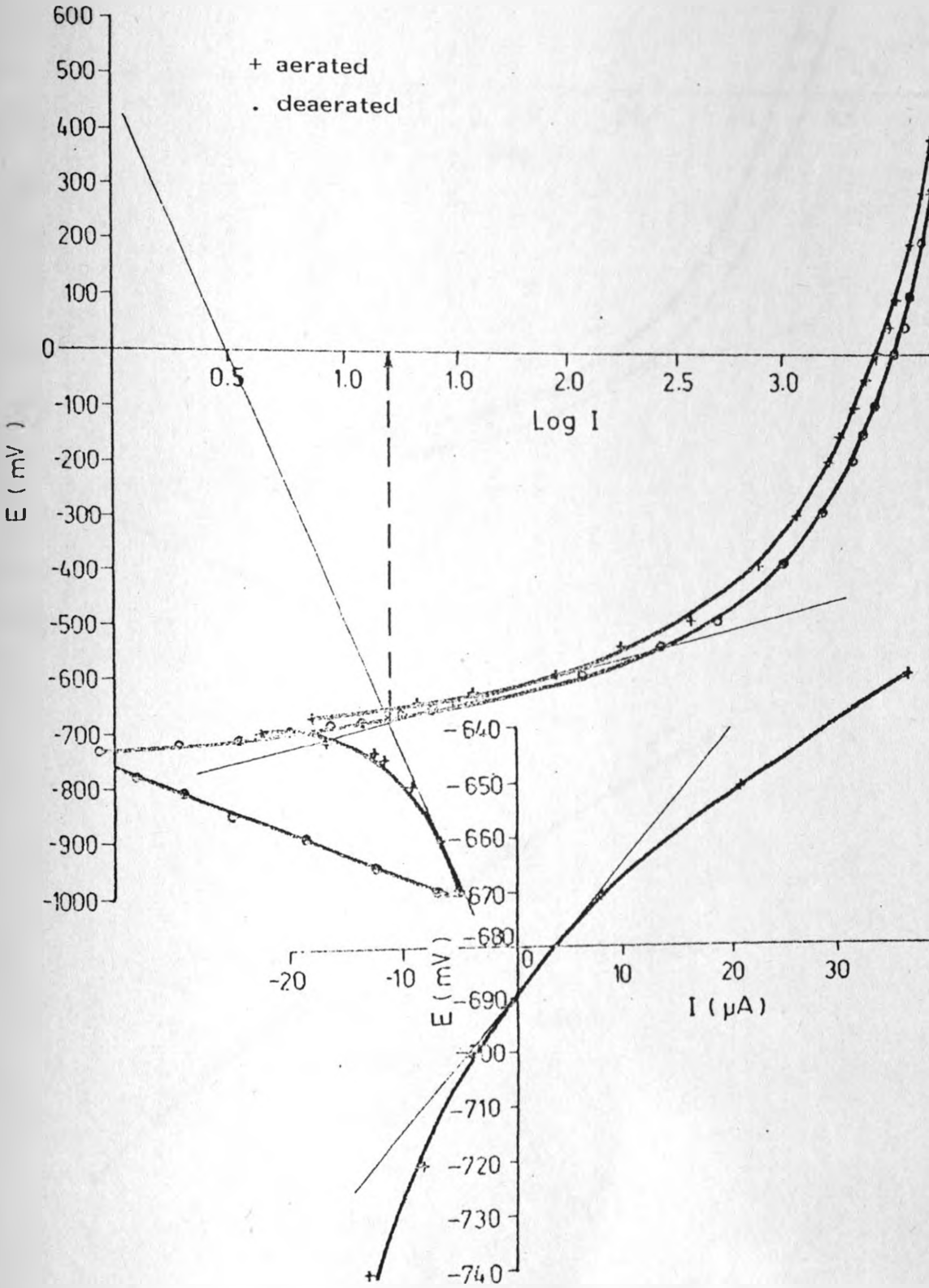

Fig. 14: Corrosion current determination for sample No. 14.

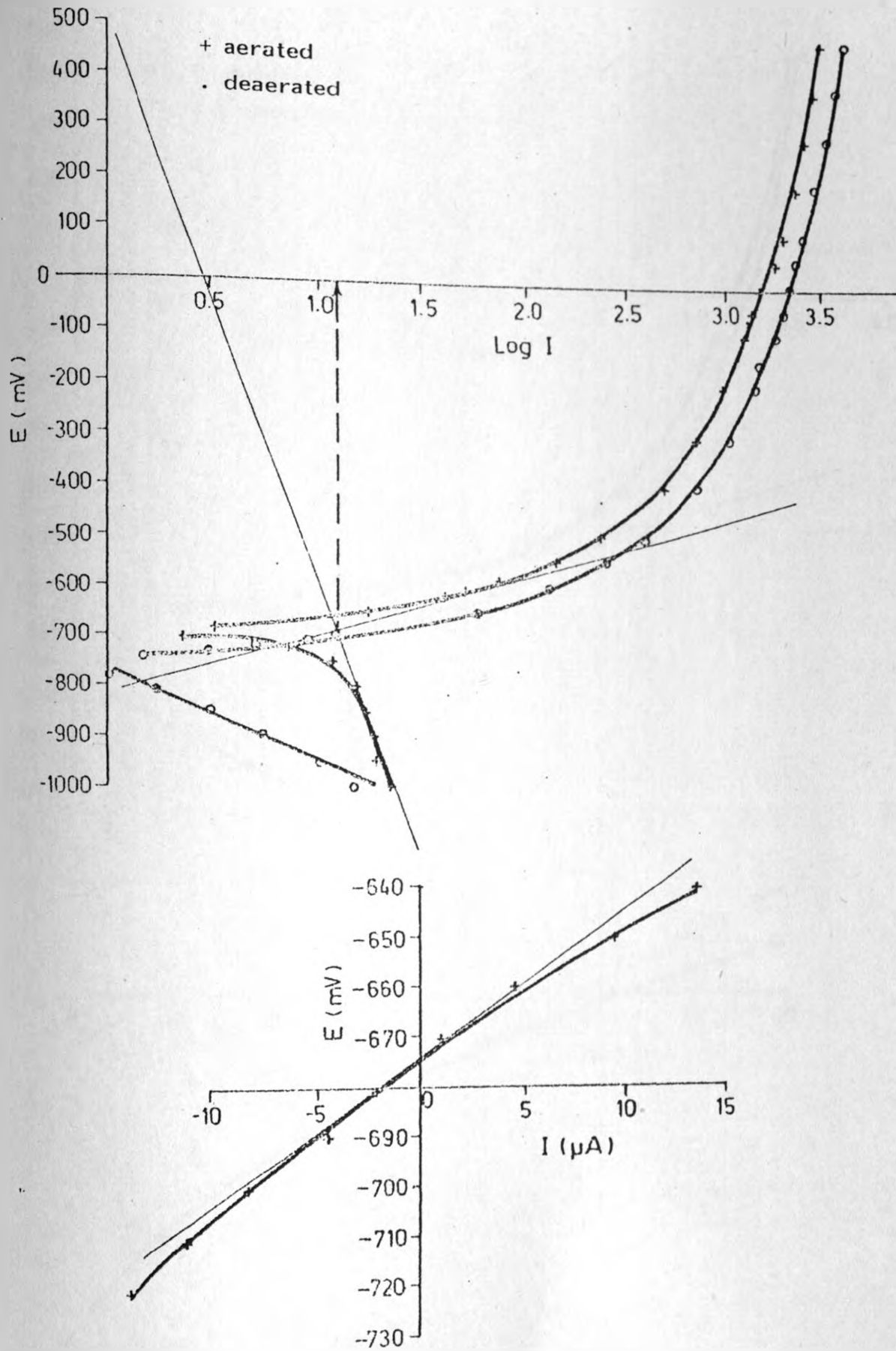

Fig. 15: Corrosion current determination for sample No. 15.

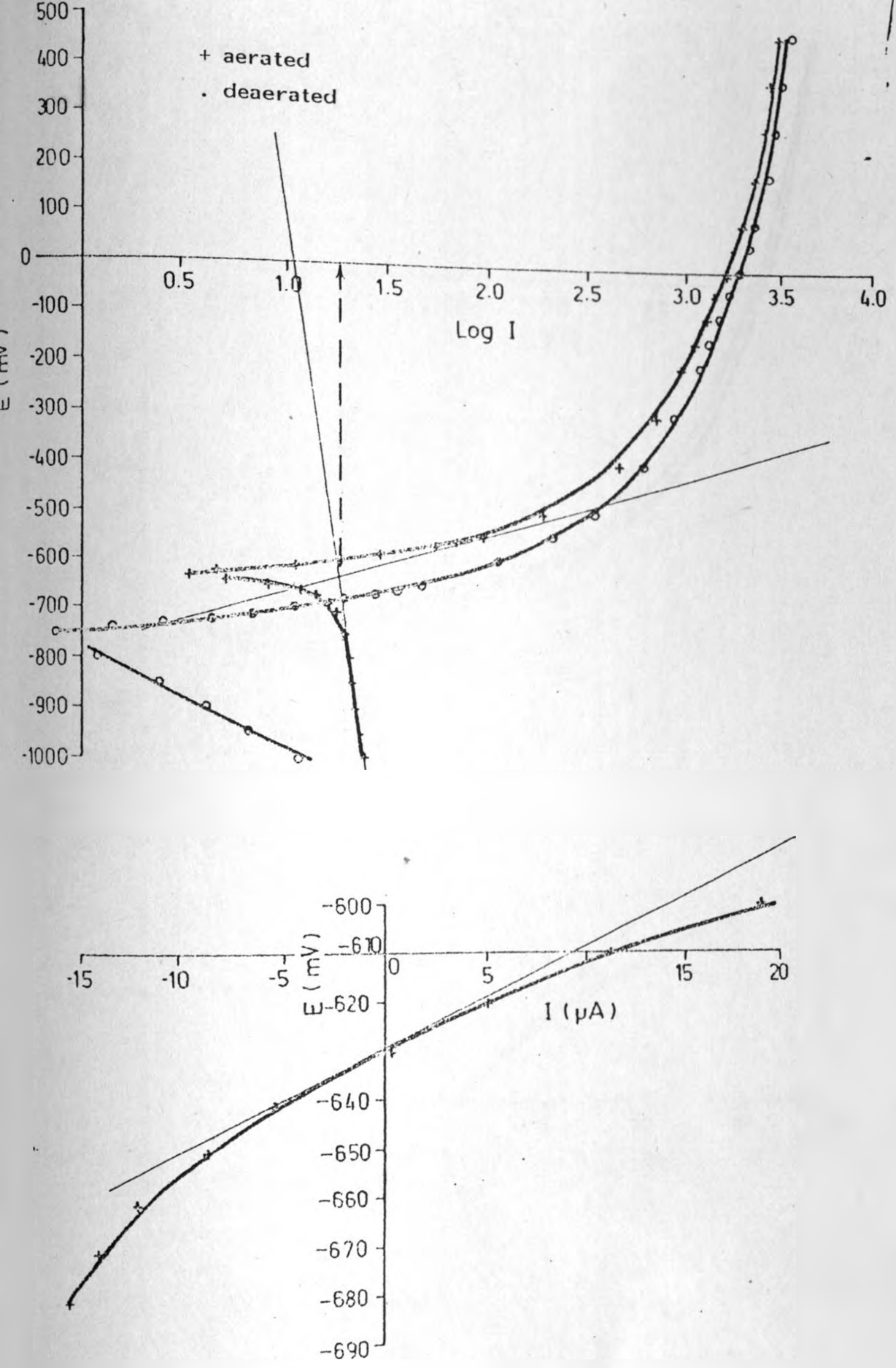

Fig. 16: Corrosion current determination for sample No. 16.

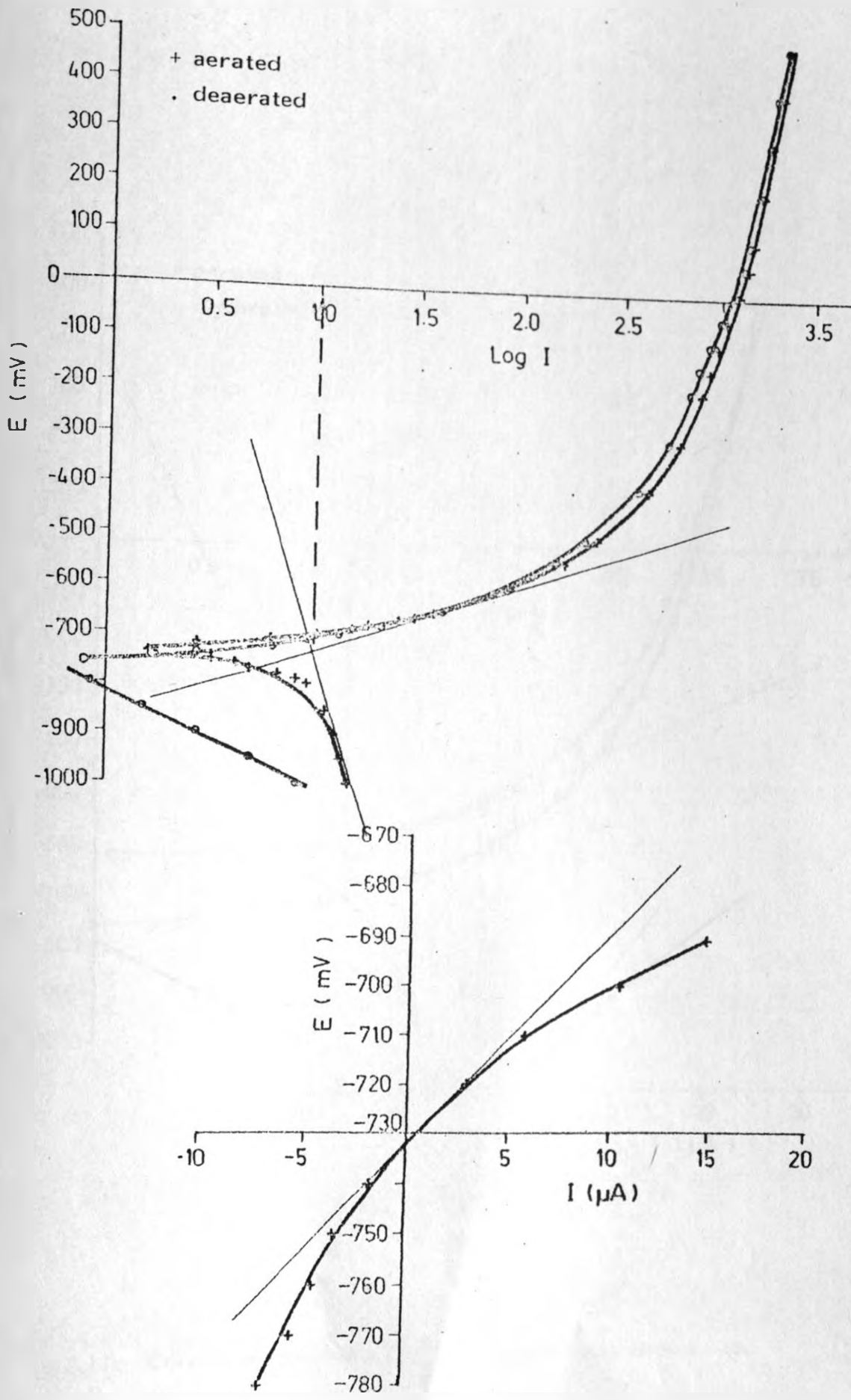

Fig. 17: Corrosion current determination for sample No. 17.

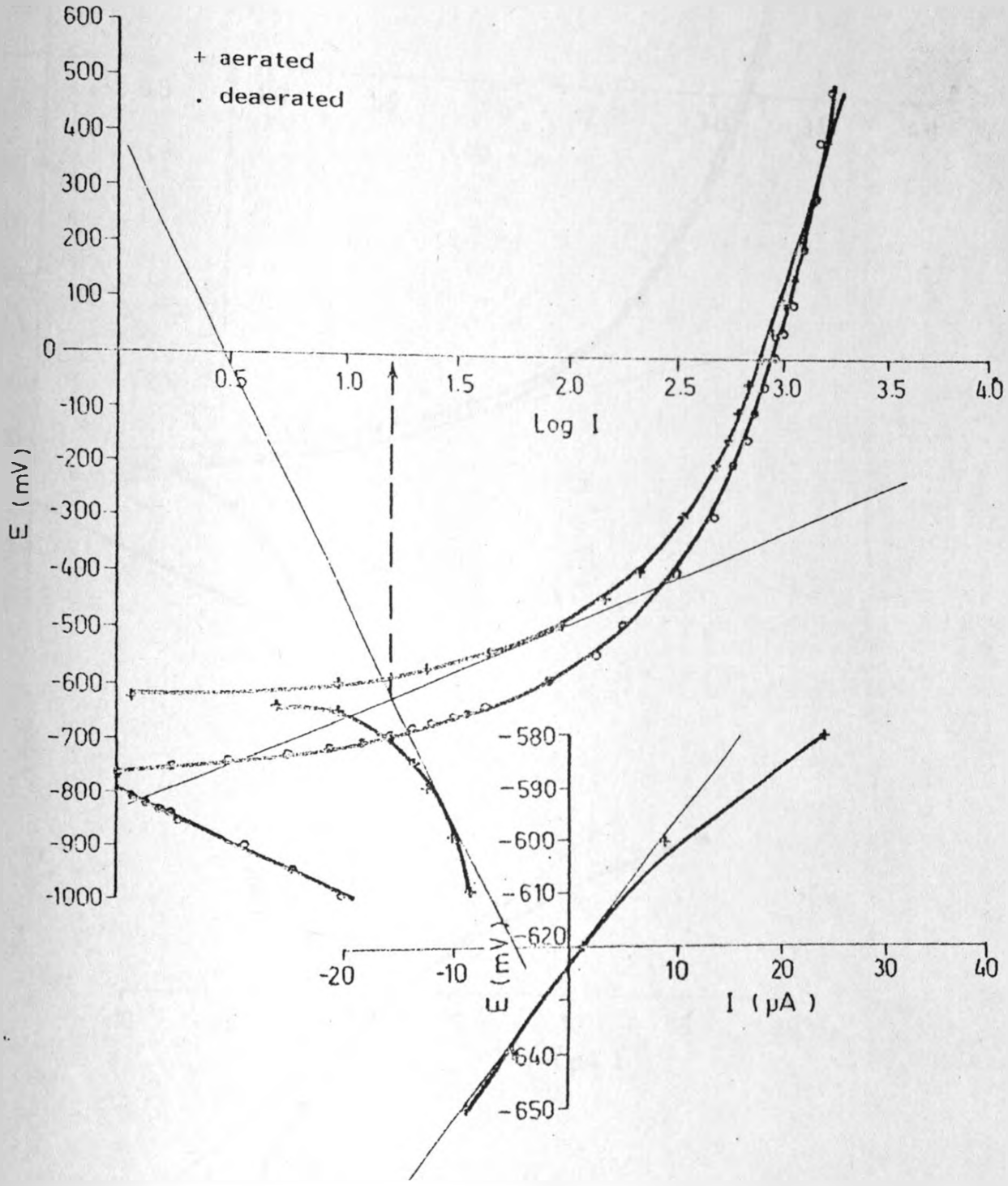

Fig. 18: Corrosion current determination for sample No. 18.

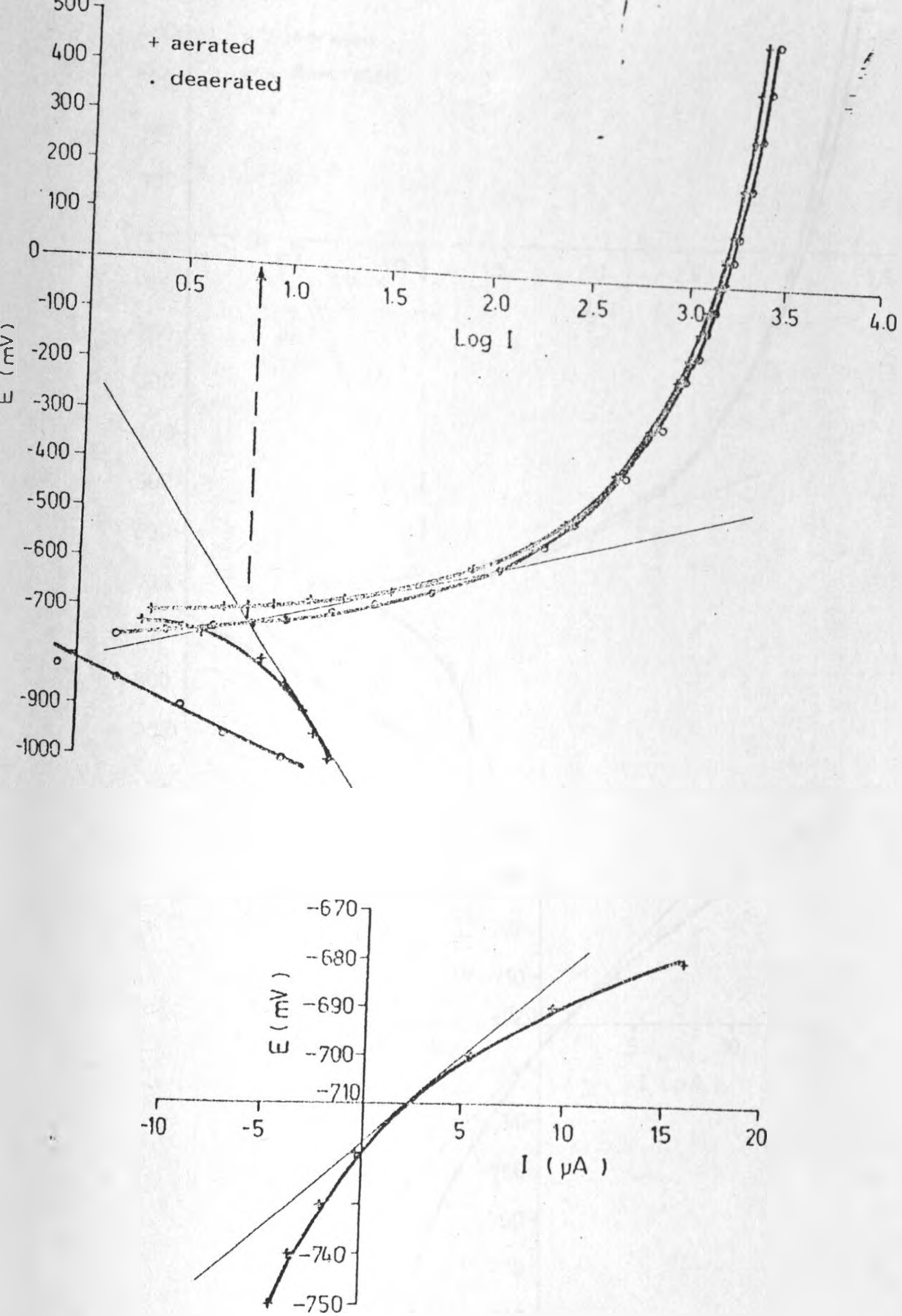

Fig. 19: Corrosion current determination for sample No. 19.

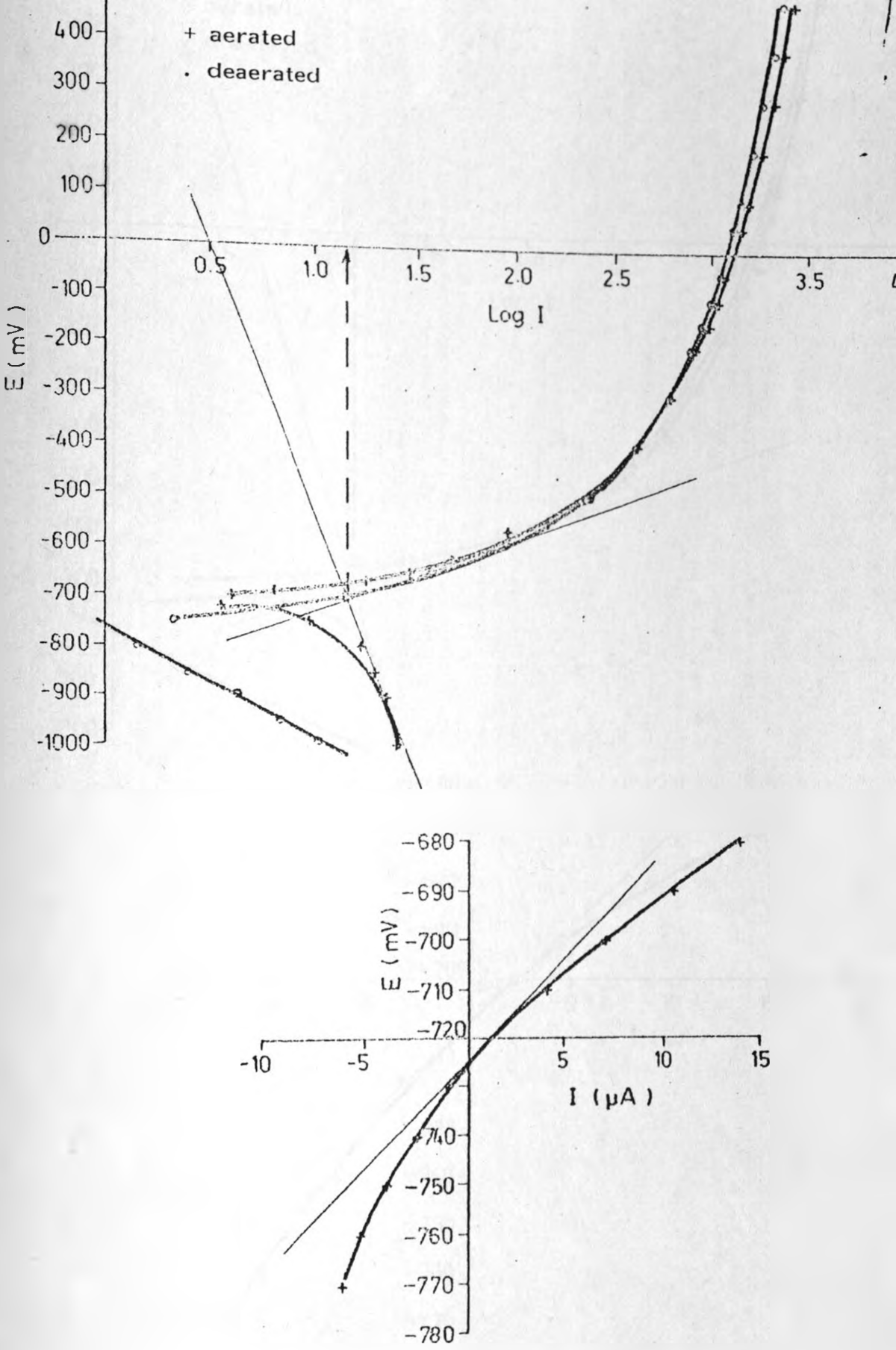

Fig. 20: Corrosion current determination for sample No. 20.

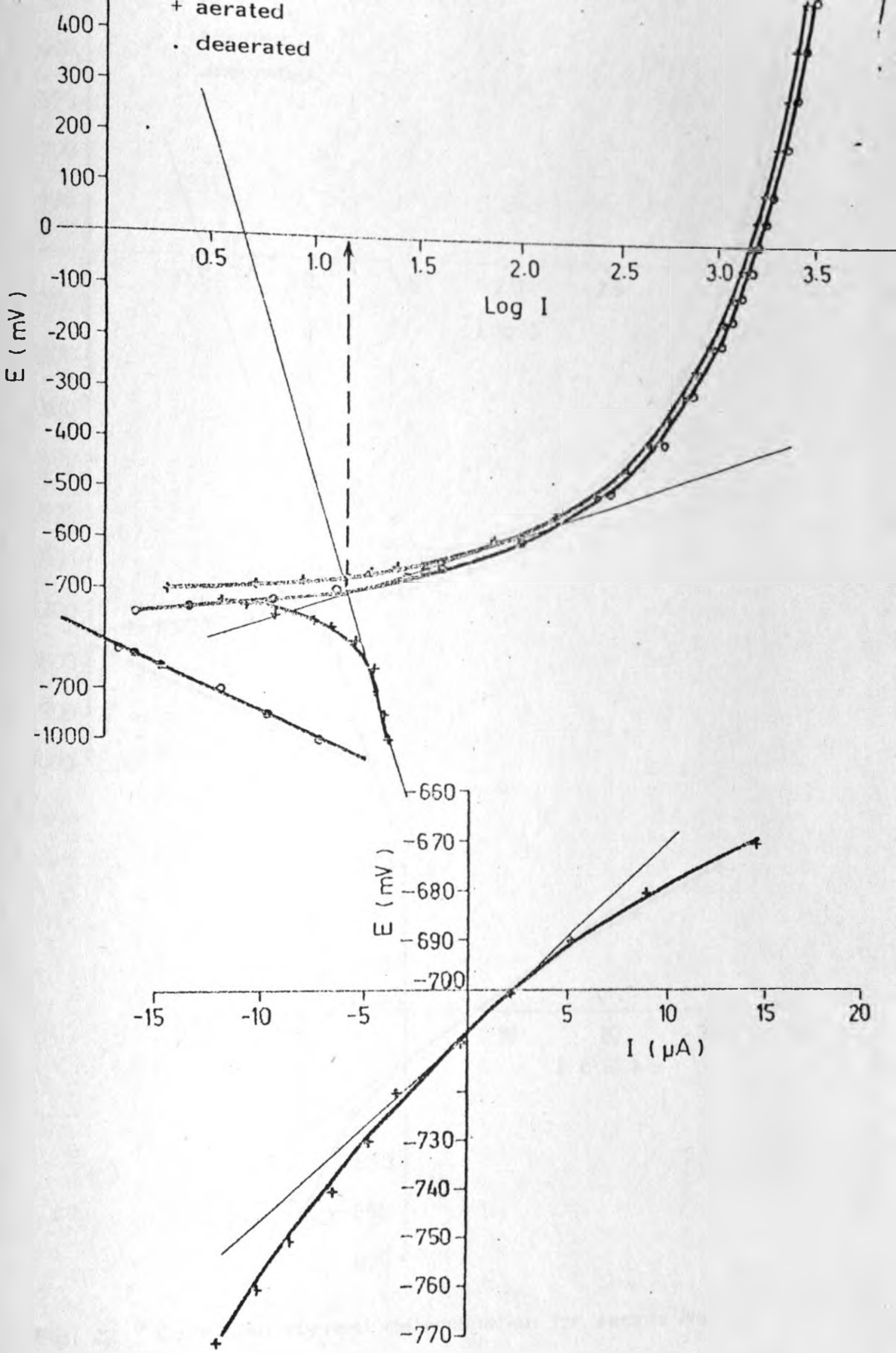

Fig. 21: Corrosion current determination for sample No. 21.

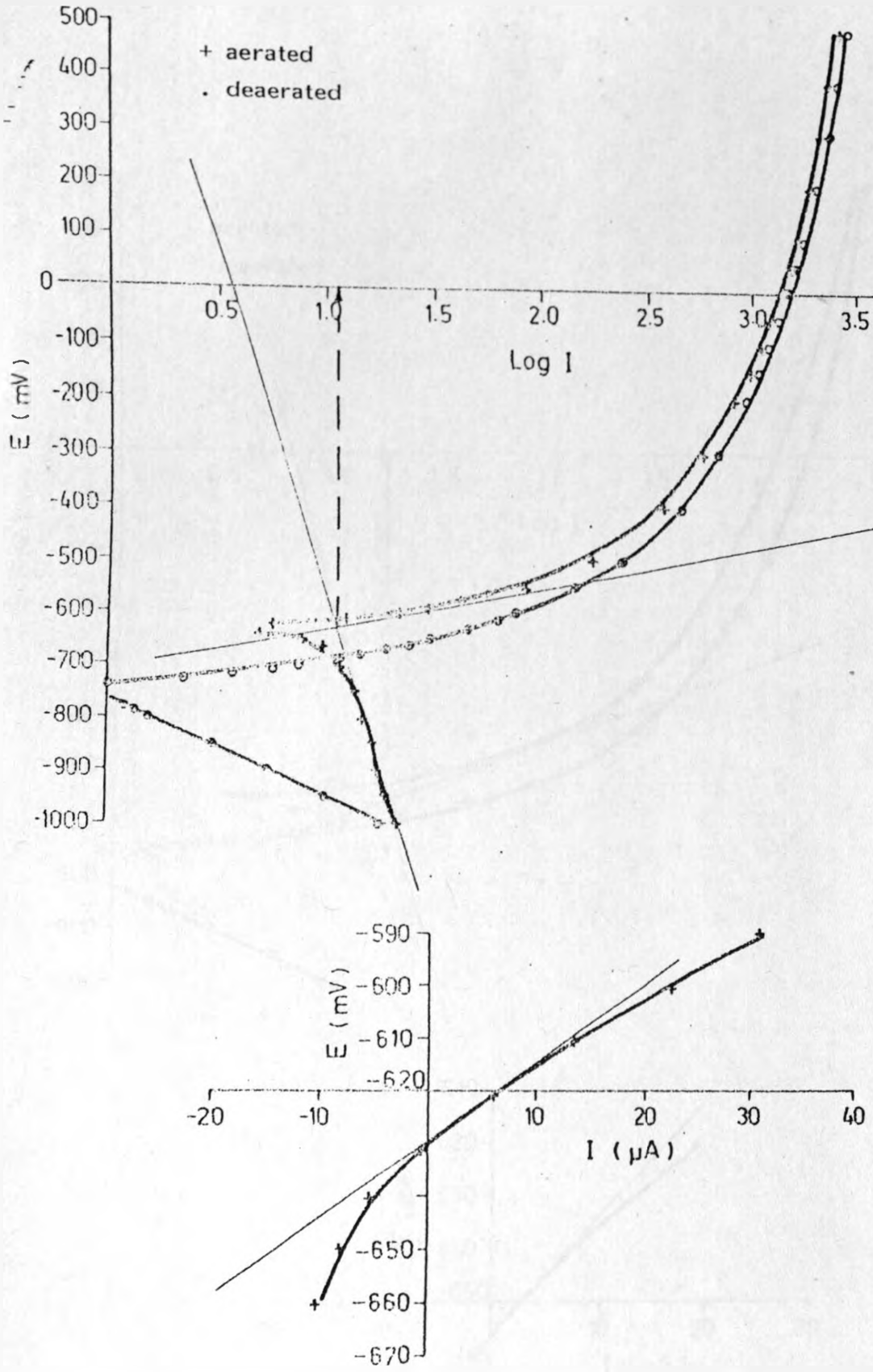

Fig. 22: Corrosion current determination for sample No. 22.

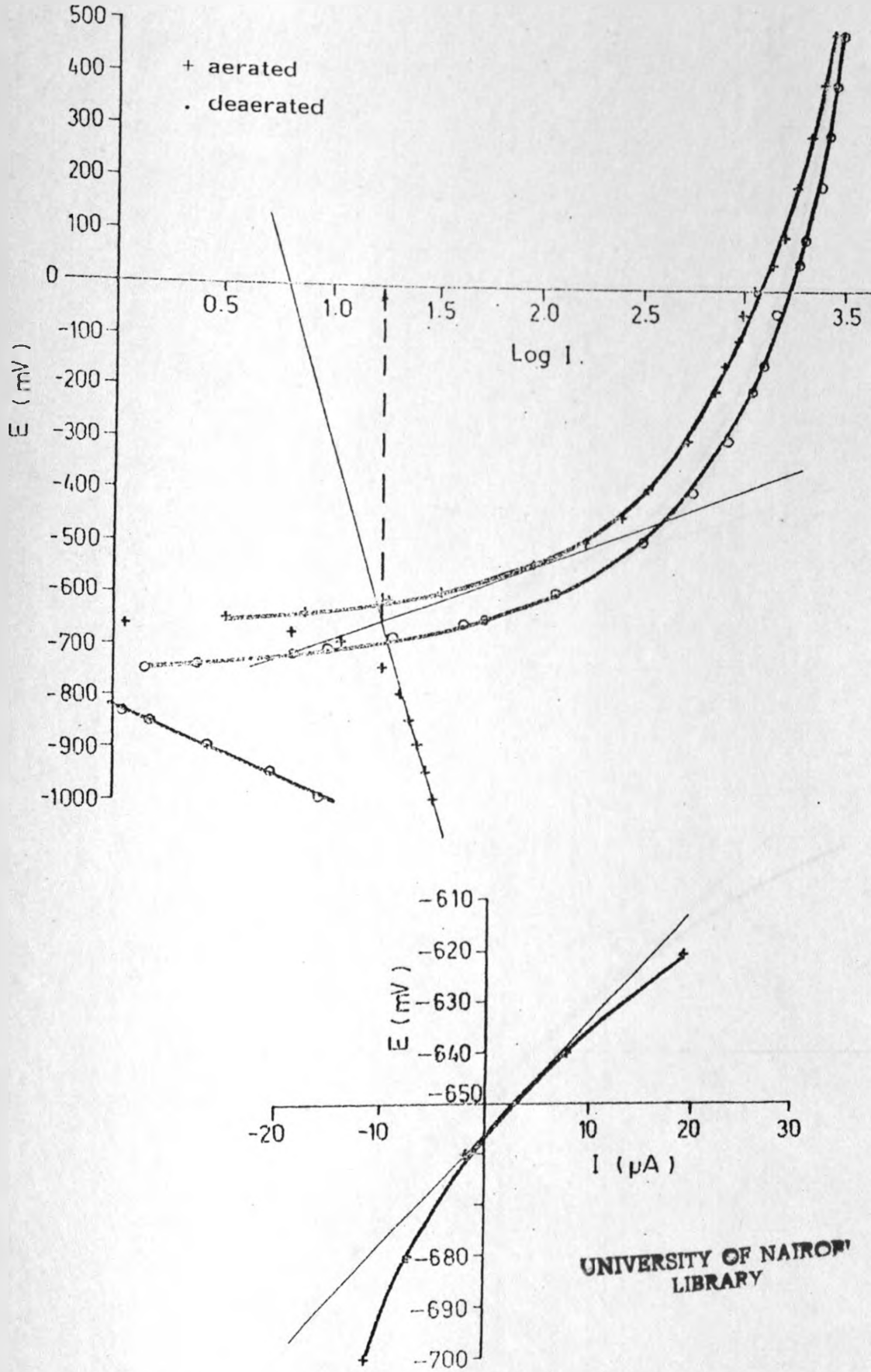

Fig. 23: Corrosion current determination for sample No. 23.

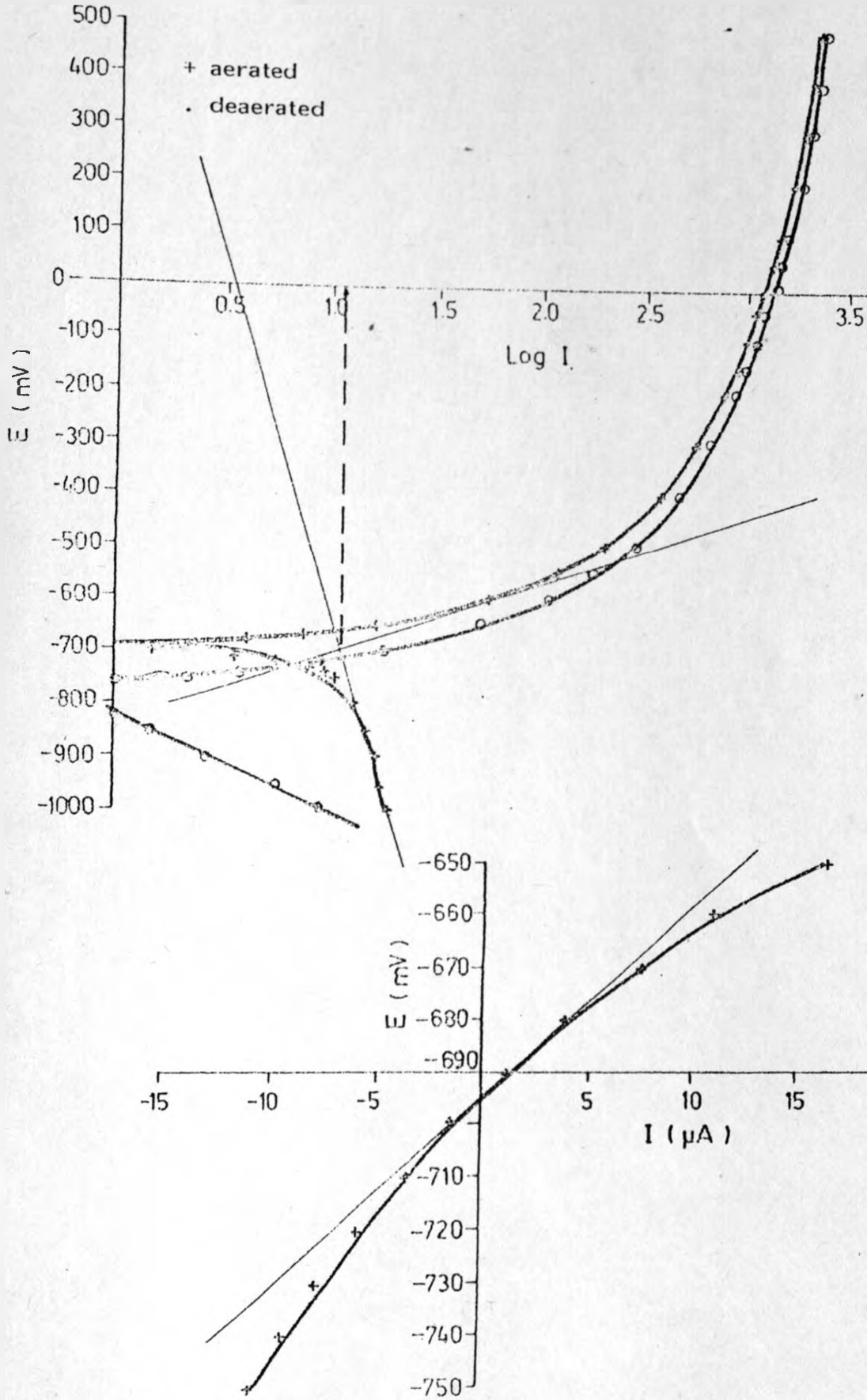

Fig. 24: Corrosion current determination for sample No. 24.